

University of Windsor

## Scholarship at UWindor

---

Electronic Theses and Dissertations

Theses, Dissertations, and Major Papers

---

2011

### Thin Film Metallization and Protective Top-Coat Development

Jack Bekou  
*University of Windsor*

Follow this and additional works at: <https://scholar.uwindsor.ca/etd>

---

#### Recommended Citation

Bekou, Jack, "Thin Film Metallization and Protective Top-Coat Development" (2011). *Electronic Theses and Dissertations*. 174.

<https://scholar.uwindsor.ca/etd/174>

This online database contains the full-text of PhD dissertations and Masters' theses of University of Windsor students from 1954 forward. These documents are made available for personal study and research purposes only, in accordance with the Canadian Copyright Act and the Creative Commons license—CC BY-NC-ND (Attribution, Non-Commercial, No Derivative Works). Under this license, works must always be attributed to the copyright holder (original author), cannot be used for any commercial purposes, and may not be altered. Any other use would require the permission of the copyright holder. Students may inquire about withdrawing their dissertation and/or thesis from this database. For additional inquiries, please contact the repository administrator via email ([scholarship@uwindsor.ca](mailto:scholarship@uwindsor.ca)) or by telephone at 519-253-3000ext. 3208.

**Thin Film Metallization and Protective Top-Coat Development**

By

Jack Bekou

A Thesis  
Submitted to the Faculty of Graduate Studies  
Through the Department of Mechanical, Automotive and Materials Engineering  
In Partial Fulfillment of the Requirements for  
the Degree of Master of Applied Science at the  
University of Windsor

Windsor, Ontario, Canada

2011

© 2011 Jack Bekou

**Thin Film Metallization and Protective Top-Coat Development**

By

Jack Bekou

APPROVED BY:

---

Dr. Xueyuan Nie, Program Reader, Department of Mechanical, Automotive & Materials  
Engineering

---

Dr. Walid Abdul-Kader, Outside Program Reader, Department of Industrial & Manufacturing  
Systems Engineering

---

Dr. Derek Northwood, Co-advisor, Department of Mechanical, Automotive & Materials  
Engineering

---

Dr. Paul Henshaw, Co-advisor, Department of Civil and Environmental Engineering

---

Dr. Henry Hu, Chair of Defense, Department of Mechanical, Automotive & Materials  
Engineering

May-19-2011

## DECLARATION OF ORIGINALITY

I hereby certify that I am the sole author of this thesis and that no part of this thesis has been published or submitted for publication.

I certify that, to the best of my knowledge, my thesis does not infringe upon anyone's copyright nor violate any proprietary rights and that any ideas, techniques, quotations, or any other material from the work of other people included in my thesis, published or otherwise, are fully acknowledged in accordance with the standard referencing practices. Furthermore, to the extent that I have included copyrighted material that surpasses the bounds of fair dealing within the meaning of the Canada Copyright Act, I certify that I have obtained a written permission from the copyright owner(s) to include such material(s) in my thesis.

I declare that this is a true copy of my thesis, including any final revisions, as approved by my thesis committee and the Graduate Studies office, and that this thesis has not been submitted for a higher degree to any other University or Institution.

## ABSTRACT

This research involved an investigation to find an alternative technology to chrome plating. The proposed system used a plastics substrate, a metalized layer, and a protective top-coat. The interfaces between the layers are the challenges and thus various experiments are conducted to examine the different possibilities for each layer and find the most suitable combination for the system meeting the appearance and functional requirements. Various studies, using different techniques such as scanning electron microscopy, energy-dispersive X-ray spectroscopy, Fourier transform infrared spectroscopy and profilometry have been presented to examine different failure modes and identify the root cause of the failures. This analysis was used to improve the system in the subsequent iterations.

Two systems were developed. System “A” consists of polycarbonate, a stainless steel metalized layer, and a silicone based top-coat. System “B” consists of polycarbonate, a stainless steel metalized layer, an aluminum metalized layer and a silicone based top-coat.

## DEDICATION

Dedicated to my family

## ACKNOWLEDGEMENTS

First and foremost, I would like to sincerely thank my co-advisors Dr. Derek Northwood and Dr. Paul Henshaw for their support, advice and the opportunity to complete my Master's degree under their supervision.

I would also like to thank my committee members, Dr. Xueyuan Nie and Dr. Walid Abdul-Kader for their valuable input and guidance.

I would also like to thank John Robinson for his help with the preparation of samples for microscopy analysis.

## TABLE OF CONTENTS

DECLARATION OF ORIGINALITY .....	iii
ABSTRACT .....	iv
DEDICATION.....	v
ACKNOWLEDGEMENTS.....	vi
LIST OF TABLES.....	x&xi
LIST OF FIGURES .....	xii&xiii
<b>CHAPTER</b>	
<b>I. INTRODUCTION</b>	
1.1 Background Information	1-2
1.2 Objective of Project / Thesis	3
1.3 General Challenges	4
<b>II. LITERATURE REVIEW</b>	
2.1 General Literature Overview	5
2.2 Traditional Chrome Plating for Plastic Parts	5-6
2.3 Metallization of Plastics	7-8
2.4 Base-coat Before Metallization	9
2.5 Film Stress in Metallized Layers	9-11
2.6 Hexamethyldisiloxane (HMDSO)	11
2.7 Plasma Treatment of Polymers	11-13
2.8 Mechanical Properties of Thin Films	14-15
<b>III. DESIGN, MATERIAL, METHODS, AND REQUIREMENTS</b>	
3.1 Requirements for This Technology	16-18
3.2 Experimental Procedure & Materials	18-21
3.3 Analytical Techniques	22
<b>IV. INITIAL DEVELOPMENT AND EARLY RESULTS</b>	
4.1 Initial Development and Early Results	23
4.2 Substrate Selection – Polycarbonate	24
4.3 Adhesion of the Metalized Layer as a Function of Time	24-25
4.4 Ultraviolet Light Transmission Study	25-30



	<b>4.5 Iridescence Appearance</b>	<b>31</b>
<b>V.</b>	<b>SYSTEM "A" DEVELOPMENT AND RESULTS</b>	
	<b>5.1 System "A" Introduction</b>	<b>32</b>
	<b>5.2 Stage-1 of System "A" Development</b>	<b>32</b>
	<b>5.2.1 Objective</b>	<b>32-33</b>
	<b>5.2.2 Observations / Data / Results</b>	<b>33-39</b>
	<b>5.2.3 Main Conclusions</b>	<b>34-35</b>
	<b>5.3 Stage-2 of System "A" Development</b>	<b>40</b>
	<b>5.3.1 Objective</b>	<b>40</b>
	<b>5.3.2 Observations / Data / Results</b>	<b>40-45</b>
	<b>5.3.3 Main Conclusions</b>	<b>41</b>
	<b>5.4 Stage-3 of System "A" Development</b>	<b>46</b>
	<b>5.4.1 Objective</b>	<b>46</b>
	<b>5.4.2 Observations / Data / Results</b>	<b>46-47</b>
	<b>5.4.3 Main Conclusions</b>	<b>46</b>
	<b>5.5 Stage-4 of System "A" Development</b>	<b>47</b>
	<b>5.5.1 Objective</b>	<b>47</b>
	<b>5.5.2 Observations / Data / Results</b>	<b>47-54</b>
	<b>5.5.3 Main Conclusions</b>	<b>54</b>
	<b>5.6 Stage-5 of System "A" Development</b>	<b>55</b>
	<b>5.6.1 Objective</b>	<b>55</b>
	<b>5.6.2 Observations / Data / Results</b>	<b>55-66</b>
	<b>5.6.3 Main Conclusions</b>	<b>66</b>
	<b>5.7 System "A" Summary</b>	<b>67</b>
<b>VI.</b>	<b>SYSTEM "A" DEVELOPMENT AND RESULTS</b>	
	<b>6.1 System "B" Introduction</b>	<b>68</b>
	<b>6.2 Stage-1 of System "B" Development</b>	<b>68</b>
	<b>6.2.1 Objective</b>	<b>68</b>
	<b>6.2.2 Observations / Data / Results</b>	<b>69-71</b>
	<b>6.2.3 Main Conclusions</b>	<b>71-72</b>
	<b>6.3 Stage-2 of System "B" Development</b>	<b>72</b>
	<b>6.3.1 Objective</b>	<b>72</b>
	<b>6.3.2 Observations / Data / Results</b>	<b>72-74</b>

6.3.3 Main Conclusions	74
6.4 Stage-3 of System "B" Development	75
6.4.1 Objective	75
6.4.2 Observations / Data / Results	75-79
6.4.3 Main Conclusions	79
6.5 Stage-1 of System "B" Development	79
6.5.1 Objective	79-80
6.5.2 Observations / Data / Results	81-92
6.5.3 Main Conclusions	93
6.6 System "B" Summary	93
<b>VII. CONCLUSIONS AND RECOMMENDATIONS</b>	
6.1 Conclusions	94-95
6.2 Recommendations	95
<b>REFERENCES</b>	96-98
<b>VITA AUCTORIS</b>	99

## LIST OF TABLES

Table 2.1: PVD Coating Comparison	8
Table 5.1: Process Parameters – Stage-1 of System-A	35
Table 5.2: Formulations for Primer-A – Stage-1 of System A	35
Table 5.3: Heat Age and Water Immersion Results. Note that TCA refers to top-coat “A”	36
Table 5.4: Primer Composition – Stage-2 of System-A	41
Table 5.5: Process Parameters for Stage-2 of System-A	43
Table 5.6: Summary of Tape Pull Adhesion after 16 Hr Water Immersion for Stage-2 System-A	44
Table 5.7: Summary of Tape Pull Adhesion after Water Immersion	45
Table 5.8: Summary of Performance of the Number of Samples with Respect to Bake Time	45
Table 5.9: Process Parameters for Stage-3 of System-A	47
Table 5.10: Primer Formulations for Stage-3 of System-A	47
Table 5.11: Process Parameters for Stage-4 of System-A (UV coating)	50
Table 5.12: UV Top-coat Film Build for Stage-4 of System-A	51
Table 5.13: Primer Formulations for Stage-4 of System-A – Thermal Coating	53
Table 5.14: Process Parameters for Stage 4 of System-A – Thermal Coating	54
Table 5.15: Process Parameters for Stage-5 of System-A	56
Table 5.16: Initial Adhesion Results for Stage-5 (UV run) of System-A	56
Table 5.17: Primer Formulations for Stage-5 of System-A – Thermal Coating	57
Table 5.18: Process Parameters for the Thermal run Stage-5 of System-A	57
Table 5.19: Test Results for Complete Matrix Testing for System-A	57
Table 5.20: Integrated Areas Under the Curves for Figure 5.13	66
Table 6.1: Adhesion Relationship between Target Power and Sputtering Time for an Aluminum Target	70
Table 6.2: Process Parameters for Stage-1 of System-B	70
Table 6.3: Initial Adhesion and Adhesion After 10 Day Water Immersion Test Results for Stage-1 of System-B. Note: All samples formed pinholes after the water immersion	71
Table 6.4: Process Parameters for Stage-2 of System-B	73
Table 6.5: Initial Adhesion and Adhesion After 10 Day Water Immersion Test Results	

for Stage-2 of System-B	74
Table 6.6: Process Parameters for Stage-3 of System-B	77
Table 6.7: Initial Adhesion and Adhesion After 10 Day Water Immersion Test Results for Stage-3 of System-B	78
Table 6.8: Process Parameters for Stage-4 of System-B	81
Table 6.9: Initial Adhesion and Adhesion after 10 Day Water Immersion Test Results for Stage-4 of System-B	82
Table 6.10: Results for Complete Matrix Testing for System-B	82
Table 6.11: CASS versus Salt Spray Testing	84

## LIST OF FIGURES

Figure 1.1: Potential Automotive Applications for Chrome Replacement	2
Figure 1.2: Basic Concept for Chrome Replacement	3
Figure 2.1: Basic Concept for Chrome Replacement	7
Figure 2.2: Adhesion and Surface Tension of A Polymer Surface Versus Plasma Treatment	12
Figure 3.1: Process Flow with a Thermally Cured Top-coat System	20
Figure 3.2: Process Flow with a UV Cured Top-coat System	20
Figure 3.3: Thermal Profile for the UV Cured Top-coat System	21
Figure 3.4: Thermal Profile for the Thermal Cured Top-coat System.	21
Figure 4.1: Surface Energy as a Function of Time for Metalized Layer of Aluminum	23
Figure 4.2: % Adhesion Loss vs. Sputter Time.	25
Figure 4.3: Topo-graphical Map of Light Transmission Data for the Metalized Surface Only	27
Figure 4.4: Top View of Light Transmission Data for the Metalized Surface Only	28
Figure 4.5: Topo-graphical Map of Light Transmission Data for the Metalized Surface & Top-coat.	29
Figure 4.6: Top View of Light Transmission % Data for the Metalized Surface & Top-coat	30
Figure 4.7: Iridescence Effect. A) sample before top-coating. B) sample after top-coating	31
Figure 5.1: System “A” Development Stages	32
Figure 5.2: Optical Imaging of Micro-cracked Metalized Surface - X200	37
Figure 5.3: Optical Imaging of “Spotting” After Water Immersion Testing	37
Figure 5.4: FTIR of Water Spotting Versus No Water Spotting	38
Figure 5.5: FTIR of Water Spotting Versus No Water Spotting. Enlarged from Figure 5.4	39
Figure 5.6: Effects of the UV Top-coat on a SST metalized Layer	52
Figure 5.7: EDX Analysis on Metalized Layer with no Primer no Top-coat, Different Beam Energies EDX Spectra	59
Figure 5.8: EDX Analysis on Metalized Layer with Primer-C and no Top-coat, Different Electron Beam Energies and Penetration Levels	60

Figure 5.9: Primer C – Cured at 85oC for 15 Minutes (SEM/EDX Analysis)	61
Figure 5.10: Primer BB– Cured at 85oC for 15 Minutes (SEM/EDX Analysis)	62
Figure 5.11: Different Primer SEM Images – Surface Wet-out	63
Figure 5.12: Sample 1, 2 3 (no bake, 7min at 110C, 15min at 85C)	65
Figure 6.1: System “B” Development Stages	68
Figure 6.2: Nichban Test Results After Water Immersion Testing with Respect to the Sputtering Time for Aluminum	79
Figure 6.3: SEM Images for Freeze Fracture of a Cross Section for a Typical Sample for System-B	85
Figure 6.4: SEM Images for Edge of the CASS Sample 77-44	85
Figure 6.5: SEM/EDX Images for Edge of the CASS Sample 77-44	86
Figure 6.6: SEM Images for Edge of the CASS Sample 77-44 – Crack Location	87
Figure 6.7: SEM/EDX Images for Edge of the CASS Sample 77-44, Crack Location	88
Figure 6.8: SEM Images for Middle of the CASS Sample 77-44	89
Figure 6.9: SEM images for Middle of the CASS Sample 77-44, Failure Location	89
Figure 6.10: Elemental Mapping for Middle of the CASS Sample	90
Figure 6.11: SEM Images for CASS Sample Showing the Different Exposed Layers	91
Figure 6.12: SEM/EDX Images for CASS Sample 77-44 shown in Figure 6.8	92

# CHAPTER I

## INTRODUCTION

### 1.1 Background Information

For decades, chromium plating has been a process of choice when building up worn components and improving wear resistance and corrosion resistance of machine elements, as well as plating parts for decorative purposes as in the case of the automotive industry. In recent years, chrome plating has come under attack because the plating process emits a substance called hexavalent chromium, which is considered to be a cancer causing substance. This substance can get in the air and can also into our water supply, so there is considerable concern about people living close to chrome plating facilities. In order to overcome this problem, regulatory agencies have instituted more stringent air quality standards on the emissions resulting from the chrome plating process. These standards have required chrome plating facilities to install increasingly sophisticated equipment to achieve compliance. The use of chrome plating is so widespread that these requirements have prompted a desire to replace chrome plating with some other coating alternative [1]. In addition, much legislation regarding the maximum amount of hexavalent chromium content allowable in many industries (especially automotive) is very strict. Furthermore, health and safety regulations related to Cr plated components is driving research and development towards finding new, environment friendly solutions.

Hard chromium is widely used in many applications. Hard chromium possesses a few characteristic properties like relatively high hardness, good corrosion resistance and a self leveling effect. Combinations of these properties have lead to use in applications where the conditions require high hardness, low friction, low wear and high corrosion resistance. Hard chromium is found in a wide range of applications like hydraulic parts for aerospace, automobiles and off-shore vehicle. The anti wear properties of hard chromium are used in applications such as coating of piston rings, and in the textile industry.

Given the health hazards in the traditional chrome plating process, there is a need for a chrome replacement process. Some of the chrome plating alternatives include, but are not limited to the following:

- Plasma spray
- High velocity oxy-fuel (HVOF)
- Twin wire arc spray
- Electro-spark deposition
- Electroless nickel
- Laser cladding

- Physical vapour deposition (PVD)

The focus of this research is to develop PVD coatings along with organic top-coatings to replace chrome plating. The PVD process is an environmentally friendly process compared to traditional chrome plating and thus there is a great motivation by the industry to develop decorative PVD coatings. This project deals specifically with automotive applications that fit the chrome replacement development. Some of the specific applications include but are not limited to the following: lift gate appliqué, fender badges, pillar appliqué trim, emblems and ornamental bezels. Examples fender badges are shown in Figure 1.1.



Figure 1.1: Potential Automotive Applications for Chrome Replacement. Examples of Fender Badges. Photos taken by Jack Bekou from The North American International Auto Show in Detroit-2010.

Metallizing for functional and decorative applications has long been an off-line batch process usually requiring climate controlled clean rooms and equipment costing in excess of \$1,000,000. Large batch processing methods allow time for parts to absorb moisture and accumulate other types of contaminants, cleaning procedures and base coats are often needed to achieve proper coating adhesion. In-line processing methods address these concerns and also increase yield and reduce the need for cost prohibitive part storage.



## 1.2 Objective of Research

The basic idea behind the development of a process to replace the traditional chrome plating process is to:

1. Injection mold a plastic substrate (as it is traditionally done) to form the main structure of the system.
2. Apply a PVD coating (using magnetron sputtering) to deposit a metallized layer with a metal like finish to achieve the reflective metallic look (mirror look).
3. Apply a top-coat (protective layer) to the metallized surface that consists of an organic clear coating that is applied by spray or flow coating and is thermally or ultraviolet (UV) cured. In some cases, a primer maybe required to increase the adhesion of the top-coat to the metallized layer as is discussed later.

Figure 1.2 shows the basic concept for this technology:

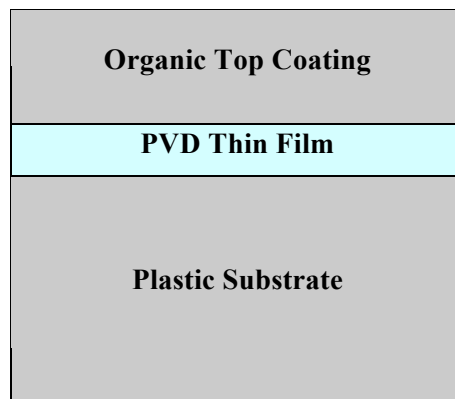


Figure 1.2: Basic Concept for Chrome Replacement

More specifically, the objective of the research is to define the specific layers that make up the overall system to produce a chrome replacement technology that meets the following pre-requisite test requirements as specified by different Original Equipment Manufacturers (OEMs):

1. Reflective appearance
2. Proper initial adhesion between all layers
3. Water Immersion Testing
4. Heat Age Testing
5. Impact Testing
6. Humidity Testing
7. Salt Spray Testing

### **1.3 General Challenges**

Due to the extensive testing required to approve this technology, where some tests require 6-8 months to complete (as outlined in Chapter II), it was determined that the above requirements are sufficient for the subject of this thesis. However, complete testing also includes some critical aspects of the system such as corrosion (CASS) testing.

The development of this project involved many challenges for each step of the process. Some of the major challenges included:

- Molding processes – minimize internal part stress.
- Part wall thickness – improve material flow and reduce part stress.
- Material selection – improve adhesion, impact resistance and appearance.
- Metalizing processes – provide the appearance requirements.
- Plasma pre-treatments – improve adhesion.
- Plasma post-treatments – improve adhesion.
- Metalizing material – improve adhesion and color (stainless steel, aluminum, chromium).
- Hard-coating Methods – provide a protective layer.
- Hard-coating Materials – achieve adhesion and weathering requirements.
- Overall Process Staging – achieve adhesion between all layers.

The main challenge was to find suitable layers for the system that allowed for proper adhesion in all interfaces in order to meet the appearance and functional requirements.

## CHAPTER II

### LITERATURE REVIEW

#### 2.1 General Literature Overview

Clean technologies developments are being pursued in all aspects of industrial manufacturing in many areas, like material, metal finishing and even plasma surface engineering. One of the most important technologies that require replacement by alternative clean technologies is traditional chrome plating for decorative and functional purposes. The electroplating of finishes, such as hard chromium, cadmium and nickel in metal finishing is today recognized as a major source of environmental pollution in every country. These electroplating technologies, that use wet bath, are not favorable anymore compared to other dry methods such as physical vapor deposition (PVD), plasma-assisted chemical vapor deposition, chemical vapor deposition and thermal spraying. In the last couple of decades, among these techniques, the results obtained with PVD coatings in metal cutting and forming show the most promising substitute for electroplating processes, which at one time, seemed to be technologically and economically irreplaceable [2].

Using PVD coatings, the technique can deposit various metals, alloys and even ceramic coatings. These coatings possess a unique set of properties based on their chemical composition, that seems to have a large range. Thus allows to form PVD thin films with various mechanical and wear resistnace properties. One of the challenges that the PVD manufacturers faced was building the proper equipment to handle high production volumes that require, in some cases, plasma treating the surface and then depositing the PVD thin films at a very high deposition rate to reduce cycle time. Therefore, it was necessary to use large PVD batch systems to accommodate for industrial mass production. The alternative for today's low price galvanic coatings is therefore dry and clean PVD technologies, fully supported by legislation on environmental protection. The economics depend directly on the substrate type and the quantity [3].

The last decade has some very strong activities to pursue a systematic replacement of the unclean technologies and specifically the traditional chrome plating with high performance PVD coatings. In the last 80 years, since hard chrome became commercially available, this industrial manufacturing method has developed into a huge, well organized, complicated and expensive business.

#### 2.2 Traditional Chrome Plating for Plastic Parts

Traditional chrome plating for plastics is an electroplating process [4]. It is a process that takes several hours to complete and it involves various steps as described below, in Figure 2.1:

1. The first step is the etch bath which consists of chromic and sulfuric acids which microscopically attack the surface of the molded plastic part. All of the butadiene molecules are removed from the plastic surface in the etching stage.
2. The second step is the an electroless plating of copper. Copper ions are reduced in the presence of formaldehyde resulting in a thin layer being plated. This step allows the plastic surface to become conductive for the next steps.
3. The third step involves electrolytic plating bath using current to deposit copper. This step is normally conducted with a low current to allow for plating thickness build up.
4. The fourth step involves depositing copper as well, but depositing with higher current. This layer serves the purpose of leveling the surface.
5. The fifth step involves electroplating semi-bright nickel, which serves the purpose of corrosion resistance.
6. The sixth step consists of electroplating bright nickel, which serves the purpose of giving a reflective appearance
7. The seventh step involves depositing a bright nickel solution with very small particles that create a porous layer, which protects against corrosion.
8. The final step involves electroplating chromium to give the final reflective look.

Figure 2.1 demonstrates all the process for the traditional chrome plating process described above. It is important to note that the traditional chrome plating process consists of all the listed long steps in addition to all the intermediate steps that are between the main outlined steps. These intermediate steps include: washing, rinsing, activating, drying, etc. Thus, there is certainly a need for development to find alternatives to the traditional chrome plating process [5-6].

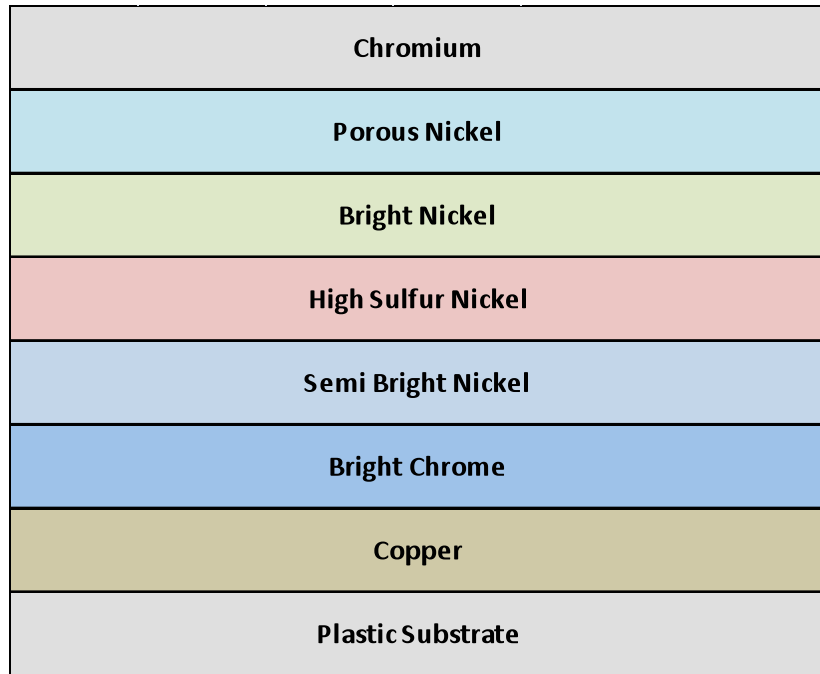


Figure 2.1: Traditional Chrome Plating Steps

### 2.3 Metallization of Plastics

In the fifties, metallization was first achieved by thermal evaporation of aluminum in the hardware, packaging, and some automotive applications. These markets attracted a larger desire to focus on productively, higher quality and lower cost. Thus, the obvious step was to create larger size chamber to accommodate higher production volumes, but the problem was pumping down the larger chambers to the desired pressure for proper metallization. Due to the water vapor that collected in the chamber, which caused the longer cycle times for pumping down the pressure, the inner surfaces of the chamber are minimized to reduce the pumping time [7].

The next step in creating these metalized reflective looks involved vapor sources other than filament due to the high demand for reflecting layers on laser readable discs. The source for metalizing had to be a reliable and efficient source, like a sputtering cathode. The next large step involved the high performance magnetron cathodes. All of this was performed for readable CDs, which are relatively flat parts. The success story of the CDs drove the development and implementation of shaped parts to be metalized [7].

Today, Physical Vapor Deposition (PVD) coating are used in many different applications. They are specifically used in decorative application as many desired looks can be achieved using PVD coatings. The coating is deposited at very low vacuum pressures and normally, a metal is deposited

for decorative purposes. The reference to decorative coating is taking into account the desired reflective silver finished look. However, there are many other considerations and limitations depending on the application as they relate to the functional requirements and life service of the product. For example, the adhesion properties of the deposited PVD thin layer are very critical. The type of the metal used during PVD coating can provide different corrosion properties to the overall system [8]. When depositing a PVD coating on plastic surface, the thin film closely mimics the surface morphology, replicating the finest features. Therefore, highly polished surfaces will give a very high reflective surface [9].

One of the most common uses for PVD coating in the automotive industry is first surface reflectors that are inside a head lamp assembly. In the reflector application, aluminum is normally the choice of metal due to its high reflectivity, relatively inexpensive cost and high deposition rates. In addition to the aluminum metal deposition, the reflectors are protected with a plasma polymerization process that involves a highly chemical resistance overlay by a monomer that is put through a plasma to be polymerized and thus provide a clear protective layer. This plasma polymerization step is done within the same sputtering metal chamber. Before the 80s, these reflectors in the headlamp did not require a plasma polymerized top-coat because the glass headlamp was totally sealed [10].

The selection of PVD coatings is really based on the application and the desired look. One of the most common deciding factors for a decorative application is the reflectivity values of the deposited metal. Table 2.1 compares some of the reflectivity values and relative cost for common metals that are used in PVD coating, in automotive applications. It is important to note that aluminum has the highest reflectivity value and the lowest cost and thus it is commonly used in automotive applications. There are other metals that provide higher reflectivity values than aluminum. Silver, for example, provides a reflectivity value of anywhere between 95-98 %. However the cost of silver is extremely high and thus it is only used in solar panel applications, where it is required. In addition, aluminum targets have high deposition rates, which helps make the cycle time shorter and that makes aluminum targets even more desirable to the industry [9].

Table2.1: PVD Coating Comparison. Note: Reflectivity values were obtained through measurement using the MiniScan XE Plus Color Meter Model No. D/8-S

<b>Metal</b>	<b>Reflectivity (%)</b>	<b>Cost</b>
Aluminum	90-93	Low
Chromium	65-72	high
Stainless Steel	68-75	medium
Titanium	60-70	medium

## **2.4 Base-coat Before Metallization**

Thus far, many researchers have attempted to use metallization to achieve the desired look of a reflective surface along with meeting the functional requirements. When metallization is used alone to coat a plastic part, it has proven that is it not sufficient to provide the proper durability, especially at the lower thickness as that can be produced using short cycle times[11].

One solution is the introduction of a base-coat layer after the injection moulding stage and before the metallized layer. The base-coat is normally a UV-curable coating that is sprayed or flow coated and serves the purposes of i) leveling the surface to allow for a smooth metallized layer deposition, and ii) increasing the adhesion properties of the system as the base-coat cross-links with the top-coat [11]. In plastics manufacture, the variability of the substrate (sometimes made of virgin resin, but often a blend of regrind and virgin resin) along with noticeable defects in the molding process make metallizing bare parts difficult [10]. Thus, special attention is required to polish the surface of the tool to achieve the highest quality of parts. The tolerance and maintenance of molds smooth enough for producing parts that can be metalized directly (at least with reasonable deposition thicknesses) is challenging.

One of the potential application for developing durable base-coat, PVD coating and top-coat systems is the alloy wheel, where serious concerns have been expressed as far as the durability of the system. While automotive interior systems using PVD have been successfully launched, the exterior trim market has been elusive. Recently some systems have gained acceptance in the automotive aftermarket where appearance is required, but some sacrifices of performance and durability have been made. Thus, fully developed systems have not been reported [11].

As the need grows for products that support a bright, chrome appearance in a wide range of industries, producers are actively seeking alternatives to the hard chrome process. Other technologies are being tried, but one of the most promising may be a combination of physical vapor deposition and a system of base and top coatings which offer both appearance and performance.

## **2.5 Film Stress in Metallized Layers**

Tensile and compressive residual stresses are present in the PVD films. Compressive stresses are due to atoms being closer to each other than they should be. However, tensile stress is due to atoms being further apart[11]. In other cases, stresses can be found in localized areas of the film due to local defects on the surface or any foreign contamination that is present before depositing the thin film. The high stress areas of the localized samples eventually lead to adhesion failures as the thin film does not adhere to the surface properly, which is observed as pinholes in the film.

In addition, the differences in the coefficient of expansion are also responsible for residual stresses in thin films. This is observed as the substrate generates a stress as the depositing temperature decreases and growth of the film, which prevents the atoms from condensing in their least energetic association with one another. The residual stresses can eventually cause a failure mode in the part that contains the thin films as the stored energy of these stresses is released. As film thickness increases, the film stress increases respectively. In addition, the elastic modulus, and the morphology and the density of the film are also other factors that affect film stress. Chromium, tungsten, and metal oxides have high modulus values which result in high film stresses and thus plastic deformation of the thin film can occur. On the other hand, materials like silver and gold have low modulus values and thus the plastic deformation of the material will allow relieving the film stresses. The stresses may not be uniform through the film thickness (i.e., a stress gradient in the deposit) if the growth mode and film density change with thickness and/or if some region has been annealed more than others during the deposition process. If the stress is not uniform through the film thickness, the film will curl when separated from the substrate—if uniform, the separated film will lie flat [12].

The high residual film stresses are responsible for adhesion failures for thin films, especially when the film thickness is large and it has a high modulus property. For example, when depositing chromium as the metal layer on glass, the film thickness needs to be controlled. By depositing too thick of a chromium layer (more than few hundred nanometers), there would be an adhesion failure due to the high residual stresses present in the deposited film. However, if the film thickness is less than 50 nanometer, the film's residual stresses are low and no adhesion failures are observed.

High film stress can also cause voids to form in the film (tensile stresses) or the film to form small hills (compressive stress) when the film has good adherence to the substrate [13]. However, there are possible ways to control film stress by changing the deposition inputs or by changing the growth mode of the film. Some of the important factors for film stress are the sputtering pressure during sputter deposition and amount of energy produced by concurrent bombardment in ion plating. [14].

A groundswell of development in nanotechnology coating additives now enables coatings to provide a dazzling range of specialized functions. Coatings can resist water, fingerprints and bacteria. Not only will future parts satisfy the cosmetic and durability requirements of customers but they may provide function not attainable with any other production method. This technology extends into so called “smart coatings” [11] where the coating can vary its properties when subjected to an external “trigger” such as temperature, moisture or light. The combination of such a new generation of coatings combined with the intrinsic appeal of bright chrome promises to take future products to the next level of performance.



## **2.6 Hexamethyldisiloxane (HMDSO)**

Hexamethyldisiloxane (HMDSO) is a organosilicon compound with the formula  $O[Si(CH_3)_3]_2$ . This volatile liquid is used as a solvent and as a reagent in organic synthesis. Plasma polymerization can be used to polymerize monomer materials into a polymer film. A great deal of work is being done to integrate plasma polymerization into PVD processing, and this has been implemented. This allows the film deposition processing and plasma polymerization topcoat processing to be done in the same equipment without having to open the system to the ambient. Precursor vapor materials of interest which produce a siloxane coating by plasma polymerization are trimethylmethoxysilane (TMMOS), tetramethyldisiloxane (TMDSO), hexamethyldisiloxane (HMDSO), and methyltrimethoxysilane (MTMOS). The mechanical and electrical properties of the siloxane coatings can be varied by controlling the degree of cross-linking and the degree of oxidation in the film [15]. In the present work, HMDSO is used as layer to promote adhesion properties between the plastic substrate and the metallized layer in some cases and between the metallized layer and the top-coat in other cases. A siloxane is any chemical compound composed of units of the form  $R_2SiO$ , where R is a hydrogen atom or a hydrocarbon group. They belong to the wider class of organosilicon compounds. Siloxanes can have branched or un-branched backbones consisting of alternating silicon and oxygen atoms (-Si-O-Si-O-), with side chains R attached to the silicon atoms [15].

## **2.7 Plasma Treatment of Polymers**

Plasma treatment can be utilized to change the surface tension of a polymer surface. The plasma treatment process can result in an over-treatment condition. In the case of over-treatment, the chemistry of the polymer surface degrades into shorter molecules (fragments) and thus a weak boundary layer is created causing poor adhesion to between the polymer surface and the deposited layer, in this case a thin film. Therefore, it is important to only plasma treat the surface for the required amount of time to achieve the optimal surface energy for maximum adhesion. Some of the gases used to generate a plasma include argon and oxygen. The use of argon is common for bombarding the surface for cleaning purposes. The use of oxygen is plasma allows organics to be converted and volatilized. This allows the cleaning of the organic contamination as well as functionalizing the surface for optimal adhesion deposition of the thin film [16].

The normal chemistry of a polymer contains high levels of carbons and thus the surface energy is fairly low. Therefore, the usage of oxygen allows the increase of surface energy. The plasma treatment removes contaminants and breaks surface bonds to form free radicals that allow the deposited thin film to adhere to the polymer surface better. Oxygen provides the reactant for chemical

recombination that converts the hydrocarbons into volatile species that can be pumped away. Without the oxygen the organic radical group would be sputtered from the surface but most likely would fall back onto the surface and re-contaminate it [18].

It is critical to understand the relationship between plasma treatment and surface tension. Figure 2.2 demonstrates a generic plot of dosage of plasma treatment versus the adhesion and surface tension, which has been categorized into three different zones as follows:

Zone A - Under Treatment

Zone B - Optimum Treatment

Zone C – Over Treatment

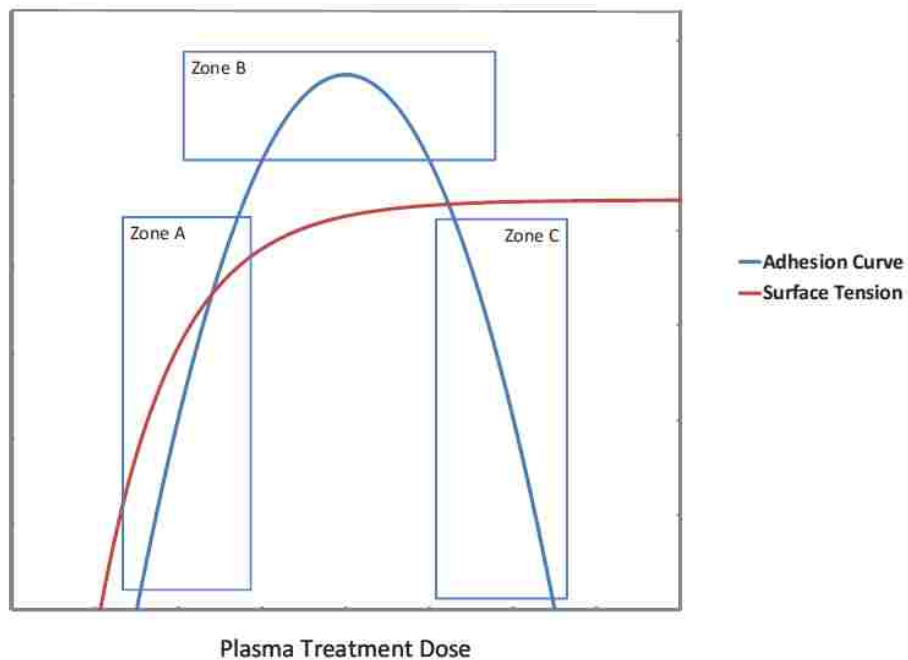


Figure 2.2: Adhesion and Surface Tension of A Polymer Surface Versus Plasma Treatment (all quantities increasing towards the top and right). [18]

In each zone, the surface tension and the adhesion properties of the surface change as described below:

In zone A, the surface contamination is removed and thus the surface tension is increased rapidly. The surface tension is not optimal in zone A and this is considered an under-treatment condition.

In zone B, The surface tension reaches optimal condition to promote maximum adhesion of the polymer surface to the deposited thin film. In this zone, further cleaning of the surface takes place without causing degradation at the interface of the bulk material and the outer surface of the polymer.

In zone C, the over-treatment condition takes place as plasma treatment causes degradation between the polymer surface and the bulk material due to the broken polymer chains responsible for the strength of that interface. However, the surface tension measurements remain the same but the adhesion properties are degraded.

Many applications require the plastic polymer to possess specific criteria based on functionality (physical, electrical and chemical requirements) and life service. These requirements might include; coefficient of thermal expansion, thermal stability, toughness and solvent absorption. However, it is seldom that the adhesion property of the polymer is a deciding factor as there exist ways to change the polymer chemistry [18]. Plasma treatment for modification of polymer surfaces has been used for a variety of applications. For example, treatment of poly(methylmethacrylate) (PMMA) intraocular lenses, used to replace the natural lens of the eye during cataract surgery, imparts hydrophobic properties and minimizes adverse interactions. Treatment of organic fibers used as reinforcement in polymer composites enhances inter-laminar adhesion to organic matrices to improve structural stability. Plasma treatment with nitrogen has been used to improve the adhesion between poly(ethylene terephthalate) (PET) or Nylon-6 tire cord and rubber. Corona discharge improves the adhesion of paint to polypropylene auto bumpers and increases the laundry shrink resistance and color depth in printing of wool fabrics. Golf balls can be plasma treated to prevent paint from chipping [17].

To initiate and sustain plasma, energy must be supplied to free electrons. The electrons interact with atoms and molecules in the gas, leading to fragmentation (dissociation) and ionization. These fragments are highly reactive. Although the probability that an electron-molecule collision will result in dissociation does not increase linearly (and can even decrease) with electron energy, it is generally true in most processing plasmas that higher electron energies will result in greater dissociation efficiencies and, subsequently, higher processing speeds.

Polymers are high-molecular-weight substances that contain repeating units of one or more low-molecular-weight monomers. They can be either linear, branched, or have cross-linked networks. Their origin may be either natural (e.g., proteins and cellulose) or synthetic (e.g., polyimides and polyethylene). [19,20,21].

The adhesion, or bond-ability, between polymer surfaces and other materials deposited onto them can often be related to the wettability as determined from contact angle measurements. Effective plasma modification of polymer surfaces for adhesion enhancement requires a thorough knowledge of the effects of system configuration and processing parameters on the plasma constituents and the effect of these constituents on polymer surfaces.

## 2.8 Mechanical Properties of Thin Films

The mechanical properties of these thin film structures are strongly influenced by micro-structural variables (e.g., average grain size, grain shape, grain size distribution, crystallographic texture, etc...). The hardness of a material is determined by its intrinsic hardness, (the hardness characteristic of the materials in the single-crystal form) and by micro-structural features that affect the deformation mechanisms. Thus, the understanding of a hard material requires detailed knowledge both about the electronic and atomic structure, and about the microstructure of the sample of interest. It is also essential to have a hardness measurement technique that provides reproducible results in order to at least qualitatively compare different samples.

The inter-atomic forces and the crystal structure dictate the intrinsic hardness of the material. Materials with a high intrinsic hardness can be characterized as having high cohesive energy, short bond length, and a high degree of covalent bonding. The strength of inter-atomic forces, and the bonding length plays an important role in determining the elastic properties of a material, and thus, also the hardness. For example, a high elastic modulus implies that the atomic potential wells have a large curvature at the position corresponding to the minimum (the equilibrium atom position) which in turn implies both a deep well and a small bond length. Intrinsically hard material also requires that the resistance to dislocation generation and propagation is high, and that the number of operative slip system is low. A high resistance to dislocation propagation and multiplication can be achieved in materials with a high bond strength. Also, highly directional bonds such as covalent bonds will restrict dislocation propagation. Diamond, the hardest material known, is a completely covalent bonded material. However, many compounds do not have pure covalent bonds, but often contain bonds of mixed character. In general, the hardness decreases as the proportion of covalent bonding decreases [22,23].

The Young's modulus (elastic modulus) of a material is a ratio of stress to strain for the material under elastic (reversible) deformation. Often it is impossible to separate the film from the substrate without altering its properties so the measurements must be made on the substrate. This often influences the properties being measured. Mechanical property measurements of films on substrates are made using beam deflection techniques where the beam is loaded with known weights and the deflection is measured with the stress as the known. Measurements can only be made as long as the film does not microcrack (tension) or blister (compression). Thin films have been shown to have very high elastic modulus and strength, presumably due to surface pinning of mobile defects (dislocations). The indentation test can be used to determine the elastic properties of coatings [23]. There is certainly a need for finding alternatives to the traditional chrome plating technology as it presents health concerns and PVD seems to have gained significant interest as an alternative solution

as it offers an environmentally friendly solution that is cost effective. One of the solutions considers utilizing a base-coat as it is being investigated in the industry. A special focus is directed at the different layers that make-up the desired alternative chrome plating system. Each layer is selected carefully to suitably interact with the next layer and fit the system as a whole. Special plasma treatments are required in some cases to activate the surface and allow the surface energy to be at its maximum level for optimal adhesion of different layers. Thus, extensive work is being conducted by many researchers to find the optimal chrome replacement technology that can meet the appearance criteria and functional requirements [1,8,9].

## CHAPTER III

### MATERIAL, METHODS, & REQUIREMENTS

#### 3.1 Requirements for this Technology

Researchers (including the student), through technical meetings and analysis in conjunction with the Original Equipment Manufacturers (OEM), have attempted to generate a set of specifications for this chrome plating replacement technology. As a result of this work, they identified the following series of tests that were to be applied to the new process for exterior automotive applications:

1. **Appearance Approval** – This standard describes the surface appearance and quality requirements for parts that utilize this technology. The requirements are described in terms of appearance attributes and surface blemishes for each zone within a part. Parts should be free of cracks or any dust particles that are visible to the naked eye. However, it should be noted that appearance is also subjective and in many cases is evaluated with trained personnel for the final approval. The purpose of these requirements is to ensure that the level of final product on vehicles meets or exceeds the level expected by the customers.
2. **Impact Resistance (ASTM D5420: Standard Test Method for Impact Resistance of Flat, Rigid Plastic Specimen by Means of a Striker Impacted by a Falling Weight (Gardner Impact)[24]** - The requirement of this test is to perform an impact test on the finished product and parts should meet a minimum of 80 in-lb of impact. In this test, a weight falls through a guided tube and impacts a striker resting on top of the testing sample. The procedure determines the energy (mass x height x gravity) required to cause a failure.
3. **Adhesion Testing (D3330/D3330M-04 Standard Test Method for Peel Adhesion of Pressure-Sensitive Tape)[25]** – This test is used to evaluate the adhesion properties of the different layers that are formed using this chrome replacement technology. The part is scratched with a cross hatch pattern, then a tape is used to remove the layer being tested.
4. **Water Immersion Resistance (D 870 – 02 Standard Test Method for Testing Water Resistance of Coatings Using Water Immersion)[26]** – In this test, samples are immersed in water (at 40°C) for 10 day. After the exposure, appearance and adhesion properties are evaluated.
5. **Heat Age Testing (no ASTM or SAE reference available)** - In this test, samples are put in an oven at 80°C for 7 days. After the exposure, appearance and adhesion properties are evaluated.
6. **Humidity Resistance (D2247-11 Standard Practice for Testing Water Resistance of Coatings in 100% Relative Humidity)[27]** – This test is used to evaluate the effects of a

high humidity environment on the coating layers. Samples are placed in a humidity chamber with a 99% relative humidity at 40°C for 10 days. After the exposure, appearance and adhesion properties are evaluated.

- 7. Salt Spray (B117-09 Standard Practice for Operating Salt Spray (Fog) Apparatus)[28]**  
– The test is designed to evaluate the resistance of the coated parts after an exposure of neutral salt spray. Samples are placed in a salt bath for 10 days and the appearance of the sample is evaluated. This test gives a good indication for the corrosion resistance properties of the samples. However, samples must pass CASS testing (as described in item number 10) in order to meet the requirements for corrosion resistance of automotive parts.
- 8. Weather Adhesion Cycle Resistance (D6944-09 Standard Practice for Resistance of Cured Coatings to Thermal Cycling)[29]** – This procedure is intended to simulate the different environment cycles (hot, cold, humid, etc) that the product would go through in its lifetime.
- 9. Stone Chip Resistance (ASTM D3170-03 Standard Test Method for Chipping Resistance of Coatings)[30]** – In this test stones are projected at the samples in highway driving conditions to evaluate the resistance properties of the coatings.
- 10. Copper-Accelerated Acetic Acid Salt Spray (CASS) Test (B368-09-03 Standard Test for Copper-Accelerated Acetic Acid-Salt Spray (Fog) Testing)[31]** – This test is used to evaluate the corrosion resistance of samples. The CASS test is widely employed and is useful for specification acceptance, simulated service evaluation, manufacturing control, and research and development. It was developed specifically for use with decorative, electrodeposited nickel/chromium and copper/nickel/chromium coatings. Use of the test has improved the quality of electroplated parts and led to the development of new and superior electroplating processes. Samples are placed in a CASS bath for 96 hours and the appearance of the sample is evaluated.
- 11. Thermal Shock (no ASTM or SAE reference available)** – The samples are subjected to a thermal shock effect to evaluate the adhesion resistance of the technology. Samples are subjected to water immersion for four hours at 38°C while bubbling air at rate of one bubble per second. Samples are removed and a "X" cut is made. Samples are placed in a freezer at -29°C for three hours. Finally, samples are removed from the freezer and a steam blast is directed at the center of "x" cut.
- 12. Water Jet (no ASTM or SAE reference available)** – This procedure is designed to simulate car wash testing where very high pressure water is used that could cause delamination to the coating.

- 13. Accelerated Weather Testing (G 155 – 05a Standard Test for Operating Xenon Arc Light Apparatus)[32]** – This test simulates an accelerated weathering environment where samples are exposed to simulated solar UV radiations. It takes 8 months to complete this test.

### **3.2 Experimental Procedure & Materials:**

The development that is summarized in this thesis follows a series of experiments. The procedure for all the experiments was as follows:

1. Injection Molding: the injection molding process involved utilizing a tool with a highly polished surface to produce the required samples. The material used for molding is polycarbonate plastic which was chosen based on extensive testing to understand the most suitable substrate for this application (see section 4.2).
2. Physical Vapor Deposition: the next step involves metalizing the sample to produce the desired reflective surface. The technique used in this experiment is sputtering deposition. The sputtering process involves physically removing atoms from the “target”, the source material, which are deposited into a substrate. Initially, the pressure of chamber is lowered to vacuum conditions ( $<5\text{mTorr}$ ) where plasma is then generated through the injection of an argon gas with voltage, which generates a plasma. A plasma consists of highly energized particles that accelerate towards the target material and bombard the surface to physically remove target material, which is thrown to deposit on the surface of the substrate [27]. The sputtering process was most suitable for depositing metal on plastic as other techniques, such as thermal evaporation, would distort the polymer as result of high temperature. Also, sputtering deposition provides high deposition rates and is widely used in the industry. In addition, the PVD chamber allowed for plasma pre-treatments and plasma post-treatment to promote adhesion of the metalized layer to a plastic substrate or to promote adhesion of a top-coat to the metallized layer. Some of the gases used in the plasma treatment processes included HMDSO, argon and oxygen in some cases. Plasma treatments use highly energized particle to increase the surface energy and thus promote adhesion.
3. Top-coating: the next step involves providing a clear coat on top of the metalized layer to provide protection to the over-all system and thus meet the functional requirements. The application of the top-coat after metallizing takes place in a clean room environment to minimize dust and any dirt in the hard-coat. The top-coat material was applied using a flow-coating technique. All the top-coat materials are a clear silicone based top-coat which have



good resistance to UV light, good abrasion resistance, and chemical resistance. The coating contains 20% solids and 80% solvents. It has a flashing point of 19.0° C.

It is important to mention that there was one sample per trial produced. Figure 3.1 is a specific process flow diagram for the experiments when utilizing a primer and a thermally cured top-coat. Figure 3.2 is a specific process flow diagram for the experiments when utilizing a UV cured top-coat. The thermal profile for the UV cured top-coat is outlined in Figure 3.3 and the thermal profile for the thermally cured top-coat is outlined in Figure 3.4. The thermal profiles for both of these processes outlined the sample's surface temperature and the surrounding air temperature during the processing of the top-coat.

The surface energy was measured using dyne pens and the methodology for using measuring the surface energy is outlined below [33]:

1. Choose an ACCU DYNE TEST marker pen of a dyne level you believe is slightly lower than that of the test sample. The dyne pens are of 2 dynes / cm increments.
2. Press applicator tip firmly down on subject material until the tip is saturated with ink.
3. Use a light touch to draw the pen across the test sample in two or three parallel passes. Disregard the first pass(es); to flush any contamination from the tip, and to ensure that the test fluid layer is thin enough for accurate measurement, evaluate only the last pass.
4. If the last ink swath remains wetted out on the test sample for three seconds or more, repeat steps 2 and 3 with the next higher dyne level marker. If the last ink swath beads up, tears apart, or shrinks into a thin line within one second or less, repeat steps 2 and 3 with the next lower dyne level marker. If the ink swath holds for one to three seconds before losing its integrity, the dyne level of the marker closely matches that of the sample.

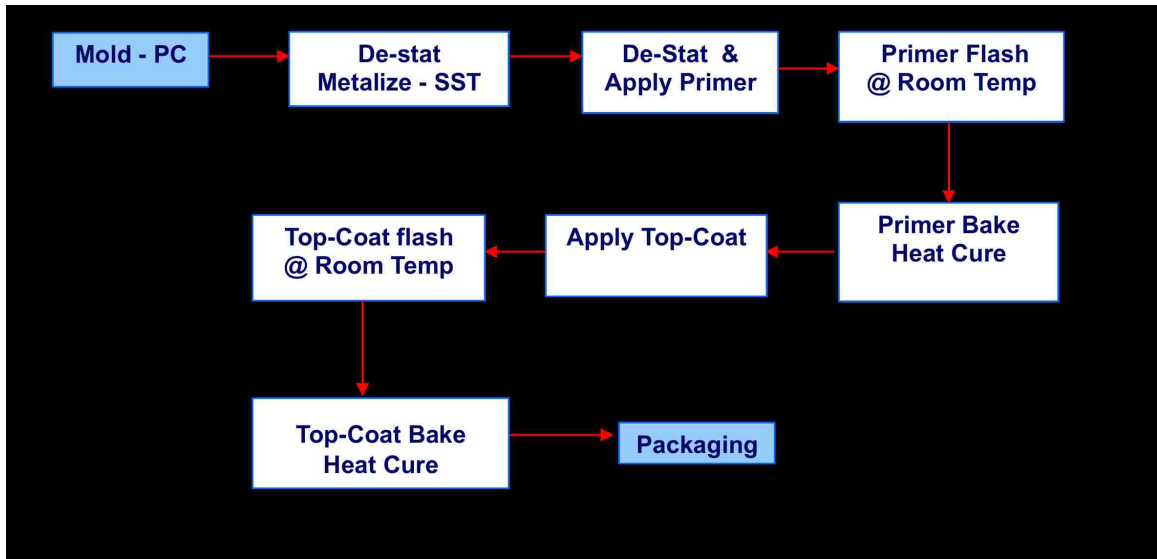


Figure 3.1: Process Flow with a Thermally Cured Top-coat System. Note that RT refers to room temperature conditions.

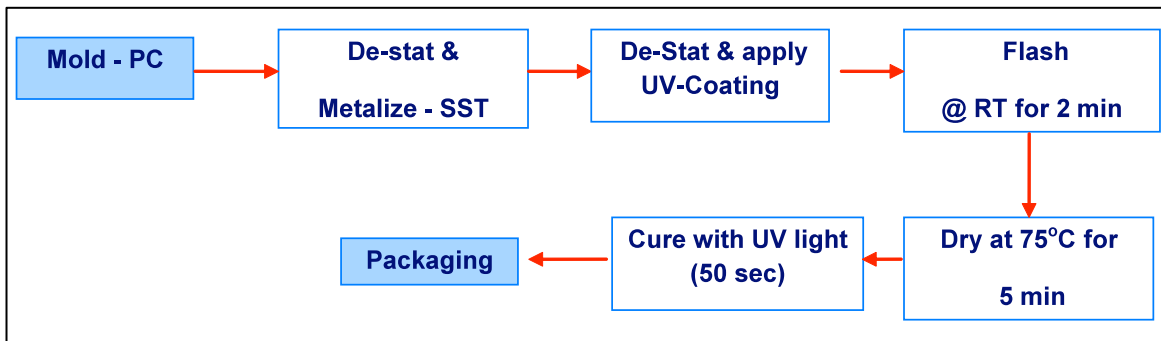


Figure 3.2: Process Flow with a UV Cured Top-coat System. Note that RT refers to room temperature conditions.

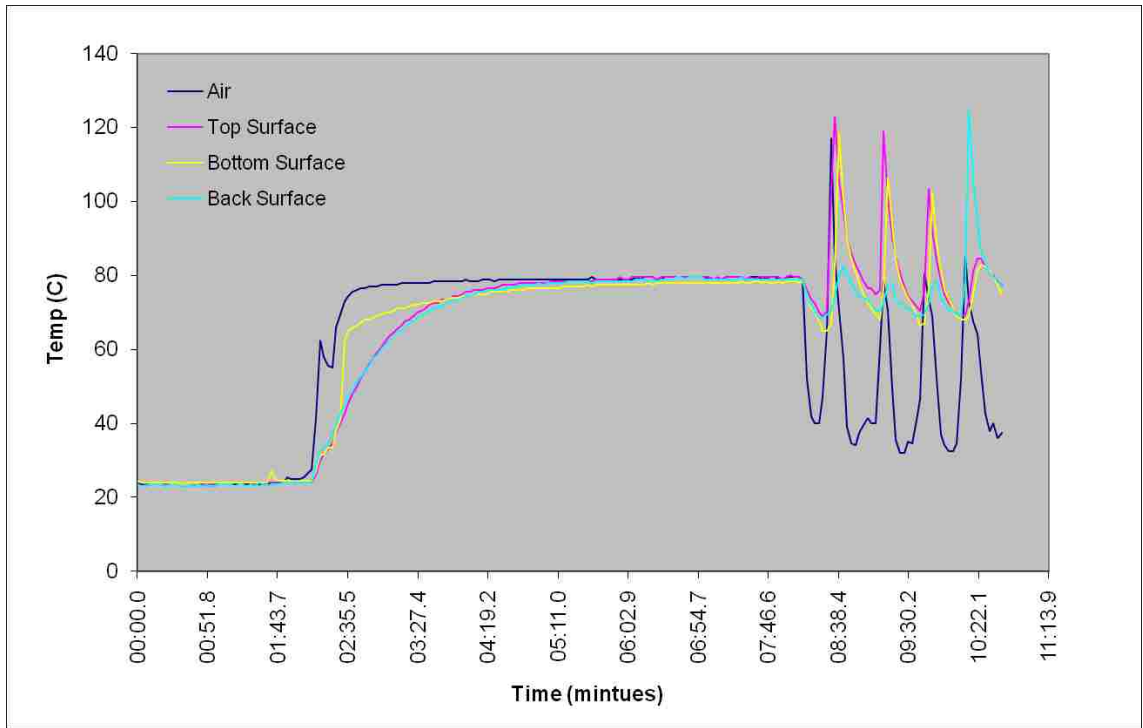


Figure 3.3: Thermal Profile for the UV Cured Top-coat System. Note that the increase at 8:38.4 is a result of entering the UV oven. From 8:38.4 to 11.13.9 minutes, repeated doses of the UV radiation are taking place.

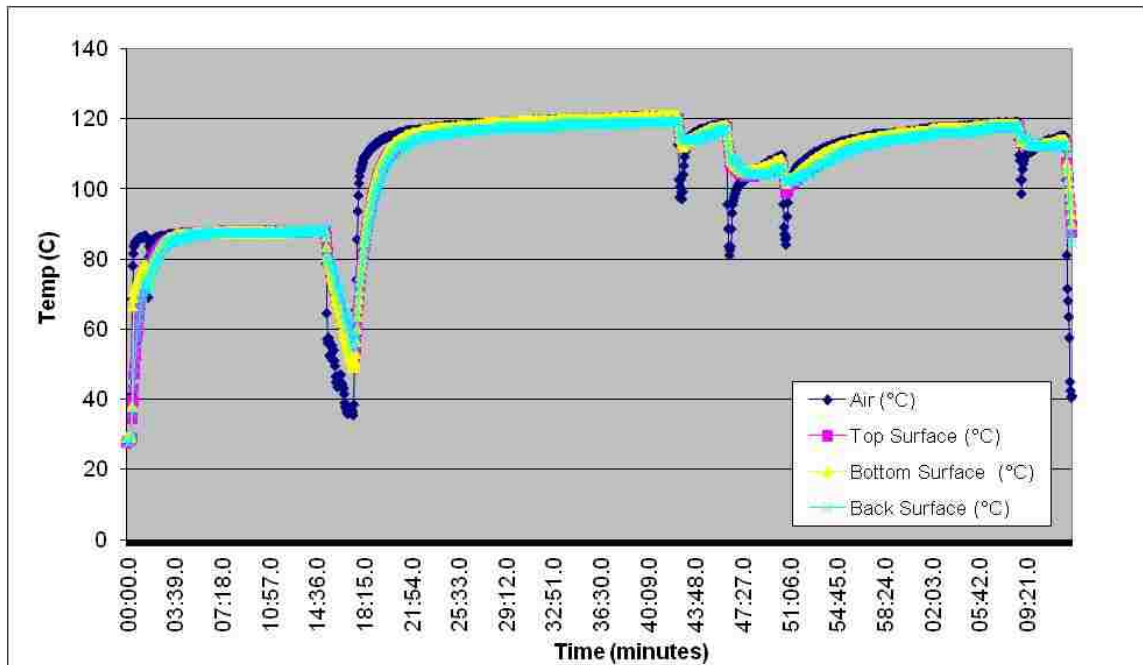


Figure 3.4: Thermal Profile for the Thermal Cured Top-coat System. Note that the increase of temperature to 80°C at 3:39.0 is a result of entering the curing oven for the primer. The increase of temperature to 120°C at 18.15.0 is a result of entering the curing oven for the top-coat.

### 3.3 Analytical I Techniques

During the sample analysis, analytical techniques were used to better identify the failure mode and understand the root cause of the problem. The following is a summary of techniques used:

1. Scanning Electron Microscopy with Energy Dispersive X-ray (SEM/EDX) Spectroscopy: Scanning electron microscopy (SEM) is widely used for surface analytical techniques. High resolution images of surface topography, with excellent depth of field, are produced using a highly-focused, scanning (primary) electron beam. SEM, accompanied by X-ray analysis, is a non-destructive approach to provide information about surface composition. The instrument used was the FEI Quanta 200 FEG microscope.
2. Fourier Transform Infrared (FTIR) Spectroscopy: is a technique which is used to obtain an infrared spectrum of absorption, emission, photoconductivity or Raman scattering of a solid, liquid or gas. An infrared spectrum of a sample is made by reflecting a beam of infrared light off of the surface of the sample. The infrared light is absorbed at specific frequencies representing the vibrations of bonds or groups in the molecule. This technique is of interest as it provides useful information about organic or inorganic coatings. The instrument used was Bruker IFS 55.

## CHAPTER IV

### INITIAL DEVELOPMENT AND EARLY RESULTS

#### 4.1 Initial Development and Early Results

In the initial experiments for the attempt to produce a chrome replacement system, the different operations (that is: molding, metallizing, and top-coating) took place in different locations based on the services provided. This meant that molding of the samples was performed at one location and the samples were sent to the metallizing facility in a different location where the samples were metallized and sent to yet a third location for hard-coating.

For the purposes of this work, this thesis focuses on the experiments that took place with all operations (that is: molding, metallizing, and top-coating) being carried out at one specific location. This allowed for better observations of all the steps and thus better analysis of the system capability. In addition, a study was conducted to understand the surface energy changes as time passed. This study proved that samples have the highest level of surface energy immediately after metallizing the plastic part, and thus adhesion is promoted easier. As time passes by and the metallized layer interacts with atmosphere, the surface energy drops. The surface energy was measured using dyne pens testing: see Figure 4.1 for surface energy values as a function of time. It is measured that the surface energy of the metalized layer is at its highest when first metalized. As time after metallizing passed by, the surface energy of the metallized layer decreased.

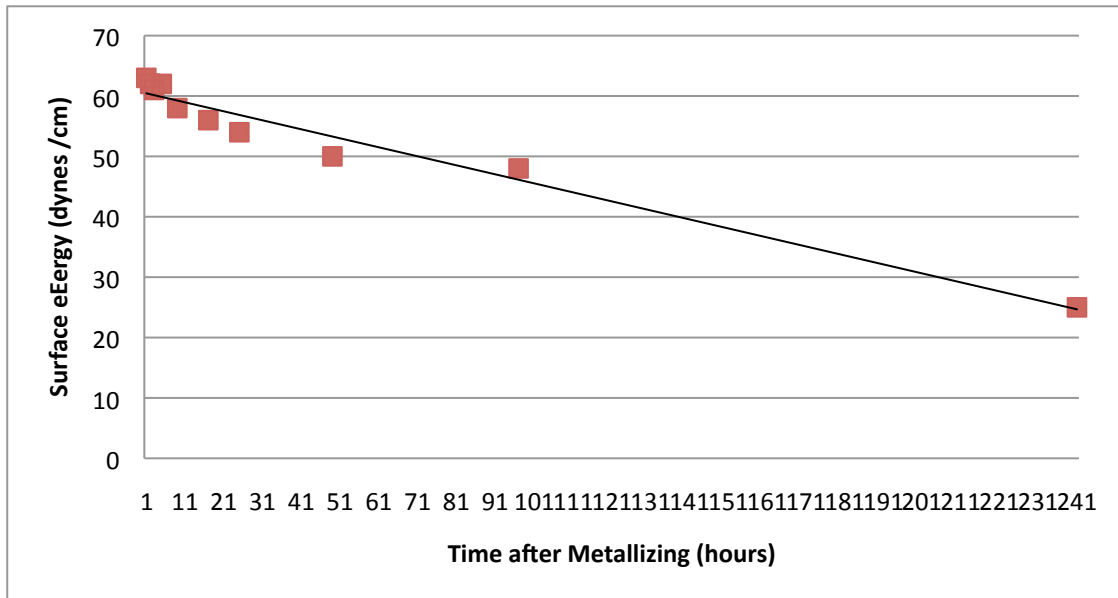


Figure 4.1: Surface Energy as a Function of Time for Metalized Layer of Aluminum

## **4.2 Substrate Selection – Polycarbonate**

Some of the critical properties that are required for the plastic substrate include the following:

- The plastic material should provide a glossy appearance after molding.
- The material should have a minimal amount of additives in it as these materials will out-gas (which is the release of low molecular weight components) during the low pressure conditions of metallization. The out-gas can be classified as "volatile" or "condensable". Volatile out-gassing consists of lower molecular weight gaseous components, such as odorants. Condensable out-gassing refers to components that are driven off under heat or ambient conditions, and which condense on relatively cooler surfaces forming an oily, waxy or solid deposit, which may be perceived as a haze or film. The absence of additives in the polycarbonate also helps with the adhesion of metal directly into the polycarbonate surface.
- The impact properties of the material should be sufficient to pass the specified requirements (ASTM D5420).

The initial development also involved determining the specifics of the most suitable layer and its interactions with the surrounding layers. For example, different plastic substrates ( polycarbonate, Acrylonitrile butadiene styrene, Poly(methyl methacrylate), and Nylon) were metallized with different metals (aluminum, chromium and stainless steel) to examine the initial appearance and the adhesion of the metallized layer to the substrate. Through these runs, it was determined that polycarbonate was the choice for the plastic substrate as it provides the initial functional requirements ( i.e. impact resistance properties ) along with a good base for adhesion of the metallized layer to the substrate.

## **4.3 Adhesion of the Metalized Layer as a Function of Time**

A study was conducted to examine the affects of film build on adhesion of the metallized layer to the polymer surface. Figure 4.2 shows the effects of increasing sputtering time, which is essentially film thickness, on adhesion. It should be noted that the sputtering material was aluminum.

It was observed that as film thickness increases, adhesion is lost. This is likely because film build usually is associated with a rise in the stress level within the film. However, changing the target material for the metalized layer could change the level of the initial adhesion.

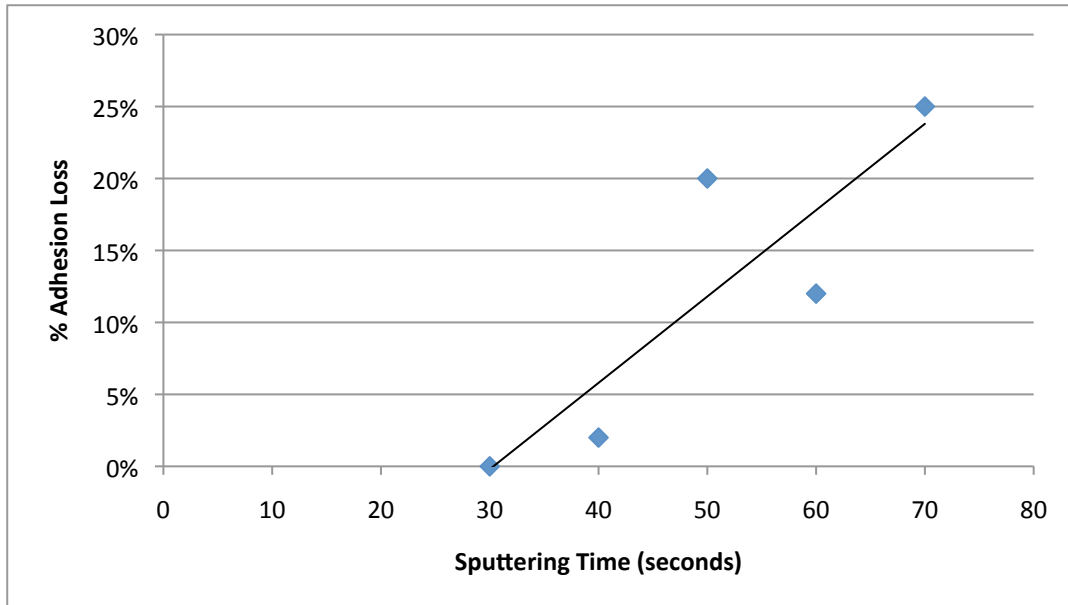


Figure 4.2: % Adhesion Loss vs. Sputter Time. Note that adhesion loss is determined by method in section 3.1[17]

#### 4.4 Ultraviolet Light Transmission Study

It is known in the industry that a polycarbonate plastic substrate requires UV protection when it is placed on the exterior of the vehicle, and thus it needs a coating that filters the harmful UV radiations [34]. It is critical to understand the capability of the metallized layer and the top-coat to protect the polycarbonate plastic substrate.

The following study was conducted to understand the protection provided in this system. In this study, clear plastic parts were used and they were coated with different thicknesses of the metallized and/or top-coat layer. A UV light, with wavelengths between 300nm and 400 nm (harmful range), was focused on the different samples and the light transmission at the opposite end of the sample was measured. Figure 4.3 represents a topographical map of light transmission (as a percentage) as a function of wavelength and film thickness for the metallized layer alone. A top view of Figure 4.3 demonstrates the amount of harmful radiation passing through at various thicknesses, which is shown in Figure 4.4. Thus, it is shown that below 360 angstroms of metal thickness, less than 2% of the UV radiation at a wavelength range of 300-400 nanometers, penetrate through to the substrate. It should be also noted that a wavelength of 315nm, there is greater than 2-4% penetration at a film thickness of about 360 angstroms.

Figure 4.5 represents a topographical map of light transmission (as a percentage) as a function of wavelength and film thickness for the metallized layer and the top-coat. The top-coat thickness was

measured to be in the 7-9 microns. A top view of figure 4.5 demonstrates what harmful radiations are passing through at what thicknesses, as shown in Figure 4.6. The top-view proves that all harmful UV radiations are blocked by the metallized layer and the top-coat. The only wavelength range that makes it through is in the range of 373nm to 400nm at a percentage of below 10%, given that the metallized layer thickness is below 400 angstroms. This study demonstrates that the harmful UV radiations are blocked. While this is not an accelerating weathering testing, it can be used to screen out systems that have only metal at a thickness less than 560 angstroms.



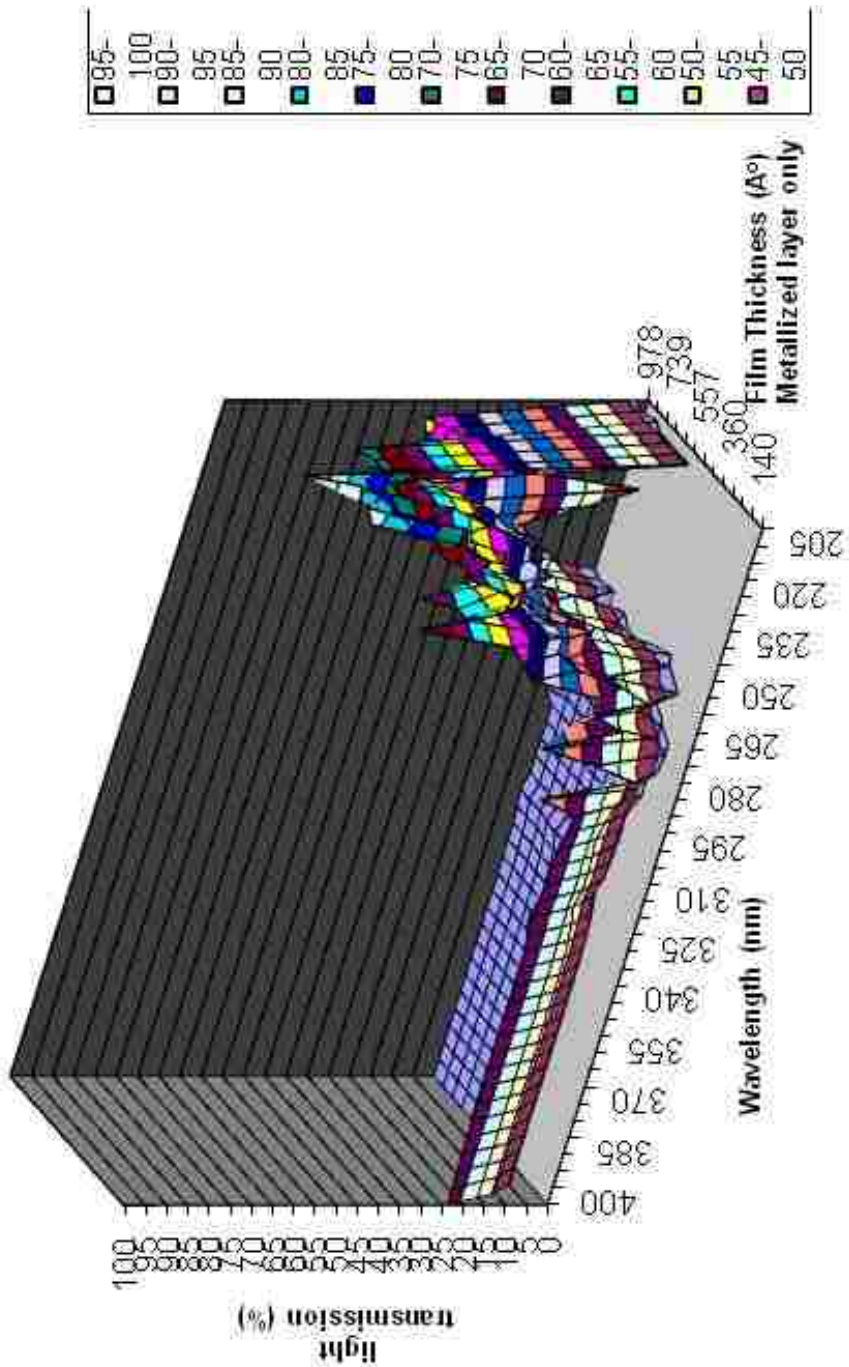


Figure 4.3: Topographical Map of Light Transmission Data for the Metalized Surface Only

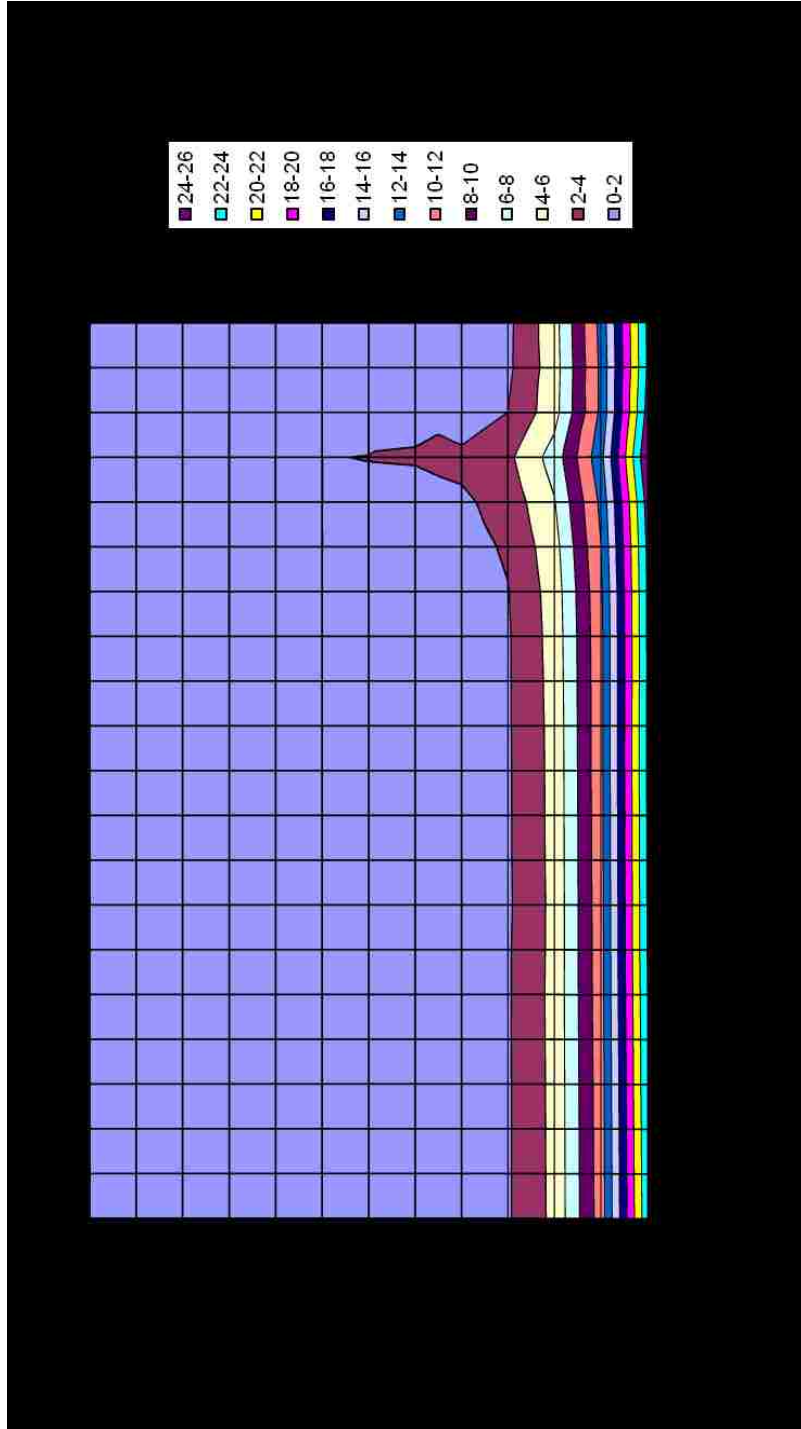


Figure 4.4: Top View of Light Transmission Data for the Metalized Surface Only

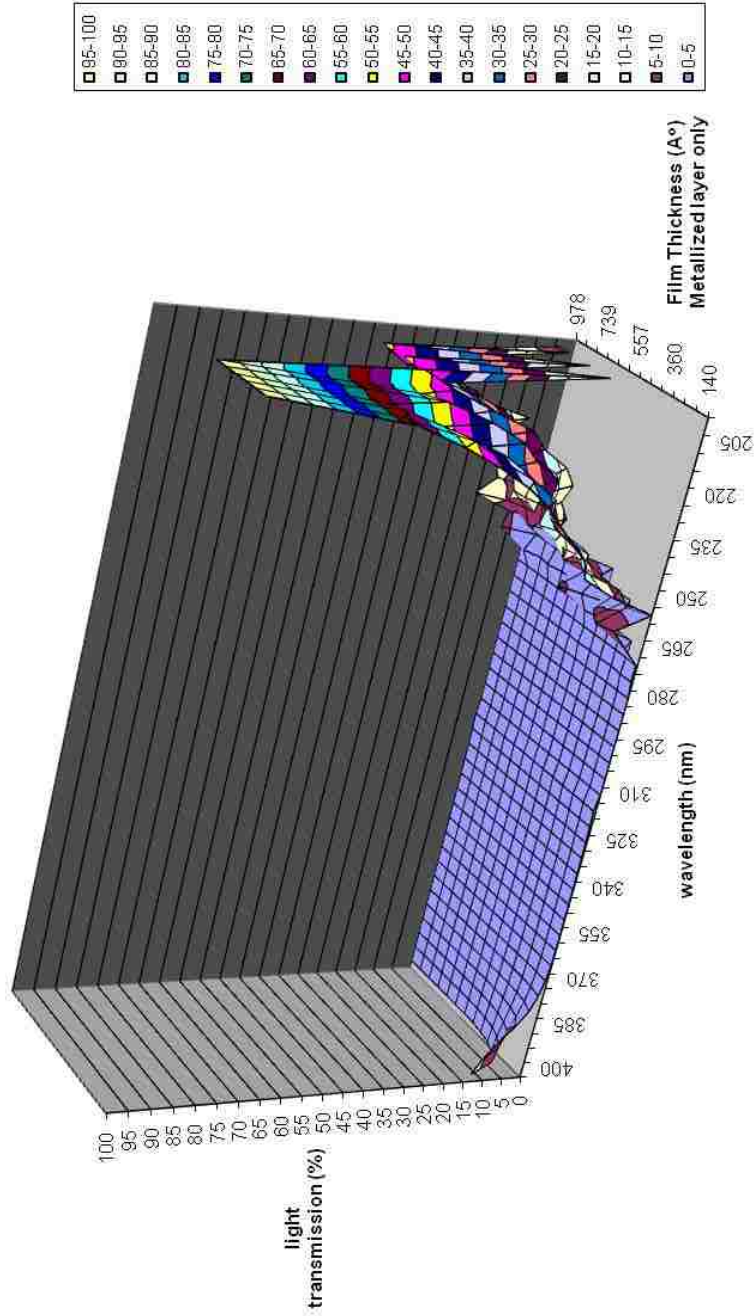


Figure 4.5: Topo-graphical Map of Light Transmission Data for the Metalized Surface & Top-coat. Note that the top-coat thickness is 7-9 microns.

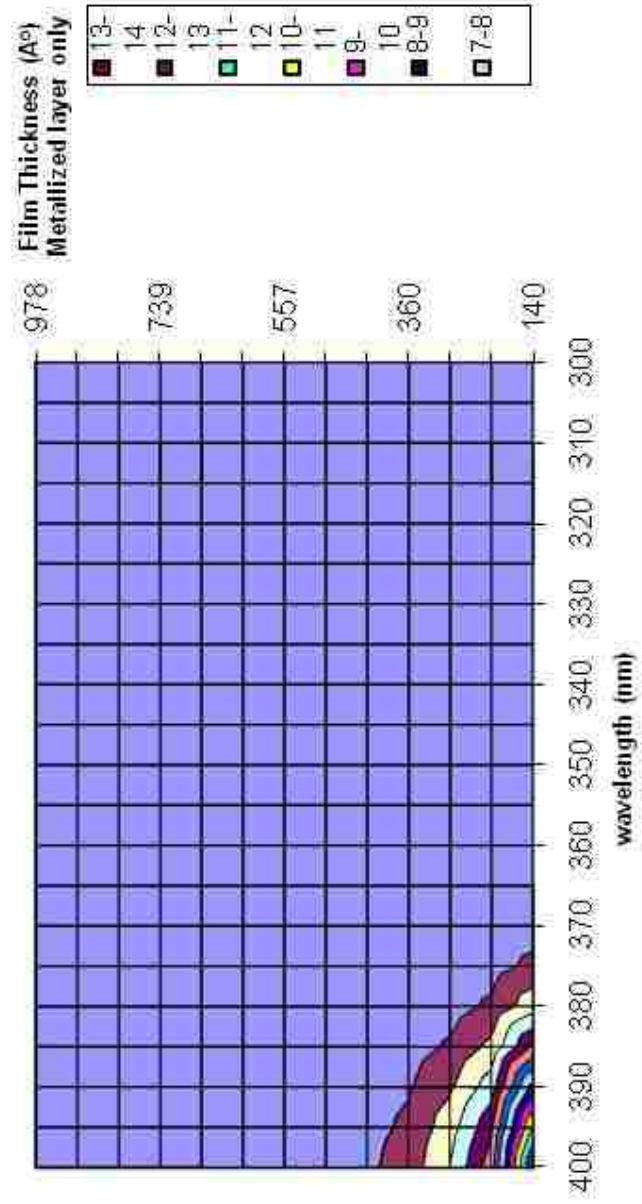


Figure 4.6: Top View of Light Transmission % Data for the Metalized Surface & Top-coat

#### 4.5 Iridescence Appearance

Iridescence is an effect caused by the interference of light waves resulting from multiple reflections of light off of surfaces of varying thickness. This visual effect can be detected as a rainbow pattern on the surface of soap bubbles and gasoline spills, and in general, on surfaces covered with thin film diffracting different frequencies of incoming light in different directions.

When coating the metallized layer with the hard protective organic top-coat and based on the metallized layer used, an iridescence phenomena (rainbow effect) is evident, see Figure 4.7. Top-coating produces a considerably more noticeable iridescence effect on a stainless steel metallized sputtered layer than an aluminum layer. The main cause of the iridescence is the mis-match between the index of refraction between the metallized layer and the top-coat as well as thickness variations in the top-coat layer. It should be noted that iridescence is seen under fluorescent lighting mainly and is largely eliminated under sun light. This iridescence effect is a subjective evaluation and the acceptance criteria is really based on the personnel evaluating the sample.

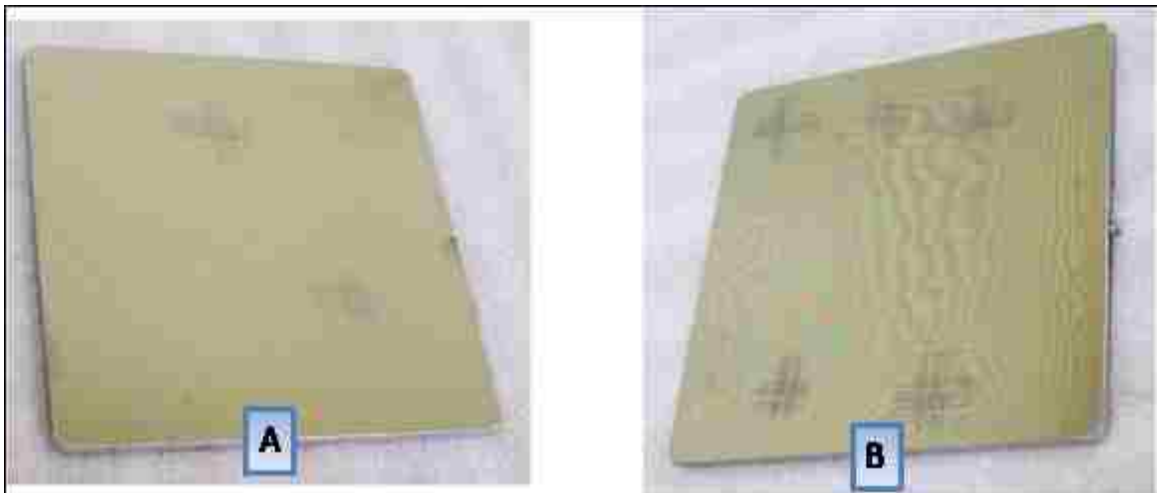


Figure 4.7: Iridescence Effect. A) sample before top-coating. B) sample after top-coating

## CHAPTER V

### SYSTEM “A” DEVELOPMENT AND RESULTS

#### 5.1 System “A” Introduction

System “A” consists of polycarbonate as a substrate, stainless steel as a metalized layer, a primer as an adhesion promoter, and a protective clear top-coat. The development for this system involved 5 stages; each stage is composed of an experiment, as shown in Figure 5.1. Each stage focuses on addressing the issues uncovered in the previous stage, which are summarized in this chapter.

Figure 5.1 outlines the 5 different stages of the development for system “A”. Stages 1,2 and 3 involved development of primer-A and stages 4 and 5 involved development of primer-B and primer-C.

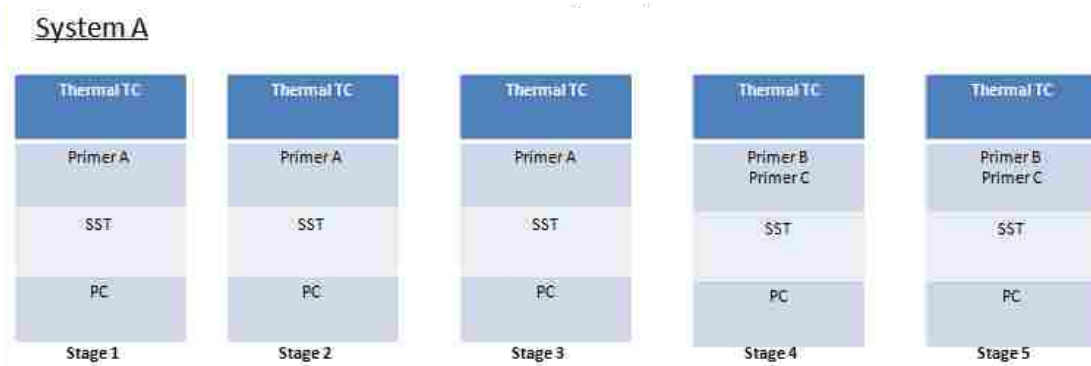


Figure 5.1: System “A” Development Stages

Samples were produced using the procedure outlined in section 3.2 “Experimental Procedure”. Sections 5.2–5.6 report the most important results of each stage.

#### 5.2 Stage-1 of System “A” Development

The following sub-sections will summarize the objective, observations, data, results, and conclusions for stage-1 of development for system-A.

##### 5.2.1 Objective

The main objective of this stage was to mold a polycarbonate substrate, metalize it with a stainless steel metalized layer, apply a primer for promoting adhesion and finally apply a thermally cured top coat. The secondary objective of this stage was to perform all steps, involved in producing samples for system-A, without any significant time intervals between the different processes. More specifically, molding, metallizing, applying primer and applying the top-coat needed to be performed in-line. This stage determined the initial feasibility for producing system-A. The first experiment for

system-A involved utilizing primer-A to promote adhesion between the metallized layer and the top-coat. Primer-A is a solvent based primer.

### **5.2.2 Observations / Data / Results**

Table 5.1 summarizes all runs tried in stage-1 of system-A development. Table 5.2 summarizes the different solvents for primer-A. All solvents used are alcohol based solvents. Runs W-A through W-G represent the usage of different primer formulations during stage-1.

#### **5.2.2.1 Primer Aging**

It was observed that the samples formed a hazy appearance after the application of the top-coat on the primer. The humidity in the clean room was low ( 27 % RH ) which might have caused the top coat to flash off quickly resulting in an appearance issue. Thus, % solids were reduced in stage-2 in an attempt to reduce the haze. The % solids for the top-coat were reported to be 18.5% as measured during the actual trial (the manufacturer recommended range is 18% +/- 3).

Thus, different parameters were changed including percentage of elements (i.e. DI Water) in the primer-A formulation in order to address the hazy appearance issue, as shown in Table 5.2. W-A and W-B have the same formulations with the exception of the solid levels. W-A contains 1.05% while W-B contains 0.8%. W-C has a higher level of DI water and 0.93% solids. W-D contains 3.9 DI water and 1.05% solids. W-F and W-G do not have any solvent-B with a 1.0% solids composition. Finally, based on the appearance of the samples, it was concluded that aging the primer is the correction factor to this haze. Aging of the primer is defined by allowing the mixture of the solvents and solids to settle for 24 hours after everything was mixed, before the usage of the primer. It is speculated that when the primer was applied without allowing it to age, the solids were not fully dissolved in the solvents resulting in a foggy or hazy appearance.

#### **5.2.2.2 Micro-cracking**

Micro-cracking of the metallized layer was seen on certain parts as the top-coat was applied and cured, see Figure 5.2. After closely examining the parts and micro-cracking, it was concluded that certain parts had internal stress. As the parts were cured after applying the coating at 125C, the internal stresses were allowed to be released as a result of annealing. Thus micro-deformation of the part causes the metallized layer to deform and thus micro-crack the metallized layer [35].

### **5.2.2.3 Testing Results**

The initial testing results for stage-1 of the development for system-A are shown in Table 5.3. It should be noted that all the different primer formulations passed the initial adhesion testing.

The heat age, humidity resistance and water immersion tests were the prerequisites for the complete performance requirements. Based on the results in Table 5.3, it is observed that there is a major appearance defect and it is not caused by heat exposure as all samples meet specifications for the heat age test. This appearance defect appears in all water immersion tests and is referred to as “spotting”. See Figure 5.3.

Water Immersion tests for samples that have sealed edges (no matter what the primer formulation was) had an appearance defect as well which illustrates that moisture undercutting through sharp edges of the sample is not the cause of the problem. Also, water immersion tests for a sample with PC/SST/top-coat -A- with no primer, has acceptable appearance after water immersion testing which demonstrates that the primer is the main cause of this issue. However, the primer is necessary to promote adhesion between the stainless steel metallized layer and the top-coat. It should be noted that samples that were exposed to the atmosphere for 12 hours, after metalizing, and then coated failed the initial adhesion testing. This suggested that the in-line, where moulding, metalizing, applying a primer and finally the top-coat without any significant time intervals (under two hours), is a critical process for maximum adhesion between the layers.

### **5.2.2.4 Fourier Transform Infrared Microscopy (FTIR)**

Studies were conducted to better understand the root cause of the appearance defect that was seen as “spotting” after water exposure. Fourier Transform Infrared Microscopy (FTIR) was performed on areas of the samples with spotting and without spotting. Figures 5.4 & 5.5 demonstrate the FTIR spectrums to show the band differences. The FTIR results show the formation of Polydimethylsiloxane (PDMS) elements as a result of moisture exposure, this is seen as spotting, which is potentially a result of an external hydrophobic surface element.

### **5.2.3 Main Conclusions**

- The process of molding, metalizing & top-coating in-line has proven beneficial, as it promoted adhesion between the different layers, to the chrome replacement system.
- Aging the primer before applying it to the metallized layer is suggested to be a critical stage. It is speculated that this aging step allows the solids to fully dissolve in the primer solution, mainly the solvents, and thus eliminate the hazy appearance defect.



- Initial tape pull adhesion performed on all PC/SST/Primer + top-coat “A” passed no matter what the primer composition was.
- Metallized stainless steel parts that were exposed to the atmosphere for 12 hours and then top-coated, failed initial pull tape adhesion.
- Water immersion samples for the PC/SST/Primer- + top-coat “A” system had an appearance defect described as “spotting”. The main cause of the “spotting” is the interaction of the primer with moisture.

Table 5.1: Process Parameters – Stage-1 of System-A. Note that sccm = standard cubic centimeters per minute

Run	Metallization - SST		Primer A - formulations							Primer A		Top coat A	
	Argon Flow (sccm)	Sputter Time (seconds)	W-A	W-B	W-C	W-D	W-E	W-F	W-G	Bake Time (min)	Bake Temp (oC)	Bake Time (min)	Bake Temp (oC)
W-A	150	50	x							5	80	45	125
W-B	150	50		x						5	80	45	125
W-C	150	50			x					5	80	45	125
W-D	150	50				x				5	80	45	125
W-E	150	50					x			5	80	45	125
W-F	150	50						x		5	80	45	125
W-G	150	50							x	5	80	45	125

Table 5.2: Formulations for Primer-A – Stage-1 of System A. Note that solvent A and Solvent B are both alcohol based solvents

Component	W-A	W-B	W-C	W-D	W-E	W-F	W-G
-----------	-----	-----	-----	-----	-----	-----	-----

Solvent A	65.0%	65.0%	63.6%	63.7%	63.8%	94.4%	95.9%
DI Water	2.6%	2.6%	4.9%	3.9%	5.0%	4.5%	3.0%
Solvent B	31.4%	31.7%	30.6%	31.4%	30.2%		
primer A	1.05%	0.80%	0.93%	1.05%	0.99%	1.06%	1.07%
total:	100.0%	100.0%	100.0%	100.0%	100.0%	100.0%	100.0%

Table 5.3: Heat Age and Water Immersion Results. Note that TCA refers to top-coat “A”. Note that all samples passed initial adhesion with all primer formulations.

Test	Material	Conditions	Duration	fail	pass	comments
Heat age	PC/SST/primer-A + TCA WA, WB, WC, WD, WE, WF, WG & no primer sample	82°C	7 days		x	Appearance and adhesion pass
Water Immersion	PC/SST/primer-A + TCA WA	40°C	10 days	x		appearance defect
Water Immersion	PC/SST/primer-A + TCA WB	40°C	10 days	x		appearance defect
Water Immersion	PC/SST/primer-A + TCA WC	40°C	10 days	x		appearance defect
Water Immersion	PC/SST/primer-A + TCA WD	40°C	10 days	x		appearance defect
Water Immersion	PC/SST/primer-A + TCA- WE	40°C	10 days	x		appearance defect
Water Immersion	PC/SST/primer-A + TCA - WF	40°C	10 days	x		appearance defect
Water Immersion	PC/SST/primer-A + TCA WG	40°C	10 days	x		appearance defect
Water Immersion	PC/SST/Primer-A + TCA WA sealed edges	40°C	10 days	x		appearance defect
Water Immersion	PC/SST/ TCA - no primer	40°C	10 days		x	no appearance defect - but adhesion loss

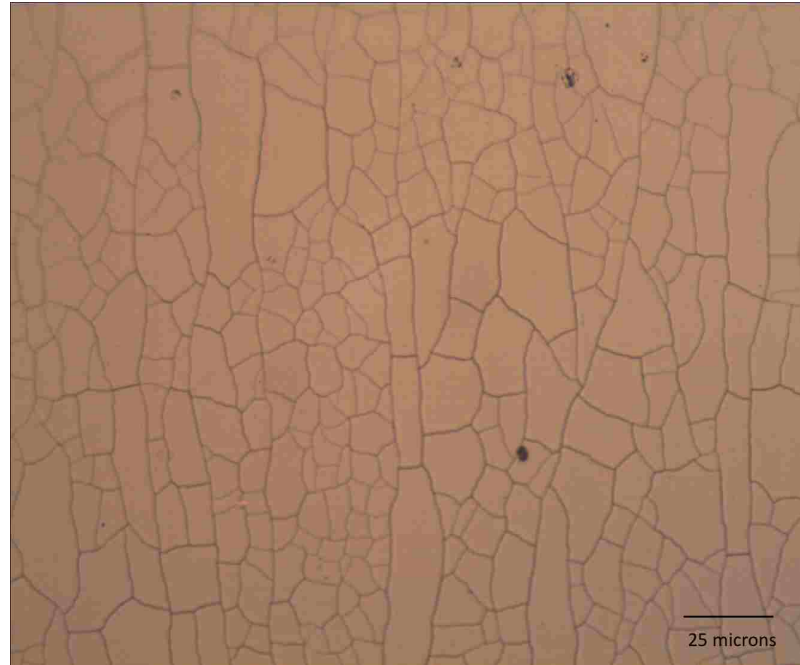


Figure 5.2: Optical Imaging of Micro-cracked Metalized Surface - X200

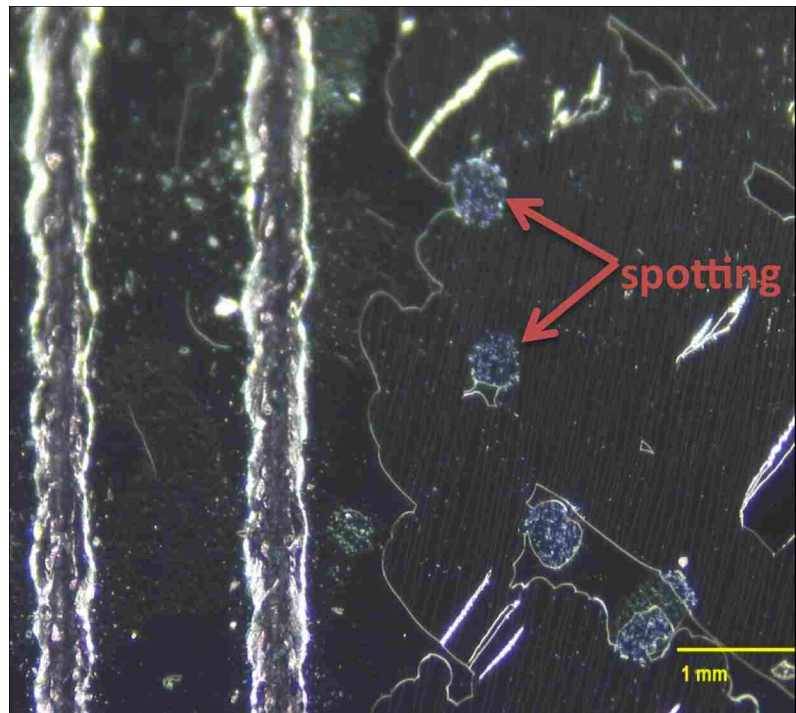


Figure 5.3: Optical Imaging of “Spotting” After Water Immersion Testing.  
Note: the top-coat is coming off as a result of adhesion pull.

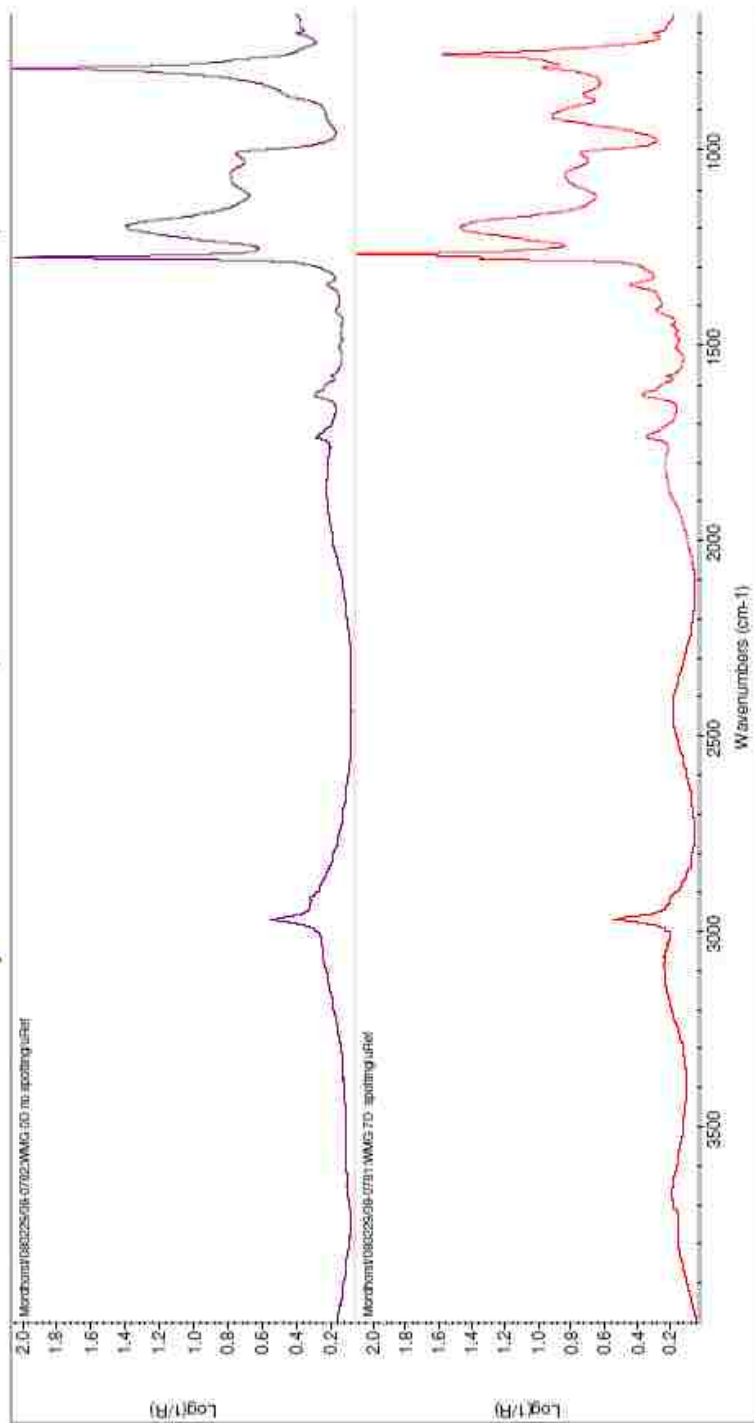


Figure 5.4: FTIR of Water Spotting Versus No Water Spotting

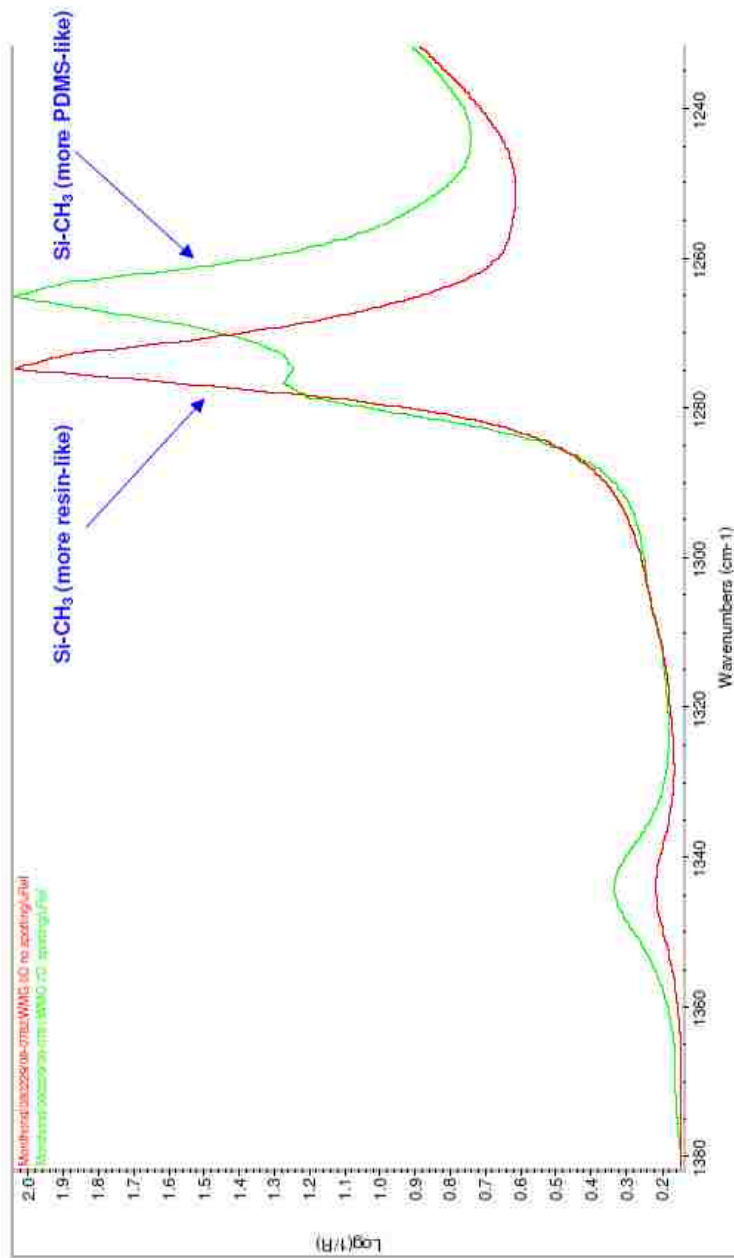


Figure 5.5: FTIR of **Water Spotting** Versus **No Water Spotting**. Enlarged from Figure 5.4

### **5.3 Stage-2 of System “A” Development**

In stage-2, the process steps utilized were the same as of those in stage-1 as outlined in section 3.2.

#### **5.3.1 Objective**

Based on the results of stage-1, stage-2 was focused on correcting the appearance defect and the moisture related failures in stage-1. Different variables were changed to best optimize this experiment and examine variables that could be the root cause of this failure. Some of the variables that were examined are:

- 1) Substrate (aged PC, fresh PC & PBT)
- 2) Metallized Layer (different film thicknesses)
- 3) Primer (only primer-A)
- 4) Primer Bake Time (different primer bake times)
- 5) Primer Solid Levels (various solid levels in the primer)

#### **5.3.2 Observations / Data / Discussion**

The primer formulation matrix in Table 5.4 shows a detailed percentage composition of each element of the primer. It is important to note that all primer-A used in this run was prepared the day before the tryout as this step was found to be beneficial to the process ( see section 5.2.2.1 Primer Aging ). The differences between WA-1, WA-2 & WA-3 are the difference in solid levels which are 0.5%, 0.75% and 1.0%, respectively. The variations in the solid levels for the primer will allow us to understand its effects on appearance and adhesion. WA-4 is prepared with equal amounts of solvents to see how this affects the flash off time and thus the appearance and the haze. The boiling points for solvent A and solvent B are 121°C and 78°C respectively. Thus, the higher the percentage of solvent B, the quicker the evaporation (flash off) of the primer resulting in appearance defect that appear as flow strikes. However, solvent A has too high of boiling temperature for it to be used by itself.

Each parameter was examined at different stages to optimize the process. Table 5.5 was created to summarize all the runs. Samples 1 through 23 were produced on the first day of the stage. In these samples, old and freshly molded parts were evaluated using different primer formulations under two different primer bake times. The initial adhesion was acceptable for all these samples. Samples were then submitted to a 16 hour water immersion test at 40°C. The appearance was acceptable with all samples however the adhesion results were as shown Table 5.6.

It can be seen that any samples with 5 minutes bake time (runs 1 and 9-20) for the primer do not pass adhesion tape pull after water immersion.. Furthermore, higher film thickness of the top-coat had better results as film build seems to prevent permeation of moisture to the metallized layer and substrate (runs19-22). Samples 24 through 29 were submitted to water immersion. The results are summarized in Table 5.7. Samples 24 – 29 definitely show some improvements in terms of being able to identify the critical variables. In this run, different primer bake times were examined to eliminate the 30 minute bake time for the primer. The results for 10 minutes seemed to be border line, 15 minutes showed some positive encouraging results, and 30 minutes seemed to cause some failures because of the high temperatures. Table 5.8 summarizes the number of samples that completely failed, marginally failed and met specification based on bake time. Thus, the 15 minutes bake time is the performed the best because it had no failures. An important note to make here regarding the consistency of keeping the oven temperatures at the desired range. The data recorder showed that it takes about 5 minutes for the surface temperature to reach the required temperature and there is some heat loss as oven door is closed/opened which translates into a 5 to 10°C decrease that takes 5 minutes to make up. Also the primer bake oven never achieved 100°C as it was supposed to and the temperature went up to 92°C only. Considering the sensitivity of this operation stage (primer bake temperature & time), the bake temperature and time were closely monitored in the next stages. However, the appearance of all the noted samples in Table 5.6 and 5.7 did failed the appearance requirement after the water immersion test as they exhibited , spotting, that was described in stage-1. The results indicate that the main factors for adhesion failures are:

- 1) primer bake temperature
- 2) primer bake time
- 3) film thickness
- 4) % Solid in primer

### **5.3.3 Main Conclusions**

- Although the primer bake time of 5 minutes have shown initial positive results (stage-1). However, the 24-hour water immersion test is causing a top-coat / metallized layer failure.
- The appearance defect, spotting, was observed in stage-2 after the water immersion test.
- There seemed to be a lot of “border-line” results that might conflict with each other.
- A 15 minute primer bake time was best for initial adhesion.

Table 5.4: Primer Composition – Stage-2 of System-A

Component	WA-1	WA-2	WA-3	WA-4
Solvent A	65.0%	65.0%	65.0%	48.3%
DI Water	2.5%	2.5%	2.5%	2.5%
Solvent B	32.0%	31.8%	31.5%	48.4%
Primer A	0.51%	0.75%	1.00%	0.75%
total:	100.0%	100.0%	100.0%	100.0%



Table 5.5: Process Parameters for Stage-2 of System-A – Note that the top coat for all the samples was cured at 125C for 45 minutes

Run	Substrate	Metallization		Primer formulation				Primer bake	
	Polycarbonate	Argon Flow	Sputter Time	W/A-1	W/A-2	W/A-3	W/A-4	Bake Time (min)	Bake Temp °C
1	x	150	50	x				5	80
2	x	150	50		x			5	90
3	x	150	50			x		5	90
4	x	150	50				x	5	90
5	x	150	50	x				30	90
6	x	150	50		x			30	90
7	x	150	50			x		30	90
8	x	150	50				x	30	90
9	x	150	50	x				5	90
10	x	150	50		x			5	90
11	x	150	50			x		5	90
12	x	150	50				x	5	90
13	x	150	50	x				5	40
14	x	150	50		x			5	40
15	x	150	50			x		5	90
16	x	150	50				x	5	90
17	x	150	50			x		5	90
18	x	150	50				x	5	90
19	x	150	80		x			5	90
20	x	150	80				x	5	90
21	x	150	80		x			30	90
22	x	150	80				x	30	90
23	x	150	50		x			30	90
24	x	150	50			x		10	90
25	x	150	50			x		15	90
26	x	150	50			x		30	90
27	x	150	50			x		10	100
28	x	150	50			x		15	100
29	x	150	50			x		30	100

Table 5.6: Summary of Tape Pull Adhesion After 16 Hr Water Immersion for Stage-2 System-A. Note: TC/SST refers to the interface between the top-coat and the stainless steel layers. SST/PC refers to the interface between the stainless and polycarbonate layers

Run	Film Thickness (µm)		Tape Pull After short water-immersion		Failure Interface	
	top	bottom	top	bottom	TC/SST	SST/PC
1	4.1	5.7			x	
5	3.9	4.9			x	
6	4	5.1				
7	4.5	5.3				
8	4.9	4.4			x	
12	3.9	5			x	
14	4.1	5.3			x	
15	4.3	6			x	
16	3.9	5.8			x	
17	4	6			x	
18	4.5	5.7			x	
19	4.6	5.2			x	
20	4.2	4.9			x	
21	4.7	4.9			x	
22	3.8	5				
23	4	5.1				x

Complete adhesion failure > 70%  
 some failure > 10% & <70%  
 meets specifications

Table 5.7: Summary of Tape Pull Adhesion After Water Immersion. Note: TC/SST refers to the interface between the top-coat and the stainless steel layers. SST/PC refers to the interface between the stainless and polycarbonate layers

Run	Film Thickness (µm)		Tape Pull after short water-immersion		Failure Interface	
	top	bottom	top	bottom	TC/SST	SST/PC
24	5	6			x	
25	4.8	5.6			x	
26	4.7	5.9			x	
27	n/a	n/a			x	
28	n/a	n/a			x	
29	n/a	n/a			x	

Complete adhesion failure > 70%  
 some failure > 10% & <70%  
 meets specifications

Table 5.8: Summary of Performance of the Number of Samples with Respect to Bake Time ( 5, 10, 15 and 30 minutes bakes )

Bake Time (min)	Number of Samples		
	complete failure > 70% adhesion removal	marginal failure some failure > 10% and <70%	meet spec
5	9	0	0
10	0	2	0
15	0	0	2
30	1	2	5

## **5.4 Stage-3 of System “A” Development**

### **5.4.1 Objective**

The objective of stage-3 is to eliminate the appearance and adhesion defects that were observed in the primer-A and top-coat layer in system-A. These defects were observed after a water-immersion test.

### **5.4.2 Observations / Data / Discussion:**

Various parameters were examined and summarized in Table 5.9. The purpose of run 30 was to replicate the results from stage-2 which involved spotting. Runs 31,32 and 33 involve O<sub>2</sub> post-treatment of the SST layer to provide more oxides for the primer-A adhesion promotion. Runs 34 and 35 involved HMDSO post-treatments. The primer formulation components are summarized in Table 5.10. Note that Solvent-C was added to the primer formulation as it had proven beneficial to clearing the primer. However, it was noticed that WA-6 caused the metallized surface to crack as the concentration of the solvent C was higher and thus we were observing evidence of solvent attack. After water immersion tests, samples still showed the same defect as before and it appeared as if the coating layer was lifted when parts were removed from the water. However, the coating could be rubbed off when the part was removed from the water immersion. Therefore, more testing is required. It is important to mention that a PC/Primer-A & top-coat “A” was produced without the metallized layer and was submitted to water immersion. The results of this sample showed a similar failure. This proves that the primer / top-coat “A” interface is the defect initiation layer.

### **5.4.3 Main Conclusions**

- The post-treatment of oxygen and HMDSO after the metallization step did not help eliminate the appearance defect, spotting. In fact, the adhesion was degraded as a result of this post-treatment
- Different primer compositions need to be investigated as a means of eliminating the appearance defect resulting from water immersion testing.

Table 5.9: Process Parameters for Stage-3 of System-A

Run	Substrate	Metallization		Post treatment				Primer formulation		Primer bake	
	Polycarbonate	Argon Flow	Sputter Time	Gas	Flow (secm)	Time (sec)	Power (kW)	WA-5	WA-6	Bake Temp (oC)	Bake Time (min)
30	x	150	50					x		90	15
31	x	150	50	O <sub>2</sub>	150	10	6	x	x	90	15
32	x	150	50	O <sub>2</sub>	150	20	6	x	x	90	15
33	x	150	50	O <sub>2</sub>	100	10	6	x	x	90	15
34	x	150	50	HMDSO	150	20	6	x	x	90	15
35	x	150	50	HMDSO	100	10	6	x	x	90	15

Table 5.10: Primer Formulations for Stage-3 of System-A

Component	WA-5	WA-6
Solvent-A	65.0%	89.0%
DI Water	2.5%	5.0%
Solvent-B	31.5%	0%
Solvent-C	0%	5.0%
Primer-A	1.01%	1.0%
total:	100.0%	100.0%

### 5.5 Stage-4 of System “A” Development

In Stage 4 of system-A, new primers were introduced in an effort to optimize the adhesion between the top-coat and metallized layer . In addition the new primers are intended to also fix the water spotting issues seen with the previous primer (primer-A). Thus, primer-B and Primer-C were introduced. Primer-C is a water based primer.

In addition, further development was done to examine the effect of adding different percentage of solids into the primer to improve adhesion.

#### 5.5.1 Objective

The main objective of stage-4 was to introduce and trial primer-B and primer-C to promote adhesion between the metalized layer and the top-coat. As a secondary objective, a UV curable top-coat was introduced to examine its feasibility.

## 5.5.2 Observations / Data / Results

Stage-4 involved using the polycarbonate substrate, the metalized layer of stainless steel and in one case utilizing a UV curable top-coat and in the other case, utilizing primer-B and primer-C with a thermally cured top-coat.

### 5.5.2.1 UV Runs

In the UV run, cross-hatch adhesion was performed and failure mode observed was between the metallized layer and the polycarbonate substrate. The resin of the UV top-coat contains very aggressive elements that penetrate through the metallized layer to cause this failure. This was evident in micro-graphs on an area of a metalized layer before and after applying the UV top-coat, see Figure 5.6. In Figure 5.6, it is evident that the UV coating has increased the size of the cracks as the comparison is made between before and after applying the UV top-coat to the same area on the sample (see Figure 5.6a and 5.6b respectively). Also the UV coating is an organic coating and the tape sticks to this coating to a great degree, which results in increasing the force of the pull. The parameters investigated in an effort to fix this adhesion failure were:

1. Flash Time.
2. Preheat Time.
3. Preheat Temperature.
4. Percentage of solvents in coating.
5. Type of solvent in coating.
6. Plasma polymerization in chamber as a base-coat to prevent penetration.

The UV runs are defined by using a UV curable top-coat. The process flow for the UV run is outlined in Figure 3.2. Table 5.11 summarizes all the iterations examined during the UV run. Runs 84, 85 and 86 represent different levels of solvent-A concentration 0%, 25% and 40% respectively. Runs 87 and 89 use 32% of solvent-A with sample 89 having no pre-heating stage. Runs 90 and 91 are duplicates to samples 85 and 87 respectively. Run 92 examine a higher sputtering time (70 seconds) for the metalized layer and resulted in micro-cracking of the metalized layer as film stress is directly proportional to film thickness.. Runs 93 and 94 have a pre-treatment of HMDSO for 20 seconds. Runs 95 and 96 have 40 and 30 seconds of sputtering time, respectively. Runs 97 and 98 have 40 and 30 seconds of sputtering time, respectively, with HMDSO pre-treatment for 20 seconds. Runs 99, 100 and 101 have 50, 40 and 30 seconds of sputtering time, respectively, with one minute of flash time and no pre-heating time. Runs 102 through 105 use IPA as a solvent instead of Solvent-A and use different pre-heat and flash parameters. Runs 107 through 108 use various pre-heat and flash parameters. The film build for the top-coat recorded for the UV run are summarized in Table 5.12.

It was observed that whenever the flash time and/or the drying time was decreased, this resulted in a higher film build which was evidence of solvents being trapped in the coating. Ideally, all solvents should be flashed off before exposing the coating to UV radiation to ensure proper adhesion and film build. Run 109 passed the initial adhesion for 3M tape.

It was observed that when drying (pre-heat step) was not performed to flash off solvents and a post-heat step was carried out; solvents would come out of the coating to cause an appearance issue. This emphasizes the importance of flashing off the coating prior to curing the top-coat. The following general comments should be noted:

- As sputtering time was increased to increase the metallized layer thickness, cracking occurred as parts were coated which is a result of increasing film stresses in the metallized layer.
- When using 100% coating (without any solvents), minimal cracking occurred. As solvent was added, cracking was evident as the solvent allows for deeper penetration through the metallized layer. The coating formulation was made-up with pre-existing solvents to carry out the solids and thus it is not feasible to have no solvent in the UV formulation.
- Based on film thickness measurements, it was determined that 32% of solvent-A in the UV top-coat gives acceptable film build. The higher the solvent level, the lower the film build.
- The pre-heat stage for processing the UV coating is critical to allow for all the solvents to evaporate. However, the adhesion results (runs 90-98) indicate that the pre-heating stage degraded the adhesion performance compared to runs (99-101 and 104-108) which do not have a pre-heat stage but they have better adhesion performance.
- Film thickness variations were evident. Note that runs 94-96 and 98 have almost a factor of 2 between the difference between the top and bottom thicknesses.
- Coating clarity was improved as the solvent level was increased. This was observed through coating a clear polycarbonate plaque, where the coating clarity can be observed as the plaque is put against a light source, where the light transmits through the plaque.
- The UV top-coat adhesion to the stainless steel layer requires further improvements. It should be noted that 3M tape pull is the main tape for adhesion and that Nichiban is a more aggressive tape that serves the purposes of distinguishing between “border line” results.

Table 5.11: Process Parameters for Stage-4 of System-A (UV coating). Note that Sol-A refers to Solvent-A, IPA refers to Isopropyl Alcohol

Run	Metalizing - SST			Coating Parameters UV top-coat							
	Time (sec)	HMDSO Flow (scm)	HMDSO Time (sec)	Flash Time (min.)	Drying Temp. C	Preheat Time (min.)	UV-A Dosage	UV-A Intensity	UVB Dosage	% Solvent in Coating	Solvent-A / IPA
84	50			2	75	5	5.8	1.25	5.5	0	Sol-A
85	50			2	75	5	5.8	1.25	5.5	25	Sol-A
86	50			2	75	5	5.8	1.25	5.5	40	Sol-A
87	50			2	75	5	5.8	1.25	5.5	32	Sol-A
89	50			2		0	5.8	1.25	5.5	32	Sol-A
90	50			1.5	75	2.5	5.8	1.25	5.5	25	Sol-A
91	50			1.5	75	2.5	5.8	1.25	5.5	32	Sol-A
92	70			1.5	75	2.5	5.8	1.25	5.5	32	Sol-A
93	70	150	20	1.5	75	2.5	5.8	1.25	5.5	32	Sol-A
94	50	150	20	1.5	75	2.5	5.8	1.25	5.5	32	Sol-A
95	40			1.5	75	2.5	5.8	1.25	5.5	32	Sol-A
96	30			1.5	75	2.5	5.8	1.25	5.5	32	Sol-A
97	40	150	20	1.5	75	2.5	5.8	1.25	5.5	32	Sol-A
98	30	150	20	1	75	2.5	5.8	1.25	5.5	32	Sol-A
99	50			1	0	0	5.8	1.25	5.5	32	Sol-A
100	40			1	0	0	5.8	1.25	5.5	32	Sol-A
101	30			1	0	0	5.8	1.25	5.5	32	Sol-A
102	40			1	65	1	5.8	1.25	5.5	32	IPA
103	30			1	65	1	5.8	1.25	5.5	32	IPA
104	40			2	0	0	5.8	1.25	5.5	32	IPA
105	30			2	0	0	5.8	1.25	5.5	32	IPA
107	40			1.5	0	0	5.8	1.25	5.5	32	Sol-A
108	40			1.5	0	0	5.8	1.25	5.5	32	Sol-A
109	40			1.5	65	2.5	5.8	1.25	5.5	32	Sol-A



Table 5.12: UV Top-coat Film Build for Stage-4 of System-A

Run	Film Build			Initial Adhesion	
	Top (microns)	Middle (microns)	Bottom (microns)	3M (% Removal)	Nichiban (% Removal)
84	14.9	20.8	24.4	15%	75%
85	7	7	12	10%	70%
86	4.1	5.2	7.6	5%	40%
87	6	7.6	10	2%	75%
89	7.2	8.4	10.1	10%	70%
90	6.1	8.4	12.1	15%	70%
91	9.4	11.8	15.9	15%	70%
92	7.2	9.5	11.1	5%	75%
93	7	9.1	11.4	5%	15%
94	6	8.5	11.7	5%	40%
95	6.6	8.3	11.4	15%	70%
96	6.5	8.6	11	10%	70%
97	7	9.4	11.2	10%	70%
98	6.7	8.6	11.4	5%	30%
99	8	12.2	15.7	0%	20%
100	7.4	11	15	0%	20%
101	8.5	11.7	15.1	0%	20%
102	10.4	12.5	13.1	10%	40%
103	10.3	12.3	15.6	10%	40%
104	10.3	12.4	13.1	10%	70%
105	10.8	12.4	14.9	10%	60%
107	8.4	11.1	14.6	0%	15%
108	6.8	9.5	12.1	0%	10%
109	8.4	11.05	13.1	0%	40%

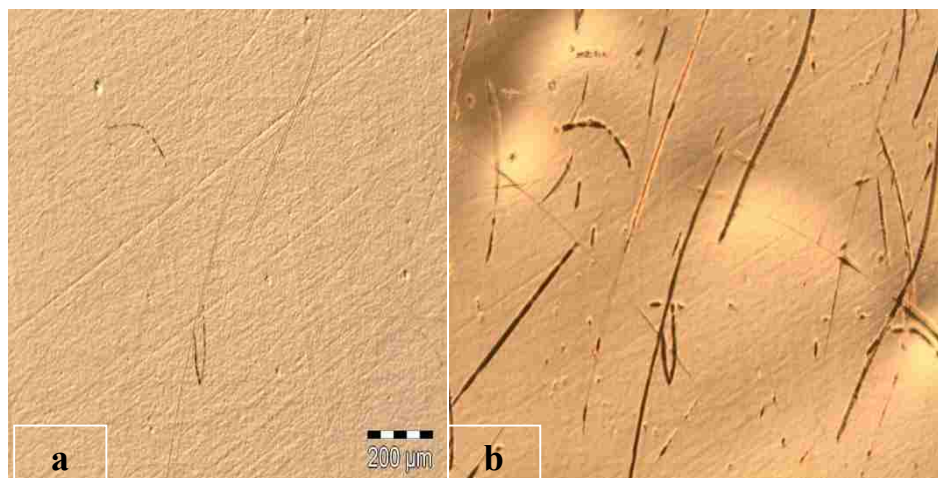


Figure 5.6: Effects of the UV Top-coat on a SST metalized Layer. a) SST Before Applying the UV Top-coat. b) SST After Applying and Curing the UV Top-coat.

#### 5.5.2.2 Thermal Run

The thermal run is characterized by a thermally cured top-coat, with polycarbonate substrate and a stainless steel metalized layer. The general process flow for the thermal run is outlined in Figure 3.1. New primers were introduced at this stage in an effort to fix the spotting. The new primers were primer-B, primer-BB and primer-C. The primer formulations for this stage are given in Table 5.13. Table 5.14 summarizes all the iterations that were performed, the initial adhesion and adhesion after 10 days of water immersion testing.

Runs 110, 111 and 112 had primers B, BB and C respectively with a 15 minutes bake time at 80°C. Runs 116, 117 and 118 had primers C, B and BB respectively with a shorter bake time of 5 minutes and a higher temperature of 86°C. Runs 119, 120 and 121 had primers C, B and BB respectively with a shorter bake time of 5 minutes and even a higher temperature of 95°C. Runs 122, 123 and 124 had primers C, B and BB respectively with a shorter bake time of 5 minutes and a highest cure temperature of 114°C. Finally, runs 113Ctrl and 114Ctrl are control samples using primer-A to duplicate and verify the failure mode observed in the earlier stages of system-A.

Initial adhesion for all samples tested with 3M tape were 100% pass. Runs 110 and 117 were the only runs that failed Nichban tape pull for the initial adhesion. The water immersion results indicate that primer-C provides the best adhesion properties to the system. In addition, shorter bake times for the primers were examined at elevated temperatures. Runs 110, 111 and 112 were baked for 15 minutes at 80°C. Runs 116, 117 and 118 were baked for only 5 minutes at 86°C. Runs 119, 120 and 121 were baked for 5 minutes at 95°C. Runs 122, 123 and 124 were baked for only 5 minutes at 114°C. The idea is to compensate for the bake time by increasing the bake temperatures. The spotting

effect was observed for runs 113 and 114 and the adhesion properties were not acceptable which verifies the results observed previously ( stage-1, stage-2 and stage-3).

The following general comments should be noted:

- Flashing off the water-based primer C takes longer than the solvent-based primer B and primer BB – about 4 minutes extra.
- When applying the B & BB primers, immediate “spotting“ formed as material is flowing. This is believed to be un-dissolved solids in the primer. However this did not present any serious appearance defect specially, after top-coating.
- Cracking of the metallized layer occurs in some cases when applying the B & BB primers (mostly at the gate location) and this was a function of internal stresses present samples as well as a solvent attack.
- Internal stresses were reduced by optimizing the molding conditions through running at hotter temperatures, providing for slow cooling of 30 seconds of cool time and no pack pressure which resulted in annealing the material and thus reducing the internal stresses.
- Overall, initial adhesion for the thermal system looks very promising and samples should go a complete round of testing. Primer-C seemed to have the best adhesion results.

Table 5.13: Primer Formulations for Stage-4 of System-A – Thermal Coating. Note: primer-C is a water based primer and no additional components were needed to be added to it. All unit are in grams.

	<b>Primer-B</b>	<b>Primer-BB</b>	<b>Primer-C</b>	<b>Primer -A</b>
Primer B	40.11	60	-	-
Solvent A	160.5	93	-	131
Primer BB	-	-	-	-
Solvent B	-	150	-	63
water	-	-	-	5
Primer A	-	-	-	2
Total	200.61	303	200	201

Table 5.14: Process Parameters for Stage 4 of System-A – Thermal Coating. Note “ctrl” is a control sample to duplicate results that were observed with primer-A.

Run	Polycarbonate substrate	Metal - SST		Primer			Initial Adhesion		Water Soak Adhesion		
		Time (sec)	Ar Flow (scm)	Primer used	Flash time ( min )	bake time ( min )	bake temp ( C )	3M (% Removal )	Nichiban (% Removal )	3M (% Removal )	Nichiban (% Removal )
110	x	50	150	primer-B	5	15	80	0%	12%	0%	15%
111	x	50	150	primer-BB	5	15	80	0%	0%	0%	10%
112	x	50	150	primer-C	8	15	80	0%	0%	0%	3%
116	x	50	150	primer-C	9	5	86	0%	0%	0%	10%
117	x	50	150	primer-B	5	5	86	0%	10%	0%	15%
118	x	50	150	primer-BB	5	5	86	0%	0%	0%	10%
119	x	50	150	primer-C	9	5	95	0%	0%	0%	0%
120	x	50	150	primer-B	5	5	95	0%	2%	0%	15%
121	x	50	150	primer-BB	5	5	95	0%	0%	0%	15%
122	x	50	150	primer-C	9	5	114	0%	2%	0%	5%
123	x	50	150	primer-B	5	5	114	0%	0%	0%	2%
124	x	50	150	primer-BB	5	5	114	0%	2%	0%	7%
113 Ctrl	x	50	150	primer-A	5	15	80	0%	0%	60%	90%
114 Ctrl	x	40	150	primer-A	5	15	80	0%	0%	60%	90%

### 5.5.3 Main Conclusions

The main conclusions for stage-4 of system-A are as follows:

- Overall, the system that is composed of a polycarbonate substrate, a stainless steel metalized layer and a UV cured top-coat does not have good initial adhesion results and it requires further development.
- Overall, the system that is composed of a polycarbonate substrate, a stainless steel metalized layer, primer-C and a thermal cured top-coat has proved to have acceptable initial adhesion properties as well as acceptable adhesion properties after water immersion testing.
- Primer-B and primer-BB have acceptable initial adhesion. However, there are some adhesion failures after the water immersion testing.

## **5.6 Stage-5 System “A” Development**

In stage-5 of system-A, the thermal and UV systems were tried. Based on the results of stage-4 of system-A, the focus of the thermal system was to produce samples for complete matrix testing.

In addition to the thermal run, the UV system was also examined to optimize its processing parameters in an effort to reduce the adhesion loss of the metallized layer to the substrate as the top-coat penetrates through the metallized layer.

### **5.6.1 Objectives**

The objective of this run is to produce samples with PC/SST/Primer-C/thermal top-coat-A and PC/SST/Primer-BB/thermal top-coat-A for further testing. Primer-C performed better than primer-BB in stage-4. However, primer-BB had good initial adhesion results and thus it was included in stage-5. In addition, the PC/SST/UV top coat system was examined to optimize processing parameters.

### **5.6.2 Observations / Data / Discussion:**

#### **5.6.2.1 UV Runs**

The UV runs use a UV curable top-coat. The iterations for the UV run are summarized in Table 5.15. As noted in Table 5.15, a primer stage was added prior to the application of the UV top-coat in an effort to increase the adhesion properties between the UV top-coat and the metallized layer and potentially prevent the UV coatings from penetrating through the metallized layer to cause an adhesion failure between the metallized layer and the substrate.

Run 127 serves as a control, without the usage of any primers. Runs 128, 129 and 130 have primer-C and have differences in the pre-heat and flash parameters. Runs 131 through 134 have primer-BB with different flash and pre-heat parameters. The addition of the primer proved not to be beneficial to this system and the initial adhesion results are summarized in Table 5.16. The initial adhesion results indicate that primer-C does provide better adhesion properties than primer-BB no primer is better. They are not within acceptable limits (greater or equal to 5% coating removal as a result of initial adhesion testing). Due to these initial adhesion failures, pursuing the UV top coating option was not continued as changing the chemical composition of the UV coating was required to advance this portion of the development and thus it was decided not to develop this UV coating option further.

Table 5.15: Process Parameters for Stage-5 of System-A.

Run	Metallization - SST		Primer				Coating Parameters					
	Sputter Time (sec)	Ar Flow (sccm)	Primer used	Flash time (min)	bake time (min)	bake temp (C)	Flash Time (min.)	Drying Temp. (°C)	Preheat Time (min.)	UV-A Dosage	UV-A Intensity	UVB Dosage
127	40	150	none	none	none	none	1.5	65	2.5	5.8	1.25	5.5
128	40	150	primer-C	8	5	110	1.5	65	2.5	5.8	1.25	5.5
129	40	150	primer-C	8	5	110	1.5	75	3	5.8	1.25	5.5
130	40	150	primer-C	8	5	110	1.5	65	3	5.8	1.25	5.5
131	40	150	primer-BB	8	5	110	1.5	70-73	2.5	5.8	1.25	5.5
132	40	150	primer-BB	8	none	none	1.5	70-73	2.5	5.8	1.25	5.5
133	40	150	primer-BB	5	5	110	1.5	75	2.5	5.8	1.25	5.5
134	40	150	primer-BB	5	5	110	1.5	65	2.5	5.8	1.25	5.5

Table 5.16: Initial Adhesion Results for Stage-5 (UV run) of System-A

Run	Initial Adhesion	
	3M	Nichiban
127	5%	10%
128	15%	20%
129	5%	15%
130	10%	15%
131	20%	60%
132	10%	30%
133	15%	80%
134	15%	70%

### 5.6.2.2 Thermal Runs

The thermal runs use a thermally cured top-coat with a polycarbonate substrate and a stainless steel metalized layer. The thermal run focused on producing samples with shorter bake times (7 minutes) at higher temperatures (110°C) that would be submitted for a complete round of testing to meet test technology specifications. Only two primers were used as shown in Table 5.17.

Samples 125 and 126 were processed with the two primers (primer-BB and primer-C) that provided acceptable results, as shown in Table 5.18. Samples 125 were then submitted for matrix testing and results are shown in Table 5.19. The system meets the specifications given in section 1.2 of this thesis.

Table 5.17: Primer Formulations for Stage-5 of System-A – Thermal Coating. Note: primer-C is a water based primer and no additional components were needed to be added to it. All unit are in grams.

	Primer-BB	Primer-C
Primer B	60	-
Solvent A	93	-
Solvent B	150	-
Total	303	200

Table 5.18: Process Parameters for the Thermal run Stage-5 of System-A

Run	polycarbonate substrate	Metal SST		Primer			
		Time (sec)	Ar Flow (scm)	Primer used	Flash time ( min )	bake time ( min )	bake temp ( C )
125	x	50	150	primer-C	9	7	110
126	x	50	150	primer-BB	5	7	110

Table 5.19: Test Results for Complete Matrix Testing for System-A

Run	Number of Samples	Test / Specifications	Results
125	3	Appearance Approval	meets specifications
125	3	Impact Resistance	meets specifications
125	3	Initial Adhesion	meets specifications
125	3	Water Immersion Resistance	meets specifications
125	3	Heat Age Testing	meets specifications
125	3	Humidity Resistance	meets specifications
125	3	Salt Spray	meets specifications

### 5.6.2.3 Primer Sample Analysis:

The following studies were conducted to better understand some of the root causes for the failure modes encountered during the experiment process for primer-A, primer-BB and primer-C. Samples with primer-C and primer-BB that had been processed at different temperatures and curing times were prepared. SEM images and EDX analysis was performed to analyze the samples and understand the surface composition of the different primers. Figure 5.7 shows EDX spectra of a stainless steel metallized layer without any primer or top-coat using different beam energies that demonstrate different levels of penetrations. At 5kV, compared to 3kV, higher levels of carbon are detected as the energy beam penetrates deeper and high peaks of Cr and Fe are observed. The SEM / EDX for Figure 5.8 shows that as electron energy beam increases, the penetration levels increase as well. This is evident as we start detecting the presence of stainless steel when using 10kV energy. In addition, it seems like the surface of primer C contains significant concentration of carbon.

Figure 5.9 shows an SEM image and an EDX spectra of a primer-C applied on a stainless steel layer and cured for 15 minutes. The SEM image demonstrates the proper surface wet-ability of the primer-C on the metalized layer. Please note that the whole surface is covered with primer and that the inclusion in the middle of the SEM image is just a high concentration area of siloxane. This is not considered a defect and it is a result of, potentially, some dust or surface imperfection of the polymer that allowed the higher primer to concentrate in that area. Figure 5.10 shows an SEM image and an EDX spectra of a primer-BB applied on a stainless steel layer and cured for 15 minutes. The SEM image demonstrates an unacceptable level of surface wet-ability of the primer-BB on the metalized layer. In addition, the SEM images show spotting defects that are shown, through EDX spectra, to have high level of metal concentrations.

Based on the SEM images shown in Figure 5.11, which compares the different primer formulations, it is observed that the primer-BB and primer-A are not wetting out the metallized surface properly as the white spots in the SEM images are metal concentrations (this is seen through the EDX spectra). However, primer-C is appearing to be wetting out the surface of the metallized layer properly.



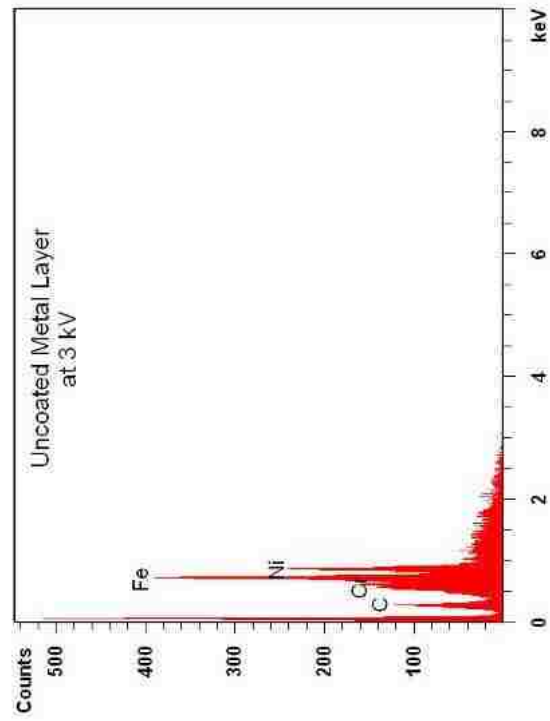
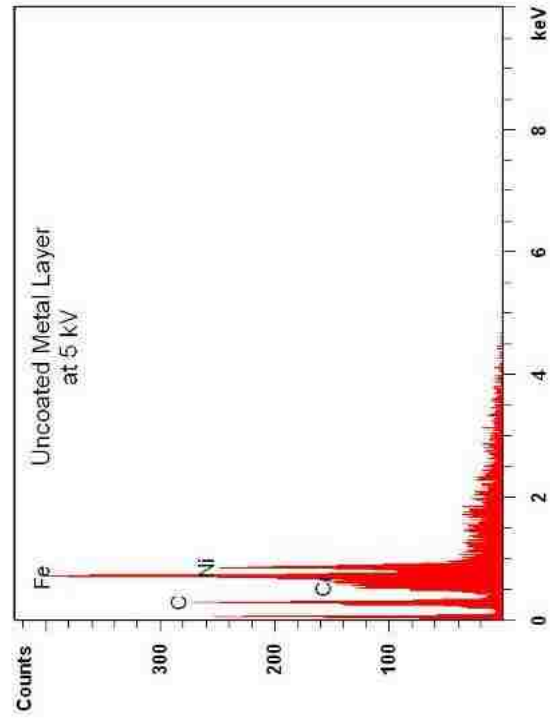


Figure 5.7: EDX Analysis on Metalized Layer with no Primer no Top-coat. Different Beam Energies EDX Spectra

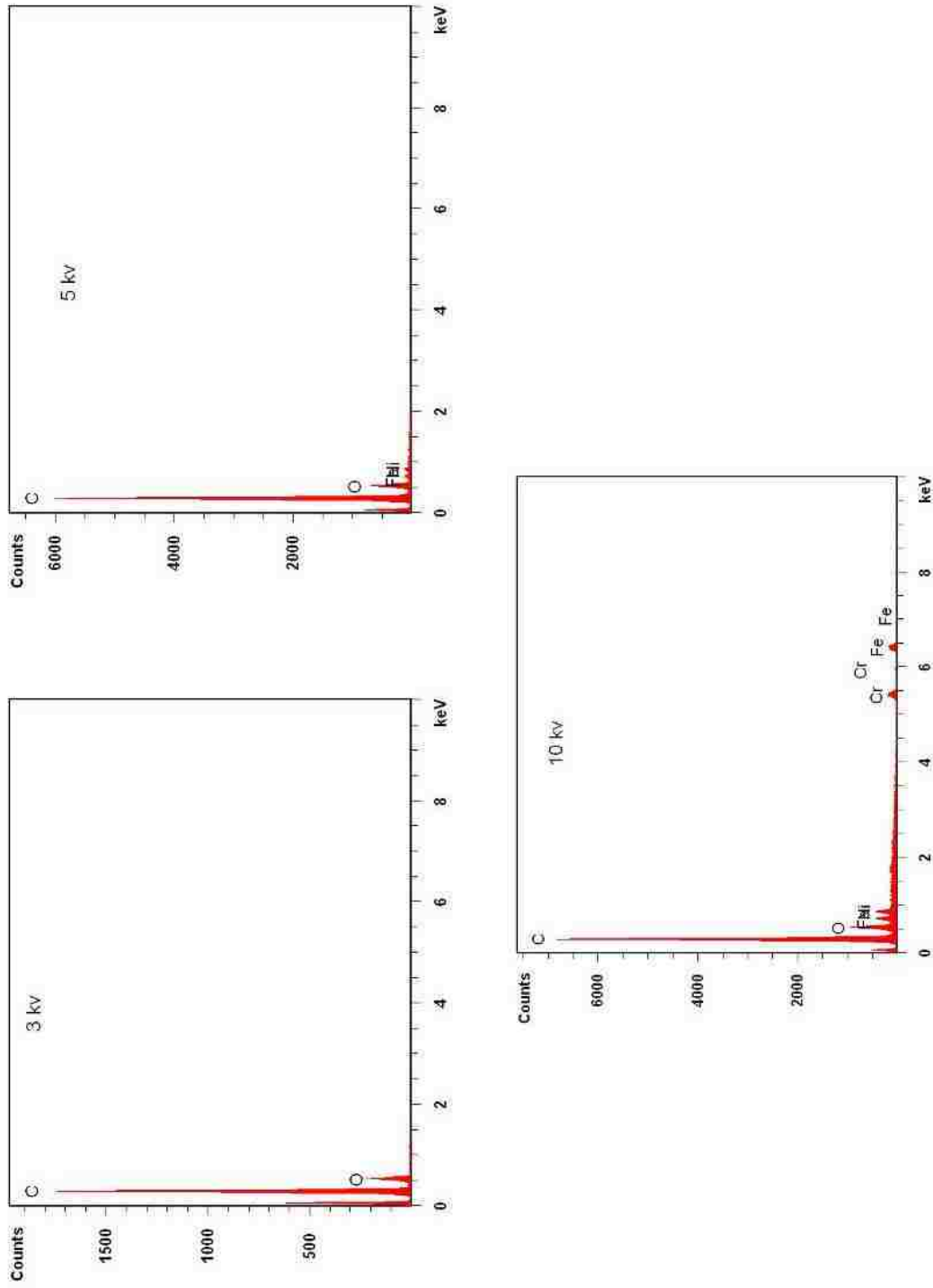


Figure 5.8: : EDX Analysis on Metalized Layer with Primer-C and no Top-coat. Different Electron Beam Energies and Penetration Levels

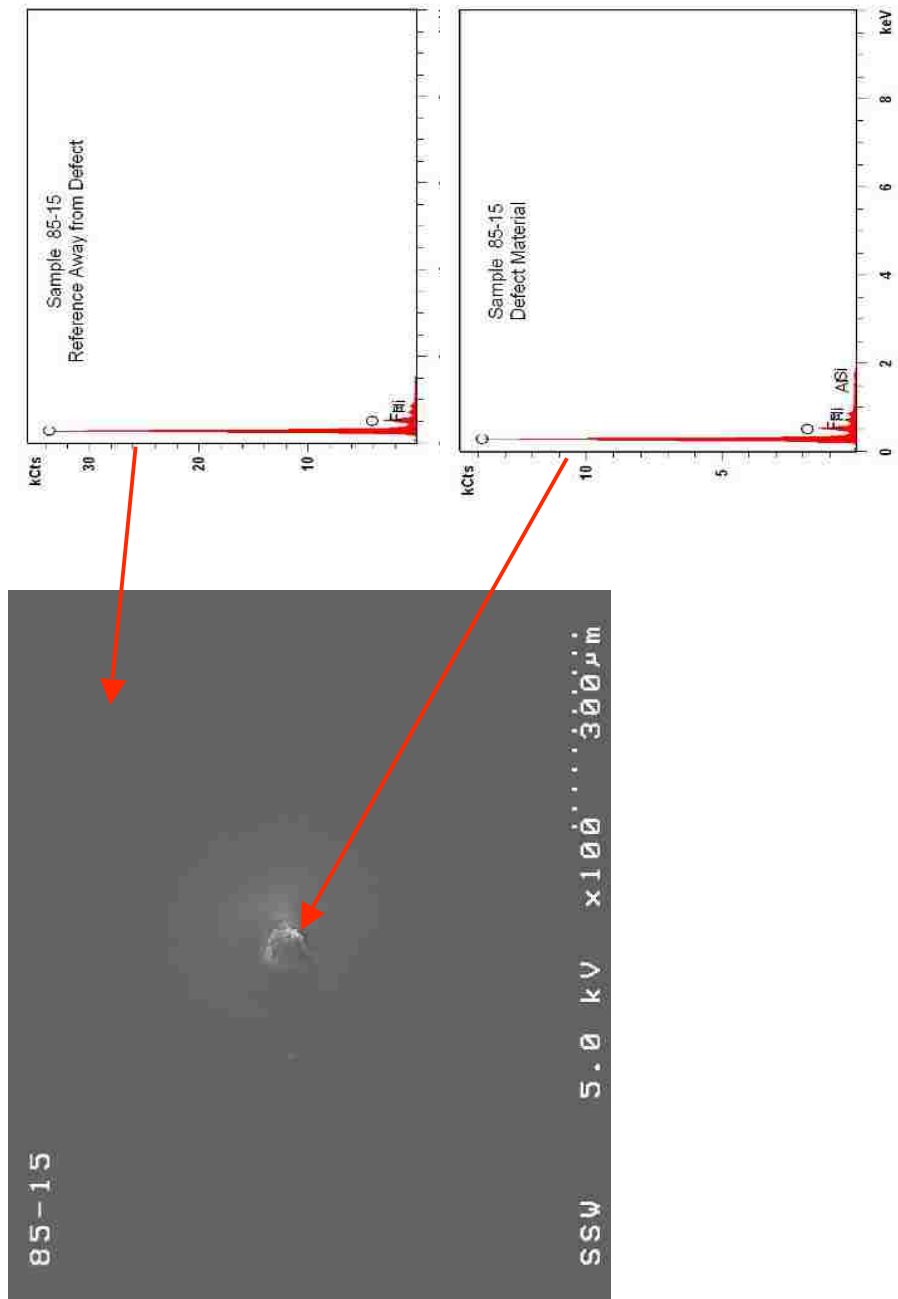


Figure 5.9: Primer C – Cured at 85°C for 15 Minutes (SEM/EDX Analysis)

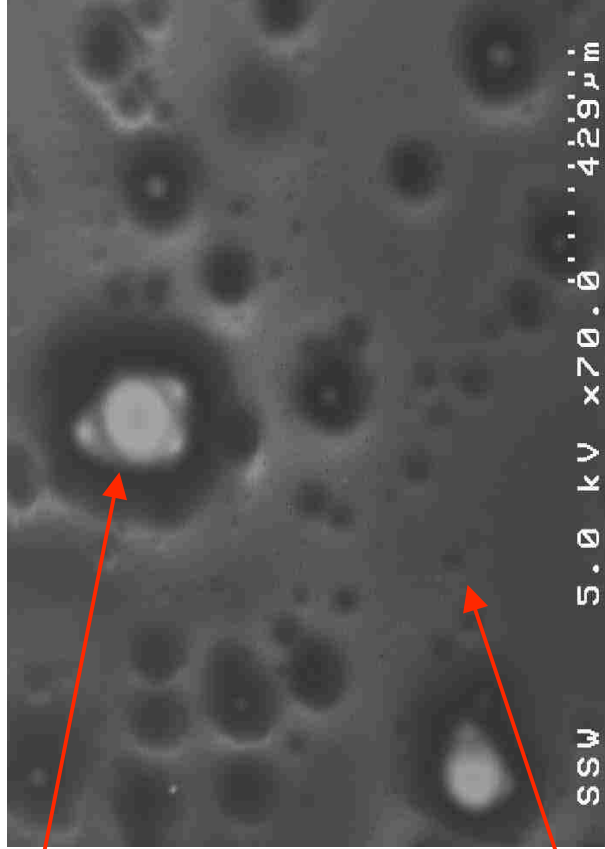
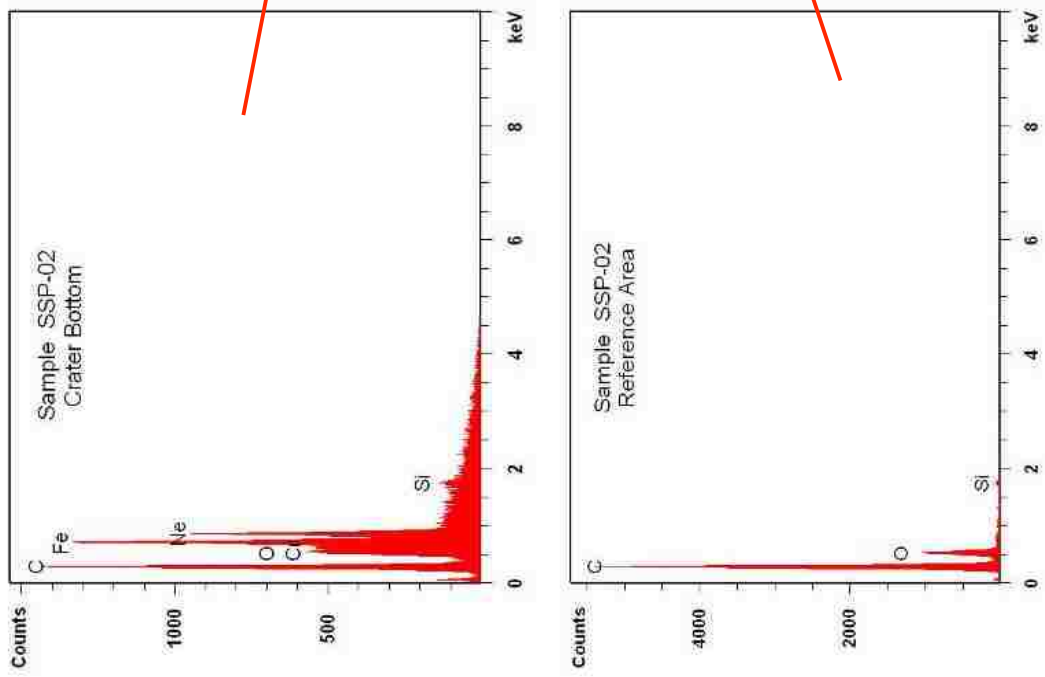
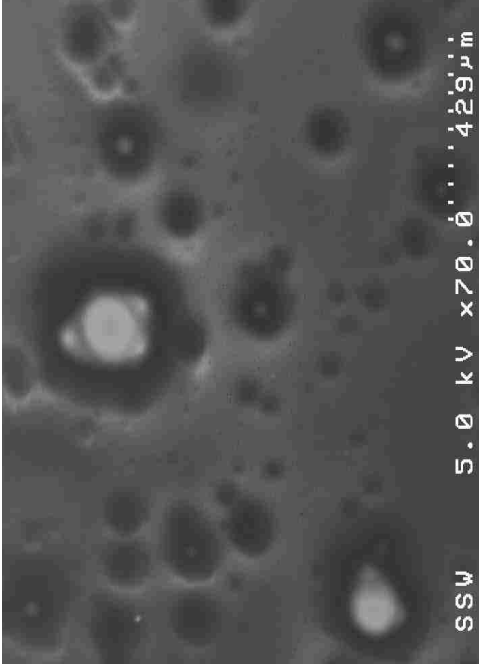


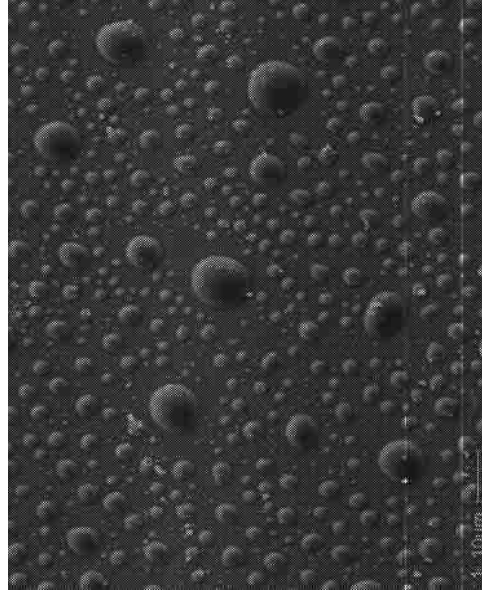
Figure 5.10: Primer BB—Cured at 85°C for 15 Minutes (SEM/EDX Analysis)



Primer  
C



Primer  
BB



Primer  
A

Figure 5.11: Different Primer SEM Images – Surface Wet-out.

Note : primer ‘‘C’’ wets-out the surface properly. Primer ‘‘BB’’ and ‘‘A’’ do not wet-out the surface

### 5.6.2.3 Primer Cure Time Analysis Using FTIR

This analysis was performed to understand the effects of curing time and temperature on the curing process in the primer. The samples were analyzed by Fourier transform infrared spectroscopy (FTIR) in reflection mode using the microscope attachment.

FTIR was used to analyze samples of primer-C

Sample 1: no bake

Sample 2: Baked at 110°C for 7 min

Sample 3: Baked at 85°C for 15 min

Three areas on each sample were analyzed and the spectra from the samples are compared in the Figure 5.12. The spectra of a representative area on each of the samples are presented individually. There appeared to be differences in the relative intensities of some of the peaks but these were not particularly obvious. Areas under the curves were integrated to determine if there were any quantifiable changes taking place.

The integrated values are presented in Table 5.20. The region of the OH peak was integrated from 3038-3713  $\text{cm}^{-1}$ . The region of the CH peaks was integrated from 2753 to 3034  $\text{cm}^{-1}$ . The region of the C=O (CO -1) was integrated from 1587 to 1767  $\text{cm}^{-1}$  and the region of the rest of the spectrum was integrated from 1183 to 1345  $\text{cm}^{-1}$ , labeled as CO-2. Ratios of the OH, CO-1 and CO-2 regions versus the CH region were calculated, assuming the CH groups are constant in the system. There appeared to be a decrease in the number of OH groups in the cured samples, relative to the uncured sample. There also appeared to be a decrease in the intensity in the CO-2 region-relative to the CH region in the cured samples, relative to the uncured sample. Thus, longer curing times have proven to be beneficial as it reduces the OH counts which contributes to better adhesion results.

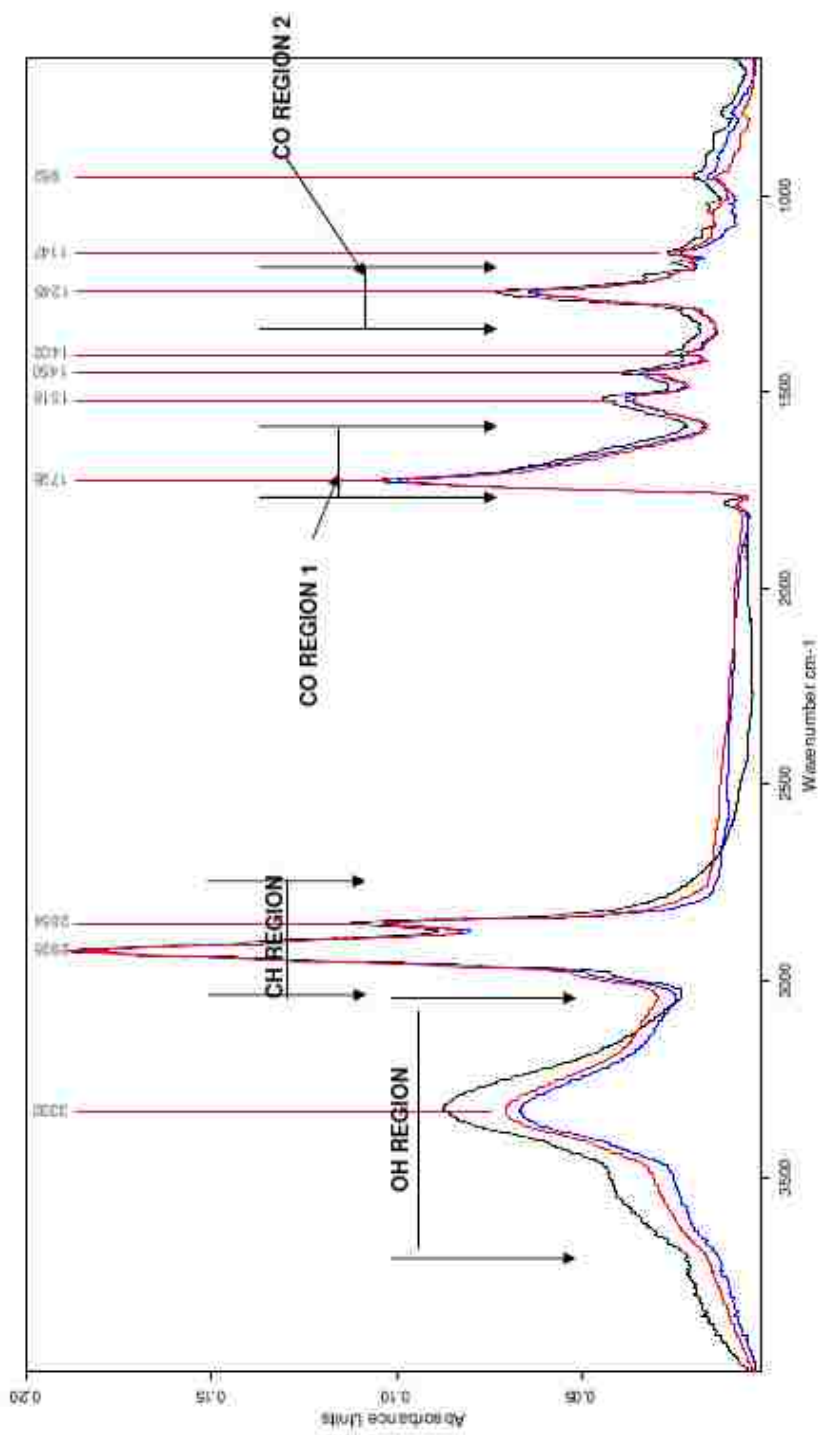


Figure 5.12: Sample 1, 2 3 ( no bake, 7 min at 110C, 15min at 85C)

Sample # 1: no Bake, Sample # 2: Baked at 110°C for 7 min, Sample # 3: Baked at 85°C for 15 min

Table 5.20: Integrated Areas Under the Curves for Figure 5.13.

<b>Sample</b>	<b>OH/CH</b>	<b>CO1/CH</b>	<b>CO2/CH</b>	<b>(OH+CO2)/CH</b>
<b>0-0</b>	1.180	0.445	0.180	1.361
	1.131	0.478	0.218	1.349
	1.196	0.439	0.177	1.372
<b>Average</b>	<b>1.169</b>	<b>0.454</b>	<b>0.192</b>	<b>1.361</b>
<b>110-7</b>	0.764	0.465	0.155	0.920
	0.636	0.472	0.154	0.790
	0.843	0.442	0.150	0.993
<b>Average</b>	<b>0.748</b>	<b>0.460</b>	<b>0.153</b>	<b>0.901</b>
<b>85-15</b>	0.798	0.433	0.151	0.949
	0.833	0.436	0.153	0.986
	0.866	0.431	0.153	1.019
<b>Average</b>	<b>0.832</b>	<b>0.434</b>	<b>0.152</b>	<b>0.985</b>

### 5.6.3 Main Conclusions

The main conclusions for stage-5 of system-A are as follows:

- The polycarbonate substrate, a stainless steel metalized layer and a UV cured top-coat system had some initial adhesion failures.
- The polycarbonate substrate, a stainless steel metalized layer, primer-C and a thermal cured top-coat system has passed the following requirements:
  - Appearance Approval
  - Impact Resistance
  - Initial Adhesion
  - Water Immersion Resistance
  - Heat Age Testing
  - Humidity Resistance
  - Salt Spray



### **5.7 System “A” Summary**

System “A” consists of polycarbonate as a substrate, stainless steel as a metalized layer, primer as an adhesion promoter, and a protective clear top-coat. The development of system-A consisted of 5 stages including finding the most suitable primer to promote adhesion between the metalized layer and top-coat and thus achieve the functional requirements. Stage 1,2 and 3 involved using primer-A that proved to have good initial adhesion properties, but did not pass the water immersion testing as it formed an appearance defect after the moisture exposure. It was determined that the root cause of the appearance defect was the primer formulation A, related to the water spotting as a result of water immersion testing. Thus, primers-B, primer-BB and primer-C were introduced in stage 4 and primer-C proved to be suitable for the system. Primer-B & primer-BB caused micro-cracking of the metalized layer due to the aggressive solvent and solid present in the primer. Eventually, primer-C, a water based primer, was the preferred primer used to produce samples to go through the testing outlined in section 1.2 and samples meet the testing specifications.

## CHAPTER VI

### SYSTEM “B” DEVELOPMENT & RESULTS

#### 6.1 System “B” Introduction

The focus of system-B is to eliminate the primer stage by utilizing different sputtering targets, to deposit yet another material using PVD, and thus achieve adhesion between the top-coat and the metalized layer without the usage of any adhesion promoters, such as primers. The development for this system involved 4 stages, each stage is composed of an experiment, as shown in Figure 6.1. Each stage focuses on addressing the issues being faced at the time, which are summarized in this chapter.

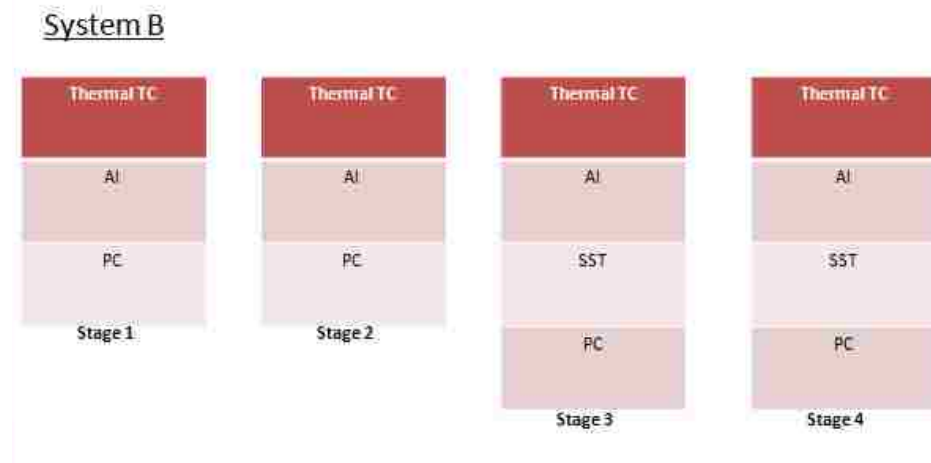


Figure 6.1: System “B” Development Stages

#### 6.2 Stage-1 of System “B” Development

The following sub-sections will summarize the objective, observations, data, results, and conclusions for the stage-1 of development for system-B.

##### 6.2.1 Objective

In the first stage of system-B development, the objective was to eliminate the primer stage and thus a different metallized layer, other than stainless steel, was tried. The obvious choice was aluminum that is 99.9% pure, due to its availability as well as its relatively low cost. The processing steps were: molding a polycarbonate substrate, metalizing with aluminum and top-coating with a thermally cured top-coat-A, which was used in the development of system-A.

### 6.2.2 Observations / Data / Discussion

Stage-1 of system-B focused on the polycarbonate and aluminum layer interface. The development process involved the usage of different techniques to increase adhesion between the metallized layer and the substrate. Initially, the series of samples in Table 6.1 were fabricated to determine the optimized target power and film build for maximum adhesion for a polycarbonate (PC) and aluminum system. For this preliminary test old PC pieces were used which had low surface energy. It is observed that higher target power gives better initial adhesion testing results as shown in runs 7 and 8 of Table 6.1. Eventually freshly molded PC pieces (with high surface energy) were used to produce the finishes as in Table 6.2. The tape pull was done using the Nichiban tape as it represents a more aggressive pull test. Based on the results from Table 6.1 the sputter time was determined to be around 40 seconds and the target power around 40 kW. As the initial parameters were determined, Table 6.2 summarizes the process parameters used in stage-1 of system-B.

Run 1 used no plasma pre-treatment to promote adhesion between the metallized layer and the polymer and it serves as a control sample. Runs 2, 3 and 4 use Argon gas as pre-treatment with various dosages. Runs 5 and 6 use HMDSO with various dosages. Samples 7, 8 and 9 use a mixture of Argon and HMDSO to pre-treat the surface. Finally, runs 10 through 16 use HMDSO as a base-coat with different base pressure and HMDSO dosages.

This system looks promising as it eliminates the primer which has a lot of variability within its composition and processing parameters. It can be seen (Table 6.3) that applying a basecoat within the chamber promotes adhesion between the substrate and the metallized layer provided there is no pre-treatment with Ar; runs 1-5 and 9 had poor adhesion. However excessive basecoat did cause initial adhesion failures in the system (run 10 in Table 6.2).

In general the process for determining the optimum treatment for any substrate is to measure the surface energy, by measuring water droplet contact angle, of the film before treatment. Then systematically measuring the increased surface energy as the treatment is increased. The aim is to maximize the surface energy. It is worth noting that once the surface has reached a maximum surface energy it is possible to over-treat the surface without seeing a decrease in the surface energy (Figure 2.1). Adhesion was promoted through some plasma pre-treatments and a base-coat and it prompted proper adhesion of the metallized layer to the plastic substrate (run 14). It should be noted that based on the results in Table 6.4, the system shows some promising results as far as robustness in the processing parameters during vacuum metallizing and hard-coating.

The samples were submitted to water immersion testing to understand how the moisture interaction affects the system. The samples formed some pinholes after the moisture exposure, which is due to

the reaction of the aluminum layer with the water. Specifically, it was observed that samples that were exposed to water immersion testing formed very small black spots which is the PC substrate as the aluminum layer has reacted with the moisture to expose the black PC.

Table 6.1: Adhesion Relationship between Target Power and Sputtering Time for an Aluminum Target

System-B	Target Power (kW)	Sputter Time ( sec)	Adhesion (% Removal)
1	30	30	10 %
2	30	40	15 %
3	30	50	35 %
4	30	60	50 %
5	35	30	15 %
6	35	40	12 %
7	40	30	5 %
8	40	40	2 %

Table 6.2: Process Parameters for Stage-1 of System-B. Note: top coat-A was applied to all samples and was cured at 125C for 45 minutes. The base-coat and the pre-treatment stages both take place within the sputtering chamber

Run	Pre-treatment				Base-coat				Metallization - Al		
	Gas	Flow (sccm)	Time (sec)	Power (kW)	Gas	Flow (sccm)	Time (sec)	Power (kW)	Base-Pressure (mTorr)	Time (sec)	Ar Flow (sccm)
1	N/A	N/A	N/A	N/A	N/A	N/A	N/A	N/A	0.025	30	150
2	Ar	80	10	5	N/A	N/A	N/A	N/A	0.025	30	150
3	Ar	80	10	5	N/A	N/A	N/A	N/A	0.025	40	150
4	Ar	80	20	5	N/A	N/A	N/A	N/A	0.025	40	150
5	Ar	80	20	5	HMDSO	150	20	6	0.025	40	150
6	N/A	N/A	N/A	N/A	HMDSO	150	20	6	0.025	40	150
7	N/A	N/A	N/A	N/A	HMDSO+Ar	150+50	20	6	0.025	40	150
8	N/A	N/A	N/A	N/A	HMDSO+Ar	150+50	20	6	0.025	30	150
9	Ar	80	20	5	HMDSO+Ar	150+50	20	6	0.025	40	150
10	N/A	N/A	N/A	N/A	HMDSO	150	60	6	0.025	40	150
11	N/A	N/A	N/A	N/A	HMDSO	150	20	6	0.05	40	150
12	N/A	N/A	N/A	N/A	HMDSO	150	20	6	0.075	40	150
13	N/A	N/A	N/A	N/A	HMDSO	150	20	6	0.04	40	150
14	N/A	N/A	N/A	N/A	HMDSO	150	20	6	0.025	40	250
15	N/A	N/A	N/A	N/A	HMDSO	150	20	6	0.06	40	150
16	N/A	N/A	N/A	N/A	HMDSO	150	20	6	0.09	40	150

Table 6.3: Initial Adhesion and Adhesion After 10 Day Water Immersion Test Results for Stage-1 of System-B. Note: All samples formed pinholes after the water immersion

Run	Initial Adhesion			10-Day Water Immersion Adhesion	
	3M (% Removal)	Nichiban (% Removal)		3M (% Removal)	Nichiban (% Removal)
1	6%	80%		0%	15%
2	6%	80%		15%	60%
3	6%	60%		6%	80%
4	4%	80%		15%	35%
5	7%	60%		35%	80%
6	0%	2%		0%	6%
7	0%	0%		0%	0%
8	0%	3%		10%	35%
9	6%	80%		45%	100%
10	0%	60%		10%	80%
11	0%	2%		0%	6%
12	0%	4%		4%	10%
13	0%	0%		2%	2%
14	0%	0%		0%	0%
15	0%	0%		0%	15%
16	0%	3%		0%	1%

### 6.2.3 Main Conclusions

- System-B is composed of molded Polycarbonate, vacuum metallized Aluminum, and thermally cured top-coat -A.
- System-B eliminates the primer stage completely which makes the system less expensive.
- A pre-treatment or base-coat of some sort is required to promote the adhesion between the metallized layer and the substrate. Note that the pre-treatment and base-coat steps are performed in the same chamber that deposits the metallized layer.
- Aluminum is the being used for the metallized layer which is an element and can be sputtered easier versus stainless steel which is an alloy, due to the different sputtering rates for the all the elements that make up the alloy.

- The samples formed some pinholes after the moisture exposure, which is due to the reaction of the aluminum layer with the water.

### **6.3 Stage-2 of System “B” Development**

Based on the water immersion results, this tryout focused on the polycarbonate and aluminum layer interface improvement. The development process involved different techniques to increase adhesion between the metallized layer and the substrate. And also creating a “barrier” layer just before metallizing to prevent the moisture from penetrating through and causing the spotting that was seen after the water immersion results. Different plasma polymerization parameters were utilized, using the base-coat option in the sputtering chamber, to optimize this system.

#### **6.3.1 Objective**

The objective of this stage was to improve system-B to eliminate the minimal amount of pinholes seen after the water immersion testing by increasing base-coat times or trying a pre-treatment in the chamber or applying a thicker aluminum layer.

#### **6.3.2 Observations / Data / Discussion**

Table 6.4 matrix summarizes all the variables and runs produced during stage-2 of system-B. As seen in Table 6.4, runs 17, 18 and 19 have increasingly more base-coat to examine how this affects the system. Runs 20 and 21 utilize a mixture of Argon and HMDSO in an effort to produce a denser layer to protect the substrate and promote adhesion. Runs 24 and 25 use a top-coat within the vacuum chamber on top of the metallized layer. Runs 27-14 and 28-7 are simulating runs 7 and 14 from stage-1 to examine repeatability. The rest of the combinations involved applying more aluminum for a denser coverage in an effort to eliminate the pinholes.

The results for initial adhesion tape and adhesion after water immersion testing are summarized in Table 6.5.

The results in Table 6.6 show that as the dose of the base-coat (in this case HMDSO) is increased, the adhesion is reduced. It is observed that the adhesion of the top-coat to aluminum metallized layer degraded as HMDSO was used on the metallized layer. Thus, HMDSO as a top-coat on the metallized layer has caused an adhesion failure between the metallized layer and the top-coat. Furthermore, sputtering aluminum with a higher flow of Argon seems to not provide a layer with more resistance to moisture penetration compared with runs 17 to 19. Also, repeatability of the pervious run for samples 7 and 14 was achieved using runs 27-14 and 28-7. Overall, pinholes were

observed after the water immersion testing for all samples and thus the system is required further improvements.

Table 6.4: Process Parameters for Stage-2 of System-B. Note: top coat-A was applied to all samples and was cured at 125C for 45 minutes. The base-coat stage takes place within the sputtering chamber

Run	Base-coat				Metallization - Al		Top-coat in Chamber		
	Gas	Ar Flow (sccm)	Sputter Time (sec)	Power (kW)	Time (sec)	Ar Flow (sccm)	Gas	Flow (sccm)	Time (sec)
17	HMDSO	150	30	6	40	150	N/A	N/A	N/A
18	HMDSO	150	40	6	40	150	N/A	N/A	N/A
19	HMDSO	150	50	6	40	150	N/A	N/A	N/A
20	HMDSO+Ar	100+100	30	6	40	150	N/A	N/A	N/A
21	HMDSO+Ar	200+200	30	6	40	150	N/A	N/A	N/A
24	HMDSO	150	20	6	40	150	HMDSO	150	20
25	HMDSO	150	20	6	40	150	HMDSO	150	30
26	HMDSO	150	20	6	60	150	N/A	N/A	N/A
27-14	HMDSO	150	20	6	40	250	N/A	N/A	N/A
28-7	HMDSO+Ar	150+50	20	6	40	150	N/A	N/A	N/A
29	HMDSO	150	20	6	50	150	N/A	N/A	N/A
30	HMDSO	150	20	6	50	250	N/A	N/A	N/A
31	HMDSO	150	20	6	60	250	N/A	N/A	N/A
32	N/A	N/A	N/A	N/A	40	250	N/A	N/A	N/A

Table 6.5: Initial Adhesion and Adhesion After 10 Day Water Immersion Test Results for Stage-2 of System-B. Note: All samples formed pinholes after the water immersion

Run	Initial Adhesion			10 Day Water Immersion Adhesion	
	3M (% Removal)	Nichiban (% Removal)		3M (% Removal)	Nichiban (% Removal)
17	1%	10%		0%	60%
18	0%	60%		6%	60%
19	4%	60%		20%	60%
20	0%	25%		6%	60%
21	0%	10%		4%	45%
24	100%	100%		100%	100%
25	100%	100%		100%	100%
26	0%	6%		0%	60%
27-14	0%	0%		0%	0%
28-7	0%	2%		0%	2%
29	0%	1%		1%	10%
30	0%	0%		0%	15%
31	0%	10%		0%	15%
32	0%	60%		2%	60%

### 6.3.3 Main Conclusions:

- Since pinholes were present after a water-immersion test, further improvement of system-B is required.
- It is proven that the HMDSO as a top-coat on the metallized layer has caused an adhesion failure between the metallized layer and the hard-coat.
- Samples were submitted to water immersion testing and results observed showed minimal improvement in terms of the pinhole concern. The system requires further improvement.

### 6.4 Stage-3 of System “B” Development



Based on the water immersion results from stage-2, the pinholes have not been eliminated and thus further development is required.

#### **6.4.1 Objective**

The objective of this stage was to produce a polycarbonate substrate that was first metallized with stainless steel as a layer to provide protection from pinhole generation, followed by a layer of aluminum and finally a thermally cured top-coat. The main idea is to eliminate the pinholes by providing a second metallized layer that is resistant to moisture penetration. In addition, the stainless steel layer will promote the adhesion between the aluminum and the polycarbonate substrate as the stainless steel layer adheres well to the polycarbonate and the aluminum layer adheres well to the stainless steel layer

#### **6.4.2 Observations / Data / Results**

This stage focused on the elimination of the pinholes that occur after the water-immersion test. Hence, the focus was the interface layer between the polycarbonate and the metallized layer (in this case the aluminum). If the hypothesis that water is penetrating through the top-coat and interacting with the metallized layer to cause the pinholes, then the goal here becomes preventing that penetration through a barrier layer. However, if the thermoplastic material has surface defects as it is molded which is initiating this problem, then it can also be concluded that water is somehow reacting with the defects that cause this issue. Table 6.6 summarizes all the processing parameters that were used in stage-3 of system-B.

All of the runs directly deal with applying a thin layer of stainless steel in the vacuum chamber, followed by aluminum sputtering. This step will allow adhesion of the aluminum layer to the substrate. Furthermore, it might prevent the pinholes problem.

Runs 43 and 44 used a stainless steel layer with 10 and 20 seconds of sputtering time, respectively. Runs 45, 46 and 47 have decreasingly less aluminum deposited with 50, 40 and 30 seconds of sputtering time respectively. They all have 20 seconds of stainless steel sputtered. Runs 48, 49 and 50 have decreasingly less aluminum deposited with 50, 40 and 30 seconds of sputtering time respectively. They all have 10 seconds of stainless steel sputtered. Run 51 has 30 seconds of sputtered stainless steel and 30 seconds of sputtered aluminum. Runs 52 and 53 have increasingly more aluminum deposited with 70 and 80 seconds of sputtering time respectively. They both have 20 seconds of stainless steel sputtered. Finally, run 54 has a pre-treatment of HMDSO and 20 seconds of sputtered stainless steel and 70 seconds of sputtered aluminum. It should be noted that one stainless steel target and one aluminum target were installed in the metallizer chamber at the same time.

The initial adhesion and adhesion after a water immersion testing are summarized in Table 6.7. One of the most important results that should be observed is the fact that no pinholes were formed after the water immersion testing. In Table 6.7, all runs pass initial adhesion 100% with the 3M tape and thus the Nichiban tape allows one to test the samples in a more aggressive manner to better understand and compare results. The results indicate that a 20 seconds sputtering of stainless steel is beneficial to promote adhesion. All the runs that had 10 seconds of sputtering for the stainless steel layer had an adhesion removal of 20% or greater as in samples, 43, 48, 49 and 50.

Samples were submitted to water-immersion to evaluate the adhesion properties after moisture exposure and results are reported in Table 6.7. It is seen that all runs meet the water immersion requirements using the 3M tape. More specifically, Figure 6.2 shows a plot of the water immersion adhesion results with respect to the aluminum sputtering times, for 20 seconds of sputtering time for the stainless steel layer. It can be observed that all runs with 20 seconds of sputtering for stainless steel have less than 13% tape pull removal, which is the best result for system-B. Further, there is no clear trend with respect to aluminum sputtering time versus adhesion.

Although it is outside the scope of the original thesis work to meet the CASS testing requirements, it is required to validate the system. Thus, it is important to report that samples failed the CASS testing (as the aluminum layer corroded) and results are reported in a later section (5.5.2.1).

Table 6.6: Process Parameters for Stage-3 of System-B. Note: top coat-A was applied to all samples and was cured at 125C for 45 minutes. The pre-treatment stage takes place within the sputtering chamber

Run	Pre-treatment			SST		AL	
	HMDSO Flow (sccm)	Time (sec)	Power (kW)	Sputter Time (sec)	Ar Flow (sccm)	Time (sec)	Ar Flow (sccm)
43	n/a	n/a	n/a	10	150	60	250
44	n/a	n/a	n/a	20	150	60	250
45	n/a	n/a	n/a	20	150	50	250
46	n/a	n/a	n/a	20	150	40	250
47	n/a	n/a	n/a	20	150	30	250
48	n/a	n/a	n/a	10	150	50	250
49	n/a	n/a	n/a	10	150	40	250
50	n/a	n/a	n/a	10	150	30	250
51	n/a	n/a	n/a	30	150	30	250
52	n/a	n/a	n/a	20	150	70	250
53	n/a	n/a	n/a	20	150	80	250
54	150	20	6	20	150	70	250

Table 6.7: Initial Adhesion and Adhesion After 10 Day Water Immersion Test Results for Stage-3 of System-B. Note: no samples formed pinholes after the water immersion

Run	Initial Adhesion		Water - Soak Adhesion	
	3M (% Removal)	Nichiban (% Removal)	3M (% Removal)	Nichiban (% Removal)
43	0%	20%	0%	8%
44	0%	0%	0%	4%
45	0%	2%	0%	12%
46	0%	2%	0%	5%
47	0%	2%	0%	6%
48	0%	20%	1%	20%
49	0%	20%	0%	35%
50	0%	30%	0%	30%
51	0%	30%	0%	20%
52	0%	2%	1%	18%
53	0%	0%	0%	4%
54	0%	0%	0%	12%

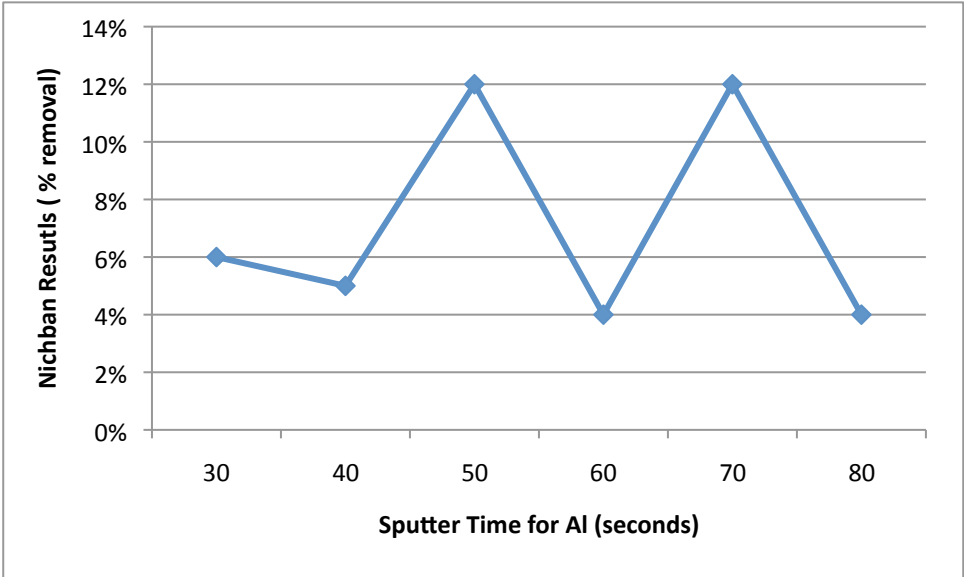


Figure 6.2: Nichban Test Results After Water Immersion Testing with Respect to the Sputtering Time for Aluminum. Note that all runs use 20 seconds of sputtering for stainless steel

#### **6.4.3 Main Conclusions**

- Sputtering a stainless steel layer before depositing the aluminum layer has proven beneficial in promoting adhesion between the plastic substrate and the aluminum metallized layer.
- System-B eliminates the primer stage completely which makes the system robust.
- All the runs that had 10 seconds of sputtering for the stainless steel layer had an adhesion removal of 20% or greater.
- All the runs that had 20 seconds of sputtering for the stainless steel layer had an adhesion removal of 13% or less. Thus, 20 seconds is preferred.
- Pinholes on the aluminum layer were eliminated after a water immersion test by the addition of the stainless steel layer.

#### **5.5 Stage 4 of System “B” Development:**

This is the last stage for system-B development. The concern has been the oxidization of the interface of the aluminum layer and top-coat layer as a result of the CASS testing (Copper Accelerated Acidic Acid Salt Spray).

##### **5.5.1 Objective**

The main objective of this run is to optimize the PC/SST+Al/top-coat system in an effort to eliminate the primer stage. More specifically, the intent was to reduce the thickness of the aluminum layer, in an effort to eliminate corrosion and yet have sufficient aluminum for the top-coat to adhere to the aluminum layer.

##### **5.5.2 Observations / Data / Results**

Table 6.8 summarizes the different combinations that were tried for stage-4 of system-B. As noted in Table 6.8, combinations 73, 74, and 75 have a constant thickness of the stainless steel metallized layer with varying thicknesses for the aluminum layers. Runs 73, 74, and 75 have sputtering times of 10, 20 and 30 seconds respectively. Run 77 is a duplicate of run 44 that ran in stage-3 to confirm results and ensure repeatability. Runs 78 – 81 involve a post-treatment of different monomers and gases in order to help the adhesion of the top-coat to the stainless steel layer. The last run 83 involves metallizing aluminum first with a thin layer of stainless steel after and on top of the aluminum.

The initial adhesion results and the adhesion results after water immersion testing are reported in Table 6.9. Runs 74 through 76 showed promising results of initial adhesion with utilizing a thin layer of aluminum. Runs 77-44 confirmed the results from stage-3. However, all the post-treatment that were examined to promote adhesion to the stainless steel layer did not help the top-coat to adhere to SST layer, as shown in runs 78 through 81.

Samples were then submitted to the first seven test specifications that are outlined in section 3.1. Sample 74-44 was selected to be submitted to these tests as it passed the initial adhesion and water immersion testing. In addition, samples 77-44 have minimal amount of stainless steel ( sputtering time of 20 seconds) which minimizes cost. Table 6.10 clearly shows that the system meets these specifications.

Table 6.8: Process Parameters for Stage-4 of System-B. Note: top coat-A was applied to all samples and was cured at 125C for 45 minutes.

Run #	SST		Al		Top-coat in Chamber		
	Sputtered Time (sec)	Ar Flow (sccm)	Sputtered Time (sec)	Ar Flow (sccm)	Gas	Flow (sccm)	Time (sec)
73	50	150	10	250	n/a	n/a	n/a
74	50	150	20	250	n/a	n/a	n/a
75	50	150	30	250	n/a	n/a	n/a
76	60	150	60	250	n/a	n/a	n/a
77-44	20	150	60	250	n/a	n/a	n/a
78	50	150	n/a	n/a	HMDSO + O2	100+100	10
79	50	150	n/a	n/a	HMDSO + O2	100+100	20
80	50	150	n/a	n/a	HMDSO + O2	100+100	50
81	50	150	n/a	n/a	HMDSO + O2 + Ar	100+100+100	20
	Al		SST				
	Time (sec)	Ar Flow (sccm)	Time (sec)	Ar Flow (sccm)			
83	50	250	10	150			

Table 6.9: Initial Adhesion and Adhesion After 10 Day Water Immersion Test Results for Stage-4 of System-B. Note: no samples formed pinholes after the water immersion

Run	Initial Adhesion		Water - Soak Adhesion	
	3M (% Removal )	Nichiban (% Removal )	3M (% Removal )	Nichiban (% Removal )
73	0%	15%	2%	17%
74	0%	0%	0%	2%
75	0%	0%	0%	0%
76	0%	0%	0%	3%
77-44	0%	0%	0%	2%
78	100%	100%	100%	100%
79	100%	100%	100%	100%
80	100%	100%	100%	100%
81	100%	100%	100%	100%
83	100%	100%	100%	100%

Table 6.10: Results for Complete Matrix Testing for System-B

Run	Number of Samples	Test / Specifications	Results
77-44	3	Appearance Approval	meets specifications
77-44	3	Impact Resistance	meets specifications
77-44	3	Initial Adhesion	meets specifications
77-44	3	Water Immersion Resistance	meets specifications
77-44	3	Heat Age Testing	meets specifications
77-44	3	Humidity Resistance	meets specifications
77-44	3	Salt Spray	meets specifications

#### 5.5.2.1 Copper-Accelerated Acetic Acid Salt Spray (CASS) Testing and Sample Analysis:

In addition to the testing performed in Table 6.11, sample run 77-44 was submitted to Copper Accelerated Acidic Acid Salt Spray (CASS) testing as this test examines the corrosion resistance



properties of system. It should be noted that is outside the initial scope of this work but it is important to report this result as it relates to validate the value of this technology.

This CASS testing was performed on run 77-44 to determine how the sample will perform as it contains an aluminum layer. The sample tested consisted of the following layers, see Figure 6.3:

1. Polycarbonate plastic substrate.
2. Stainless Steel metallized layer
3. Aluminum metallized layer
4. Protective thermally cured top-coat

This test clearly demonstrated that the presence of the aluminum layer has caused corrosion initiation and propagation that resulted in a failure. The sample exhibited discoloration as evidence of corrosion as shown in Figure 6.4 and Figure 6.5.

It is visually evident that the edges of a sample submitted to CASS testing initiated the corrosion and allowed it for propagation throughout the surface of the samples. Also, surface imperfections (scratches) did allow the initiation of the failure mode. Edges are a problem, especially sharp edges, as film (hard-coat) build up is less due to geometry.

The EDX analysis, in Figure 6.5, indicates the presence of silicone in area “1” as expected which is the presence of the top-coat as well as the paraffin wax used to seal the edges of the sample. It is observed that the aluminum metallized layer has micro-cracked initially, which caused the stainless steel layer and the top-coat layers to micro-crack as well, as shown in Figure 6.6.

The EDX spectra, in Figure 6.7, of the cracks indicate the presence of SST and Al in both areas “1” and “2”. It is observed that the aluminum film is highly corroded in area “2” and thus only traces of aluminum are present in the EDX spectra. In addition, the presence of chloride is only observed in area “1” which represents the aluminum layer and is an indication that the chloride is imbedded into the aluminum layer. This conclusion is drawn as there is no evidence of any chloride in the area number “2” which represents the stainless steel metallized layer.

Figure 6.8 and Figure 6.9 show the CASS sample 77-44 with the failure of an area in the middle of the sample. This was traced back to an initial micro-crack that allowed corrosion initiation and subsequent propagation.

It is important to note that samples had been submitted to Salt Spray Testing and have passed that requirement. However, they have failed CASS testing. The major differences between CASS and Salt Spray testing are summarized in Table 6.11. Samples pass the Salt Spray testing and yet they fail the CASS testing due to harsh environment in during the CASS test compared to that of the Salt Spray.

Table 6.11: CASS versus Salt Spray Testing

<b>Solution for CASS:</b> 5 parts by mass of sodium chloride in 95 parts of water, which makes up the Slat Solution. Plus 0.25 g of copper chloride (CuCl <sub>2</sub> ·2H <sub>2</sub> O) to each liter of the salt solution. Plus the addition of glacial acetic acid to adjust pH level.	<b>Solution for Salt Spray:</b> 5 parts by mass of sodium chloride in 95 parts of water
<b>Test Condition:</b> Temperature : 49C	<b>Test Condition:</b> 35C
<b>pH level for CASS:</b> 3.1 – 3.3	<b>pH level for Salt Spray:</b> 6.5 to 7.2

Elemental mapping of the middle micro-cracks, Figure 6.10, provides evidence of Al, Fe and Cr, as it was expected from SEM images. Figure 6.10a shows an SEM image with different shades of gray. Lighter areas represented Al atoms. Images of the metallized layer after CASS testing and after removal of the top-coat, show minimal presence of Al. The dark area in figure 6.10a contains some Fe, Cr, C and no Al. Lighter areas show Fe, Cr, and some Al. The lightest areas show a lot of Al, some Fe and Cr. Note the presence of Chlorine in the elemental mapping. Figure 6.10 b,c,d,e and f show silicone, chlorine, iron, chromium and aluminum respectively. This indicates that salt solution used in the CASS testing had penetrated through the top-coat into the metallized layer of aluminum that caused the corrosion.

Figures 6.11 and 6.12 show SEM images of the thermal top-coat removed as a result of the adhesion loss between the top-coat and aluminum layer because of corrosion of the aluminum layer. The EDX of area “1” shows the presence of low amounts of aluminum to indicate evidence of corrosion compared to area “2”. There is also iron, chromium stainless steel and chlorine. Area “2” shows high levels of aluminum, indicating no corrosion had taken place at that area. Also the presence of the different element of stainless steel is evident. Area “3” shows no evidence of aluminum, indicating corrosion of that area. It also shows high levels of carbon, which is the substrate material.



Figure 6.3: SEM Images for Freeze Fracture of a Cross Section for a Typical Sample for System-B

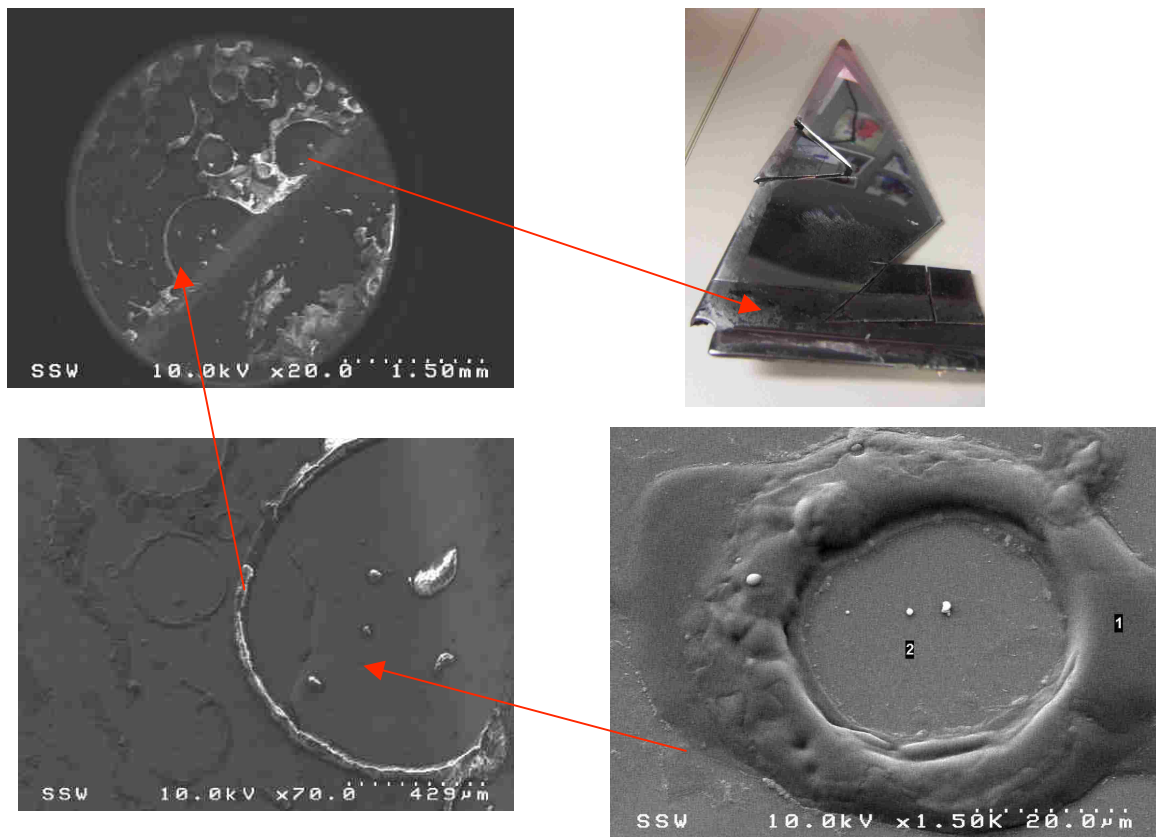


Figure 6.4: SEM Images for Edge of the CASS Sample 77-44

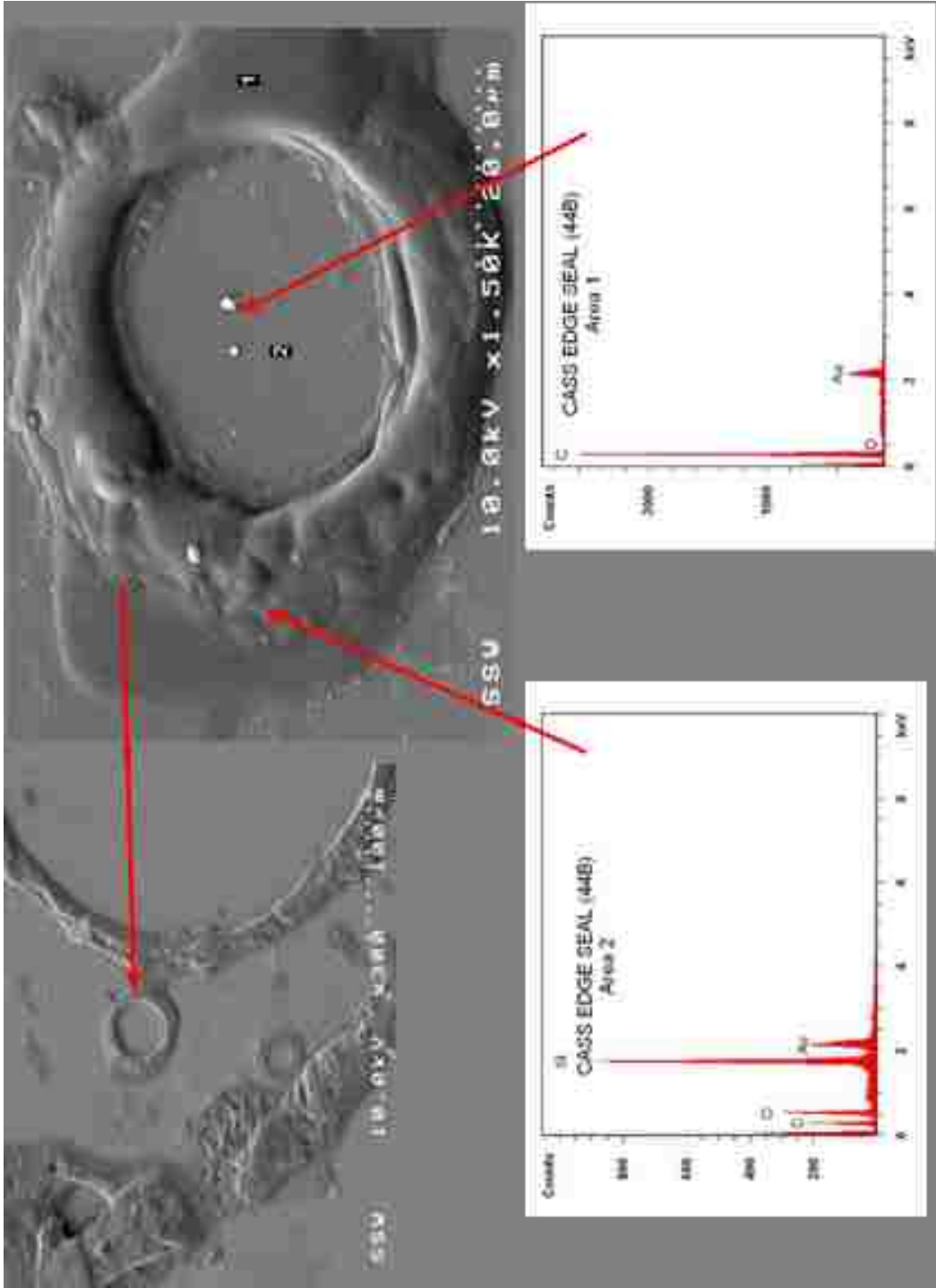


Figure 6.5: SEM/EDX Images for Edge of the CASS Sample 77-44

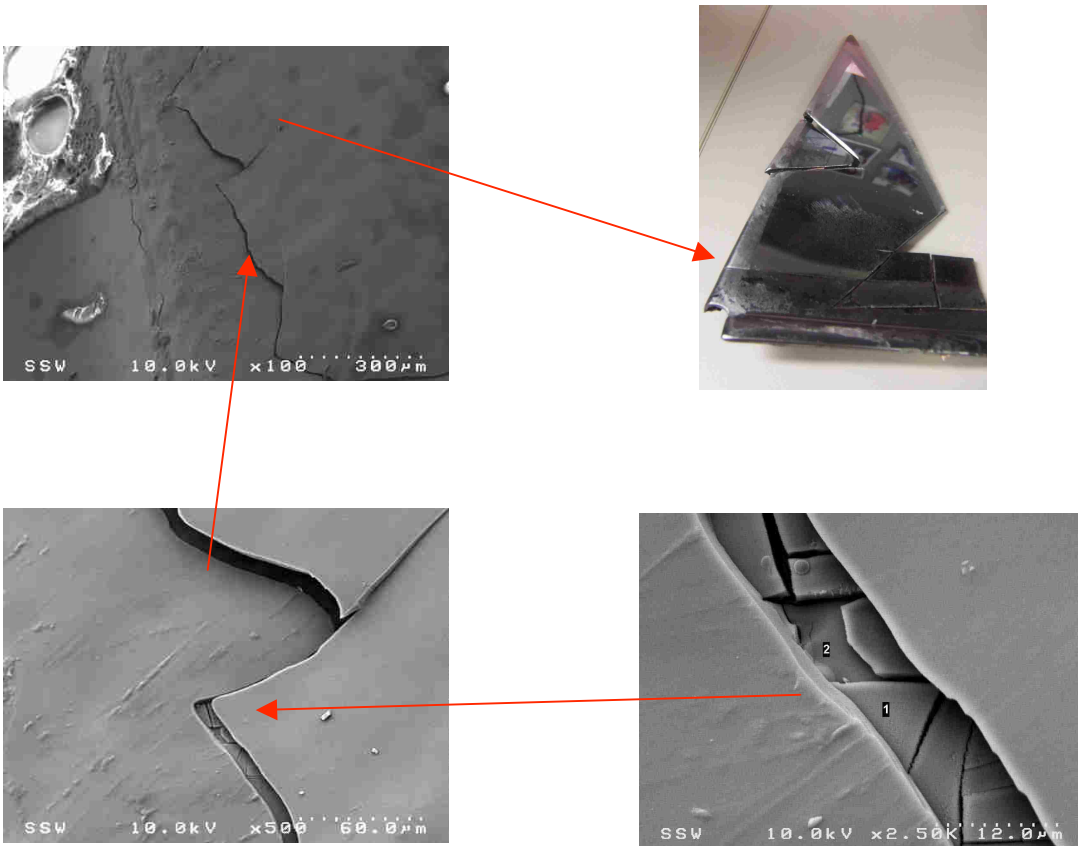


Figure 6.6: SEM Images for Edge of the CASS Sample 77-44 – Crack Location

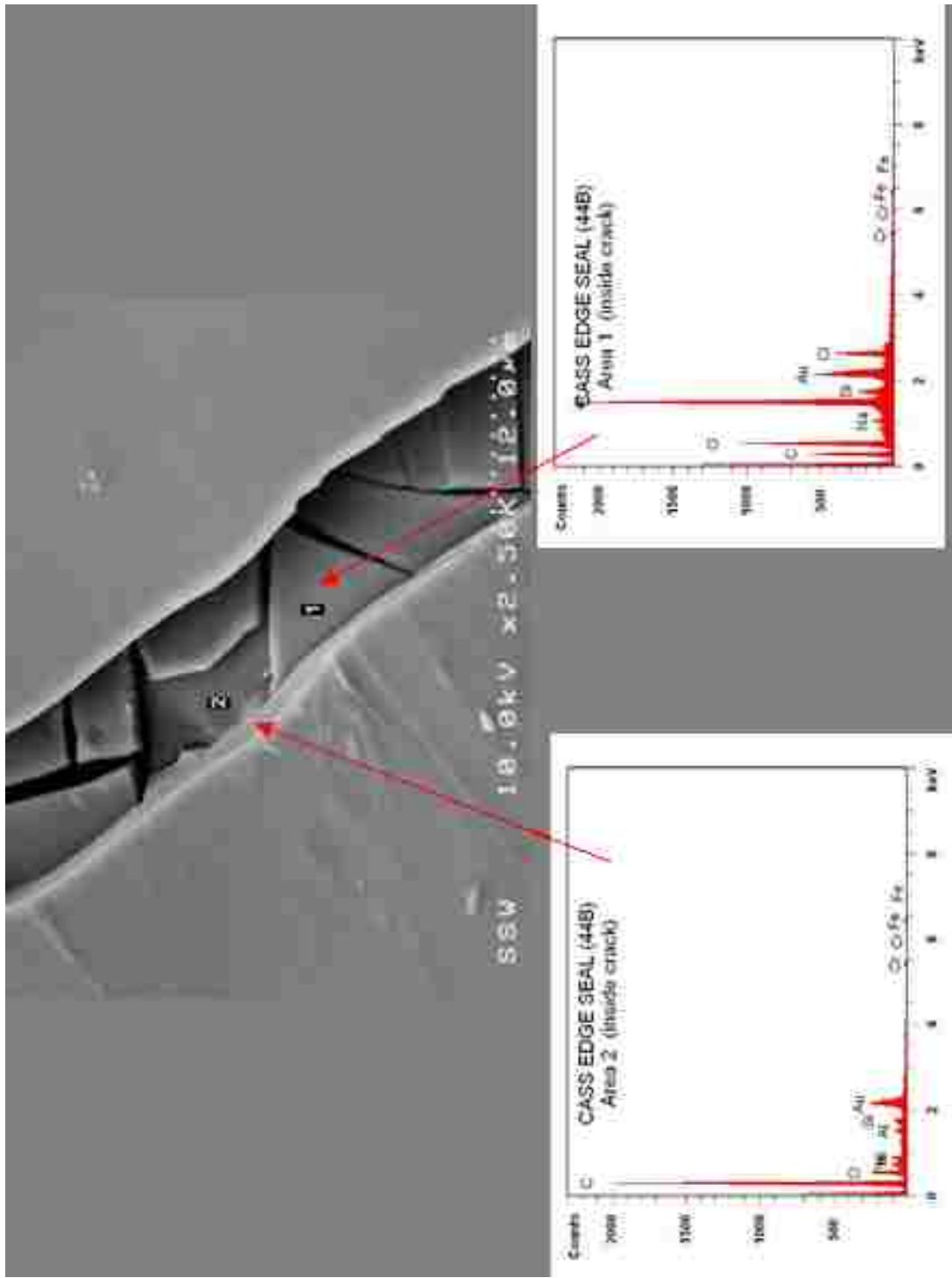


Figure 6.7: SEM/EDX Images for Edge of the CASS Sample 77-44 – Crack Location

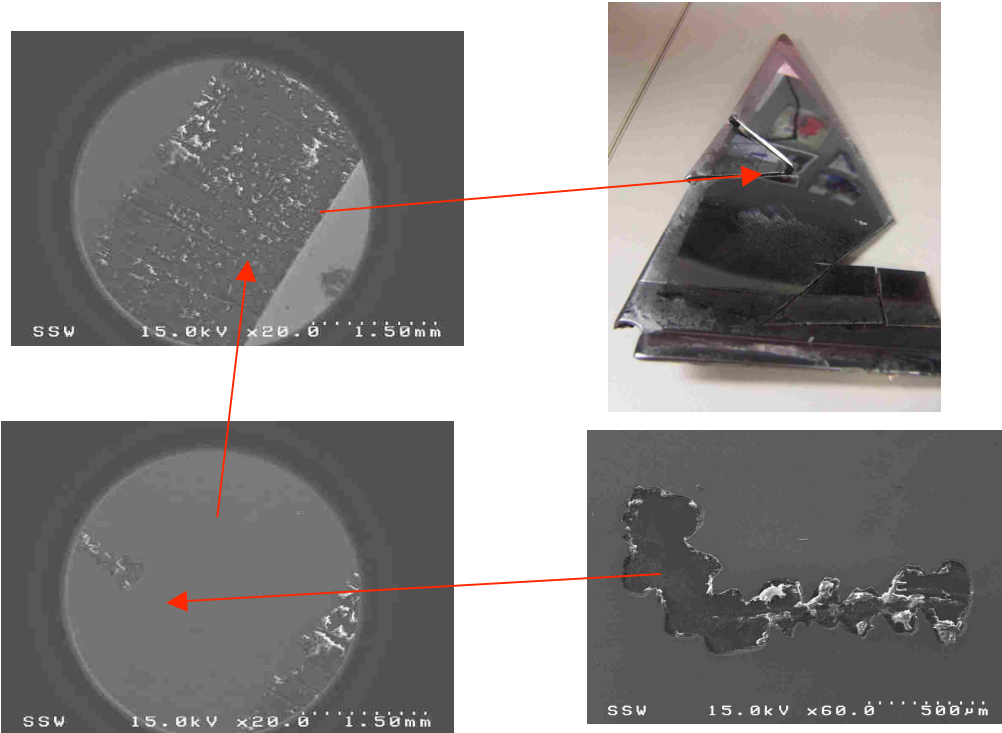


Figure 6.8: SEM Images for Middle of the CASS Sample 77-44 – Note: darker gray areas represent corroded areas failure locations

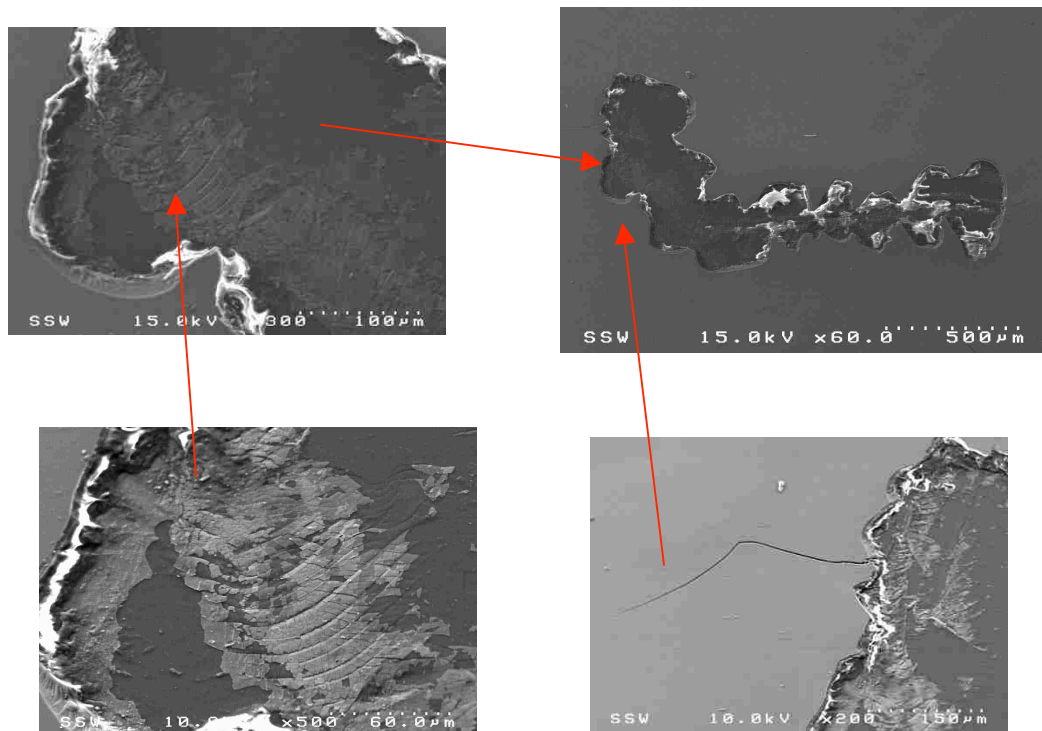


Figure 6.9: SEM images for Middle of the CASS Sample 77-44 – Failure Location

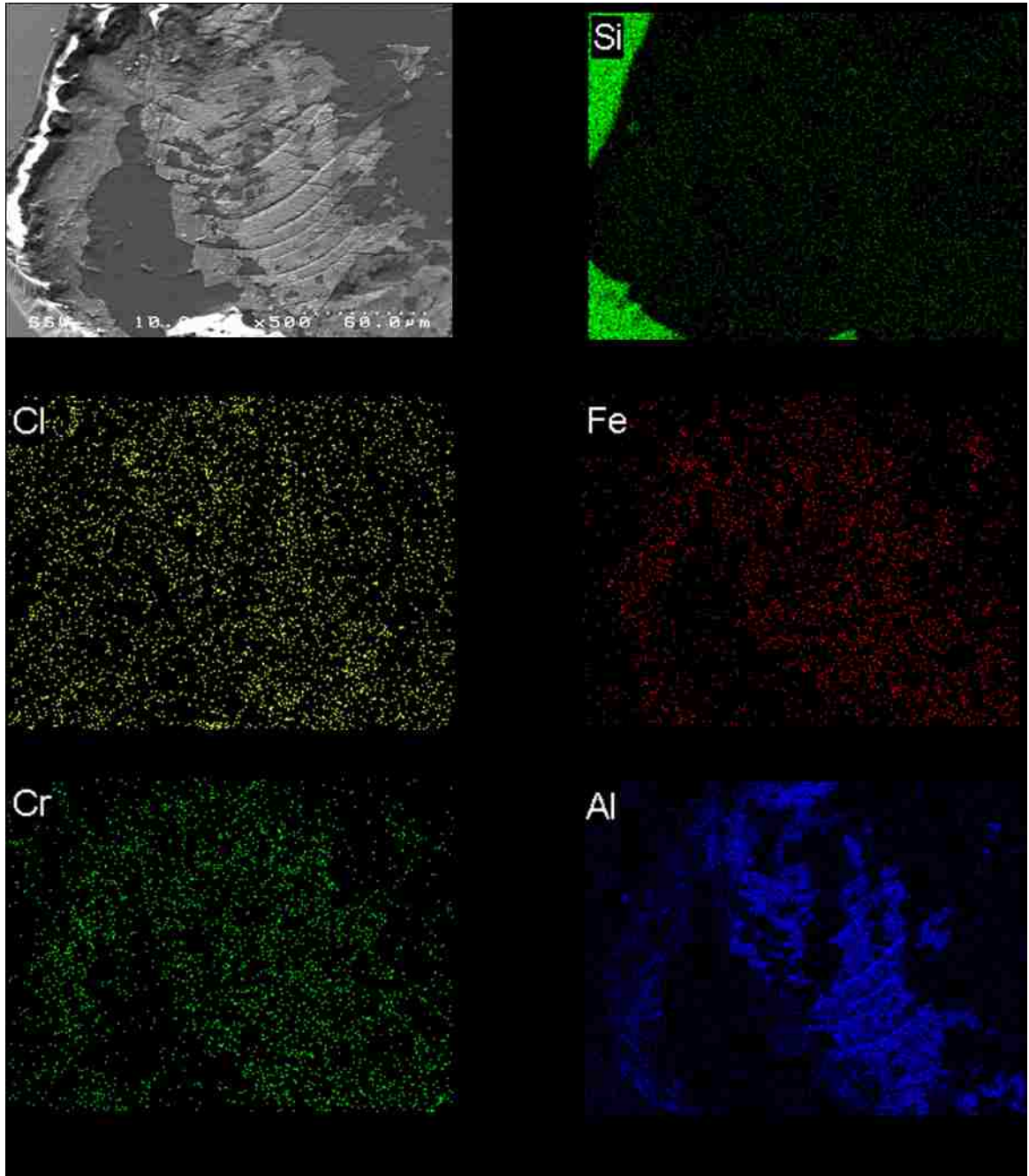


Figure 6.10: Elemental Mapping for Middle of the CASS Sample – Failure Location. Note that “a” is an SEM image of the failure location. “b” is silicone, “c” is chlorine, “d” is iron, “e” is chromium and “f” is aluminum.



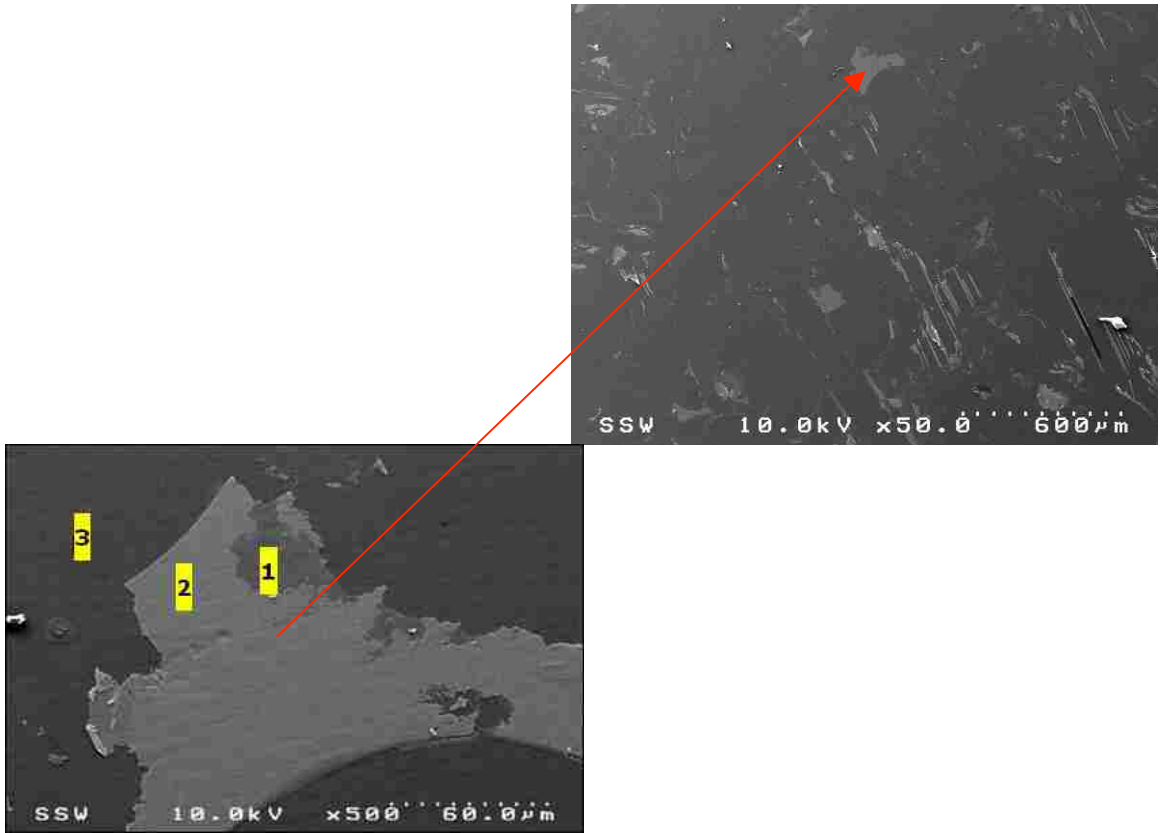


Figure 6.11: SEM Images for CASS Sample Showing the Different Exposed Layers. Note: the top coat removed and metalized layer exposed

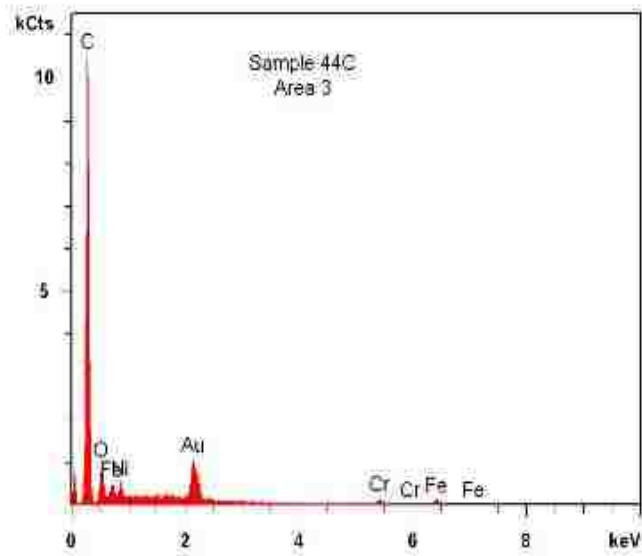
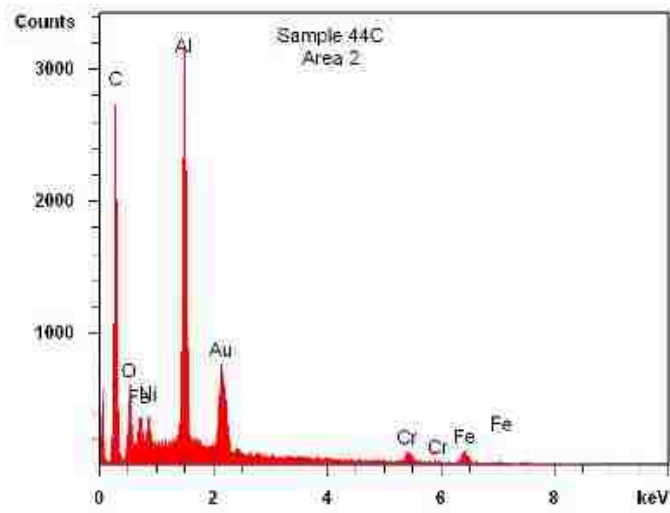
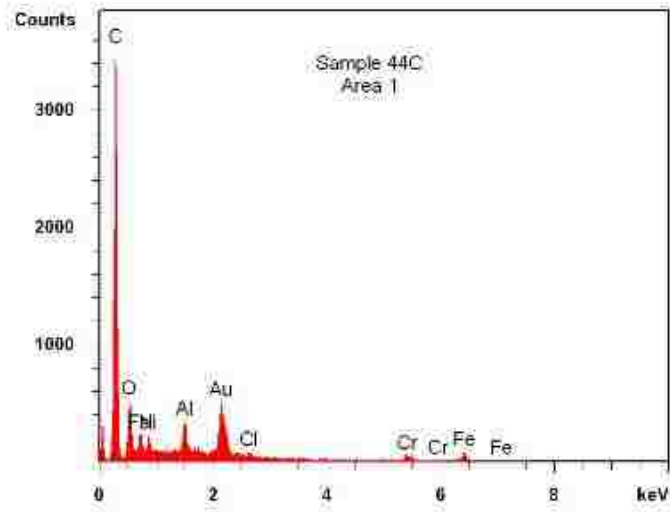


Figure 6.12: SEM/EDX Images for CASS Sample 77-44 shown in Figure 6.8  
 Note: area-1 is low levels Al and SST, area-2 is high levels of Al and SST and area-3 is no Al and only SST.

### **6.5.3 Main Conclusions**

- System-B optimization was performed to minimize the aluminum layer thickness and acceptable initial adhesion results and water immersion results were obtained.
- All plasma post-treatment runs reduced adhesion between the stainless steel layer and top-coat.
- Even with very thin layers of aluminum, system-B does not meet the performance requirements for CASS testing.

### **6.6 System “B” Summary**

System “B” consists of polycarbonate as a substrate, stainless steel as the first metalized layer, aluminum as the second metalized layer and a protective, thermally cured, clear top-coat. The development of system B involved 4 stages. The first two stages dealt with utilizing only one metalized layer, that is aluminum. However, due to pinhole formation after water immersion testing, a stainless steel layer was added. Stage 3 and 4 dealt with exploring the concept of using two metalized layers. System-B meets the seven testing requirements as outlined in section 3.1. However, due to the highly corrosive nature of the aluminum metalized layer, it was observed that sample 77-44 failed the CASS testing. It is important to note that the CASS testing falls outside the scope of satisfying this thesis but it is definitely a critical result to report.

## CHAPTER VII

### CONCLUSIONS AND RECOMMENDATIONS

#### 6.1 Conclusions:

As an alternative to traditional chrome plating, a process consisting of injection molding, physical vapor deposition and top-coating was investigated. It was concluded that using polycarbonate as a substrate material is the most suitable option for this technology as it provides the structural integrity for the system as well as the high glossy appearance for metalizing. Two systems were investigated and the following conclusions are made:

1. System "A": consists of polycarbonate as a substrate, stainless steel as a metalized layer, primer as an adhesion promoter, and a protective clear top-coat. System-A passes the functional requirements for the specifications. It was critical to use primer-C to promote the adhesion between the metalized layer and the top-coat in order to meet all of the function requirements. The main concern with system-A is related to the mis-match of index of refraction between the stainless steel metalized layer and top-coat-A which results in an iridescence appearance effect. The iridescence is a subjective matter and depending on the application, it could be accepted or rejected. Therefore, system-A meets the functional requirements with a subjective appearance effect.
2. System-B: consists of a polycarbonate as substrate, stainless steel as the base metalized layer, aluminum as the second metalized layer and a protective clear top-coat. In system-B, the primer stage was eliminated as the top-coat directly adhered to the aluminum layer. However, it was critical to add a stainless steel metalized layer to prevent any pinhole failures between the aluminum metalized layer and the polycarbonate substrate. In addition, a stainless steel metalized layer promoted the adhesion between the polycarbonate substrate and the aluminum layer, which also eliminated the pre-treatment stage. System-B meets the functional requirements for Salt Spray and all other in house testing, but it fails the Copper Acetic Acid Salt Spray (CASS) test performance requirements. It can be concluded that the presence of aluminum is causing corrosion concerns.

In general, it was concluded that performing all processing steps, that consist of injection molding, PVD coating, and top-coating without any significant amount of time between each step

proved to be critical as the surface energy of the surface is at its optimal condition for maximum adhesion between each layer.

## **6.2 Recommendations**

The recommendations for System-A would be to investigate different metalized layers, as well as different top-coat options to find a matching index of refraction and thus eliminate iridescence to meet the appearance requirements without jeopardizing the adhesion between the layers.

The recommendations for System-B would be to investigate other metallized layer options that provide the proper adhesion requirements between the substrate and metalized surface as well as the metalized surface and the top-coat. These metals should have better corrosion resistance than 99% pure aluminum to eliminate the CASS testing failures.

## REFERENCES

- [1] B Navinsek P.Panjan I. Milosev, "PVD coatings as an environmentally clean alternative to electroplating and electroless processes" *Surface and Coating Technology* 116-119 (1999) 476-487
- [2]. K.O. Legg, *Proceedings Workshop on Hard Chromium Plating: Techniques, Markets and Alternative Processes*, Saint-Etienne, (1995).
- [3] Verein Deutscher Ingenieure – Richtlinien, "Vacuum coating quality assurance, Demands on plastics to be coated" *Guideline VDI 3823, Part 2*, , Germany, (November 2006)
- [4] "Chrome Plating" [http://en.wikipedia.org/wiki/Chrome\\_plating](http://en.wikipedia.org/wiki/Chrome_plating), date accessed: (April-14-2011).
- [5] Administer, "Chrome Plating Process for Plastics"  
<http://primechrome.com/index.php/chrome-plating/chrome-plating-process-for-plastics>, date accessed: (May-19-2011).
- [6] "Introduction to Chrome Plating", <http://www.finishing.com/faqs/chrome.html>, date accessed: (May-19-2011).
- [7] H. Grünwald, "Vacuum Metallizing Plastic Parts for Five Decades— What Progress Have We Made?", *41st Annual Technical Conference Proceedings*, Society of Vacuum Coaters, (1998).
- [8] J. Barriga, "Decorative Coatings Obtained by Combination of PVD, Galvanic and Powder Coatings", *52nd Annual Technical Conference Proceedings*, Society of Vacuum Coaters, (2001).
- [9] W. Bialojan, M. Geister, " Vacuum Metallizing Plastic Parts", *Product Finishing, Focus: Plating on Plastics*, (Oct-1992).
- [10] L. Xu, R.E. Goltz, "Reflector Coatings in Automobile Lighting—Their Performance Requirements, Substrates, Materials and Processing", *44th Annual Technical Conference Proceedings*, Society of Vacuum Coaters, Philadelphia, (April 21–26, 2001).
- [11] P. Mills, "Beyond the Bling: The Development of Decorative PVD/UV Coating Systems", *Fusion UV Systems, Inc., Gaithersburg, MD; Society of Vacuum Coaters* (2008).

- [12]. P. S. Prevey,., "X-ray Diffraction Residual Stress Techniques," Materials Characterization, Vol. 10, 9th edition, ASM Metals Handbook, (R. E. Whan, et al., eds.), p. 380 (1986)
- [13]. Campbell, D. S., "Mechanical Properties of Thin Films," Handbook of Thin Film Technology, (L. I Maissel and R. Glang, eds.), Ch. 12, McGraw- Hill (1970)
- [14]. S. Yu. Gracheva, F. D. Tichelaar and G.C.A.M. Janssen "Stress in sputter-deposited Cr films: Influence of Ar pressure " ,J. App. Phy. 97, 073508 (2005)
- [15] J, Pfeifer, Hexamethyldisiloxane" <http://en.wikipedia.org/wiki/Hexamethyldisiloxane>, date accessed: (August-18-2010).
- [16] R. Rank, T. Wuensche, M.Fahland, C. Charton and N. Schiller "Adhesion Promotion Techniques for Coating of Polymer Films"; 47 Annual Technical Conf Society of Vacuum Coaters, pp. 632-937 , (2004)
- [17] F.D Egitto and L.J Matietenzo , "Plasma Modification of Polymer Surfaces" ., 36<sup>th</sup> Annual Technical Conf Society of Vacuum Coaters, pp10-22, (1993)
- [18] John Madocks , "Practical Aspects of Plasma Treatment" , SVC Bulletin, (2010).
- [19] J.S. Brinen, S. Greenhouse, and L. Pinatti, "ESCA and SIMS Studies of Plasma Treatments of Intraocular Lenses," Surf. and Interface Anal., 17, 63 (1991).
- [20] F. Millich in Encyclopedia of Materials Science and Engineering, 2nd ed., Vol. 12, p. 398, edited by H.F. Mark, N.M. Bikales, C.G. Overberger, and G. Menges, Wileyinterscience, New York, (1987).
- [21] W. Yang and N. Sung, "Adhesion Promotion Through Plasma Treatment in Thermoplastic/rubber Systems," Proc. ACS Division of Polym. Mat.: Sci. and Eng., Vol. 62, ACS Spring Meeting, Boston, MA, (1990).
- [22] R. F. Bunshah "Handbook of hard coatings: deposition technologies, properties and applications". (2001), William Andrew Publishing/Noyes
- [23] H. K, Pulker,., "Mechanical Properties of Optical Films," Thin Solid Films, 89:191 (1982)
- [24] American Standard Test Method, "ASTM D5420: Standard Test Method for Impact Resistance of Flat, Rigid Plastic Specimen by Means of a Striker Impacted by a Falling Weight (Gardner Impact)", West Conshohocken, PA, [www.astm.org](http://www.astm.org).
- [25] American Standard Test Method, "D3330/D3330M-04 Standard Test Method for Peel Adhesion of Pressure-Sensitive Tape", West Conshohocken, PA, [www.astm.org](http://www.astm.org).
- [26] American Standard Test Method, "D 870 – 02 Standard Test Method for Testing Water Resistance of Coatings Using Water Immersion", West Conshohocken, PA, [www.astm.org](http://www.astm.org).

- [27] American Standard Test Method, “D2247-11 Standard Practice for Testing Water Resistance of Coatings in 100% Relative Humidity”, West Conshohocken, PA, [www.astm.org](http://www.astm.org).
- [28] American Standard Test Method, “B117-09 Standard Practice for Operating Salt Spray (Fog) Apparatus”, West Conshohocken, PA, [www.astm.org](http://www.astm.org).
- [29] American Standard Test Method, “D6944-09 Standard Practice for Resistance of Cured Coatings to Thermal Cycling”, West Conshohocken, PA, [www.astm.org](http://www.astm.org).
- [30] American Standard Test Method, “D3170-03 Standard Test Method for Chipping Resistance of Coatings”, West Conshohocken, PA, [www.astm.org](http://www.astm.org).
- [31] American Standard Test Method, “B368-09-03 Standard Test for Copper-Accelerated Acetic Acid-Salt Spray (Fog) Testing”, West Conshohocken, PA, [www.astm.org](http://www.astm.org).
- [32] American Standard Test Method, “G 155 – 05a Standard Test for Operating Xenon Arc Light Apparatus”, West Conshohocken, PA, [www.astm.org](http://www.astm.org).
- [33] Russell E. Smith, “Test Procedure for AccuDyne Test Markers”  
<http://www.accudynetest.com>, date accessed (June-12-2011).
- [34] Phillipe Cognard, ‘Handbook of adhesives and sealants’, Volume 2 : General knowledge, application , McGraw-Hill Professional, New Curing Techniques (2006)
- [35]. Surface Engineering, ASM Handbook , Volume 5, ASM International, Materials Park, Ohio (1994)



## **VITA AUCTORIS**

Name: Jack Bekou

Place of Birth: Baghdad, Iraq

Date of Birth: 1983

Education: 2002-2006 Bachelor of Applied Science – Mechanical Engineering

University Windsor, Windsor, ON

2008-2011 M.A.Sc.– Materials Engineering

University Windsor, Windsor, ON